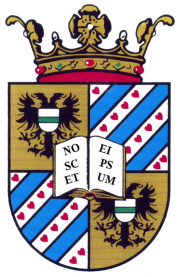

Groot Onderzoek or Master Thesis: Cosmotopology

Hugo Buddelmeijer
supervisor: *Rien van de Weijgaert*
Rijksuniversiteit Groningen

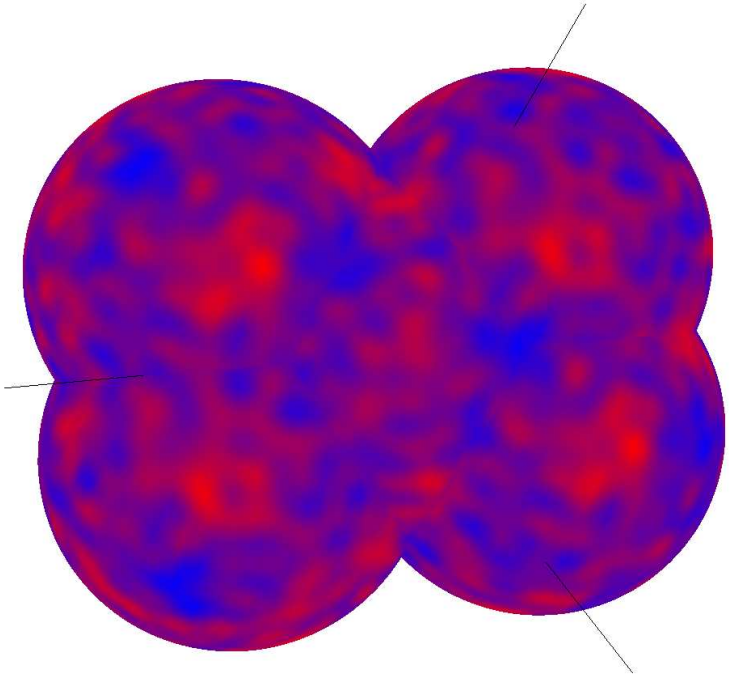

August 17, 2006

Abstract

The Universe is usually seen as either a hypersphere or an infinite Euclidean or hyperbolic space. However, the Universe might fold back into itself: there are more possibilities for the topology of the Universe that locally have one of these three metrics. In this thesis we discuss the possible non trivial topologies for two and three dimensional Universes. All two dimensional spherical and flat spaces are described, as well as all three dimensional flat spaces.

Previous methods to detect these topologies are described, as well as a new method using multipole vectors. Although they are locally isotropic, most non trivial topologies have preferred directions. The proposed method tries to detect these directions in the cosmic microwave background. Simulations for most flat orientable three dimensional manifolds are performed in order to determine the effect of a non trivial topology on the alignment of the multipole vectors. The alignment of the dipole and quadrupole to the principle axes, themselves and each other is measured.

The main conclusion is that size is more important then orientation. The particular dimensions of the Universe determine the alignments of the multipole vectors, the influence of the specific shape of the Universe is small. There appears to be a slight effect on the alignments even if the dimensions of the Universe are slightly larger then the size of the visible universe. The method is especially useful to check the viability of a proposed model for the topology of the Universe. Improvements can be made by examining more spaces, taking into account all degrees of freedom of the possible spaces and researching the effect of different positions of the observer.

"In the beginning the universe was created. This has made a lot of people very angry and been widely regarded as a bad move." – Douglas Adams

Contents

Chapter 1

Introduction

In describing the Universe at its largest scales there are two intertwined issues to address. The first one concerns with the local structure of space, its geometry. The second concerns its structure on the largest scale, its topology. Cosmology answers the question of what geometry the Universe has, but the only topological issue that it regularly addresses is the finiteness of the universe.

Nearly all cosmologies, except for ones with a closed hypersphere geometry, assume that space is infinite. This need certainly not be true and physical principles do allow for a more general view. Geometry, governed by general relativity describes the geometry of the Universe. The curvature of the Universe is determined by its mass content. It can be positively or negatively curved, or not curved at all. However, geometry does not prescribe anything about the global structure of space, this is described by topology. The global curvature of space does restrict the topological shapes the Universe can have, but there are several different topological shapes with the same geometry that general relativity can not distinguish.

As a pioneer of cosmology Albert Einstein already argued that there might be other possibilities for the topology of the Universe than the three common shapes but he acknowledged that mathematics hasn't evolved far enough yet to tackle the problem. Since then cosmology has become one of the most active research areas of astronomy and astrophysics. Yet, until recently the study of the topology of the Universe was never picked up.

In the past two decades our mathematical insight into the topology of our cosmos has advanced significantly. We have learned what the consequences of such topologies are, and found ways in which we could detect such a non trivial topology of the Universe in which we live. In this thesis we will describe what spaces are possible and how to constrain the possible configurations. We also describe the effect they might have on our universe and the attempts to detect these effects. We add a previously unused method to our arsenal using the cosmic microwave background and multipole vectors. This chapter starts with an introduction of the main principles for people without background knowledge in the fields of cosmology and topology.

1.1 History of Cosmology

Cosmology is one of the oldest sciences, it is the science of the cosmos. It has had the interest of even the most ancient civilizations. Some of the main questions that cosmologists ask about the universe are "How did it start and how will it end?", "What is its size?", "Does it have a center and if so, where is it?" and "How did all this structure in the Universe emerge?". Every age of mankind has given its own answers to these questions. Often these were more philosophical or religious than scientific. Since Einstein's theory of general relativity, which provides the general framework for the gravitational force which dominates the evolution of our Universe, and in particular since the discovery of the expansion of the Universe by Hubble in the beginning of the 20th century we have come to develop a physical compelling view of the cosmos in which we live. New theories and methods of experimentation might turn the 21st century into a true answer-giving era to the

questions of cosmology.

Cosmology studies the universe on the largest scales. It is good to realize this scale has varied over the course of history and so did the answers to these questions. A short history of cosmology (and geometry) shows how our perspective of the universe has changed over time.

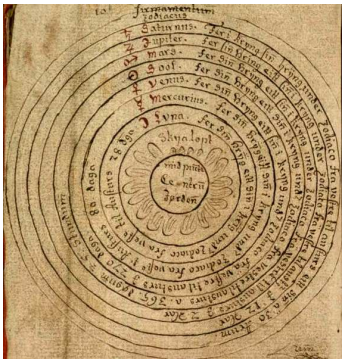

(a) An old Icelandic representation.

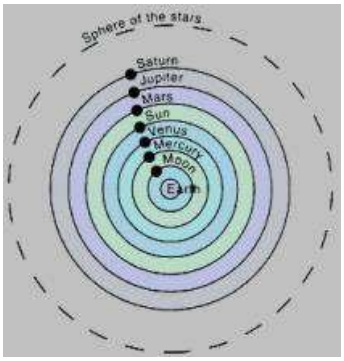

(b) A schematic representation (Poole, 1995).

Figure 1.1: The geocentric model of the universe.

1.1.1 Ancient Cosmology

In the ancient times, the knowledge about the mythical Universe was limited. The Earth was flat and the motions of the Sun, the Moon and the stars were works of the gods. The first real viable models about the universe emerged after the discovery that the Earth is (nearly) spherical. This was already known to the ancient Greeks. In the time of the Greeks many views developed, the most influential has been written down by Ptolemy around the year 150. He posed a geocentric model of the universe, the Earth is the center of the Universe (in Greek geo=Earth, centron=center). Around the Earth orbit the 7 celestial bodies, namely the Sun, the Earth and the (then 5 known) planets and the (sphere of) stars. This model stayed effective for nearly 1500 years and still has a large influence on our daily lives. The days of the week are named according to the motions of the heavenly bodies in the geocentric model. Although several people proposed that the Earth might not be fixed in space but moving, the geocentric model remained in general use to the end of the Dark Ages.

In 1514 Copernicus introduced the heliocentric model. A Heliocentric model places the Sun in the center of the universe (helios=Sun) with the planets orbiting around it. This model made it possible to predict the motion of the planets with relative ease in comparison to the geocentric model. The geocentric model had a sophisticated epicycle theory of planetary orbits which in fact remained better than the circular heliocentric model. Copernicus was not the first to describe a non geocentric view of the Universe. Philoaus (480BC-405BC) claimed a central fire, named 'estia' (hearth of the Universe) and Aristarchus (310BC-230BC) developed a heliocentric model even before Ptolemy made his geocentric model. Copernicus model was the first one that received wide acceptation.

1.1.2 Early Modern Cosmology

It must be noted that in both the geocentric and the heliocentric model, space (and time) are rigid frameworks, on which relatively the Earth or the Sun were pinpointed as the center. The Italian Galileo Galilei discovered that objects retain their speed if no force is applied to them. This was a first step to a relativistic theory of mechanics. In 1687 Isaac Newton incorporated

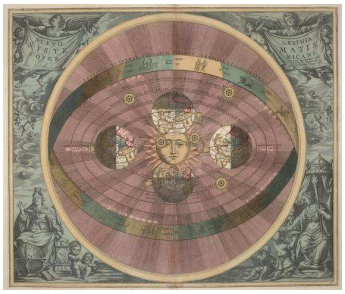

(a) An old picture of the heliocentric model, by the Dutch Cellarius (1708).

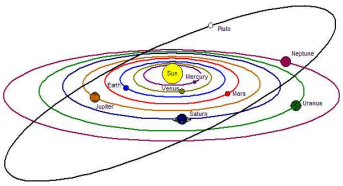

(b) A schematic image of a heliocentric model of the solar system.

Figure 1.2: The heliocentric model.

Galileis principles in his book the 'Principia' (Philosophiae Naturalis Principia Mathematica). This relativistic theory of mechanics removed the pinpointing of the Earth or the Sun as the center of the Universe. Newton's space is still a flat rigid body. In other words it represents a frame of rest in which the motion of all the elements of the universe should be measured.

This view of a universal fixed reference frame was not questioned until Ernst Mach posed in the Mach's principle that space is truly relative. This means that it is not relevant, or even impossible, to describe a position or a velocity in space, but only a position or velocity of an object with respect to another object. It suggests that there is no center of the universe. Every point in space is just as equal as any other point in space. It does raise the question about the size of the universe, in the geo- and heliocentric universes the size of space is fixed by the radius of the sphere of stars but with a truly relative space, there cannot be such a boundary. Space must be infinitely big, or so it seemed.

(a) A (very fast) car traveling 1700km/hour westward across the equator.

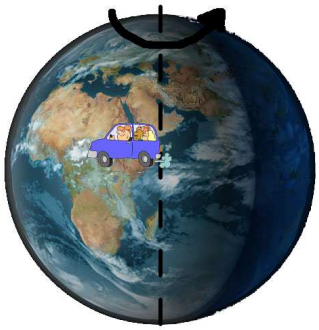

(b) The earth rotating around its axes with 1700 km/hour at the equator.

Figure 1.3: What is moving? Does the car move over the stationary surface of the Earth westwards or does the surface of the Earth move along the bottom of the car eastwards (which forces the driver to step on the gas to stay stationary)? Mach's principle says that both statements are equivalent. When something is moving, you always have to say with respect to what.

1.1.3 Modern Cosmology

In 1920 there was a discussion called the *Great Debate* between Harlow Shapley and Heber Curtis about whether the Universe consisted of just the Milky way or was composed of a number of galaxies. By the discovery of Cepheids (variable stars) in the nebulae, Edwin Hubble showed that these objects are all galaxies themselves. Hereby he proved the Universe is much larger than previously assumed.

In 1929 Hubble presented his ground breaking paper in which he shows that there are objects outside our own galaxy seem to move away from us. All spiral nebulae he observed moved away with speed proportional to their distance:

$$v = H_0 D \tag{1.1}$$

where v is the radial velocity of the nebulae, D the distance and H_0 the Hubble parameter at current time. The current value of the Hubble parameter is approximately $H_0 = 72 \pm 8 km/s/Mpc$. The Hubble parameter is often divided by 100 as $h = H/100$ so h is of order unity.

This apparent motion of the galaxies is a result of the expansion of the Universe. Space expands while the galaxies, at rest with respect to the Universe, move along our line of sight. Tracing back this apparent motion one must conclude that at a certain point in time all galaxies in the visible Universe should have been on top of each other. It has been determined that this happened about 13.7Gyr ago. The moment when this happened is called the Big Bang.

Expansion of the Universe

Perhaps the most visually appealing way to visualize the expansion of the Universe is to look at the 2 dimensional surface of a balloon. Imagine that the universe is the 2 dimensional surface of a perfectly spherical balloon, galaxies are represented by dots. If you slowly blow up the balloon, you can see that the distance between the 'galaxies' grows, with no galaxy actually moving along the balloon (as they are all fixed on the balloons surface). If there are any observers in the galaxies, they will see the other galaxies moving away from them, the more distant ones at a faster pace. They all can — incorrectly — conclude that all the other galaxies are moving away from them and that they themselves are the center of the universe, or — correctly — that their universe is expanding and that neither galaxy can claim to be the center, they are all equivalent. In this example there of course is a center of the balloon, but that point is not part of our universe, that is only the 2 dimensional surface of the balloon. In general there does not have to exist such a point. In most cases it is even meaningless to talk about it.

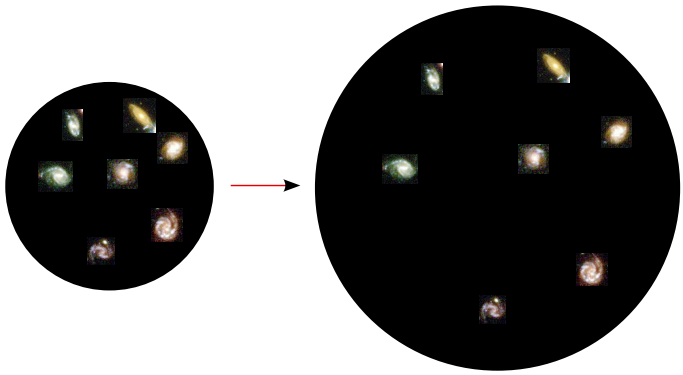

Figure 1.4: The sphere on the left represents the (2 dimensional) universe at an early time. The sphere on the right represents the universe at a later epoch. All galaxies see the distance to the other galaxies increase, at a rate proportional to their distance. Therefore observers might conclude that the galaxies are moving away from them.

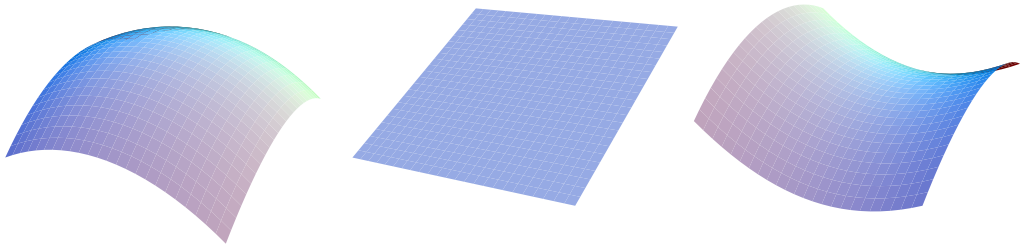

(a) Spherical (b) Flat (c) Hyperbolic

Figure 1.5: The 3 geometries.

1.2 Principles

Two important principles have emerged from the history of science to the 20th century. From the geo- and heliocentric universe we can derive the first: that we should not see ourselves as special in the universe. This is called the *Copernican principle*. From the long time it took for the Euclidean theory to be discarded the second: that we should try to put as least as possible a priori constraints on our theory.

1.2.1 Cosmological Principle

The first insight has resulted in what cosmologists call the *cosmological principle*, which is — as the name implies — one of the most important principles of cosmology. The cosmological principle says that the Universe is:

1. Homogeneous
2. Isotropic
3. Uniformly Expanding

In short, the Universe is the same everywhere (homogeneous) and looks the same in every direction (isotropic). The term 'cosmological principle' was introduced by E. Milne in 1933.

Homogeneity

Homogeneity means that the universe looks the same everywhere and has no preferred locations. While isotropy is reasonably straightforward to justify, homogeneity is harder to prove. However, there is evidence that says that there isn't any significant structure at larger then $200h^{-1}Mpc$. This means that if you smear out all matter to scales of $200h^{-1}Mpc$ the Universe will appear homogeneous.

Evidence of homogeneity of the Universe include:

1. **Redshift Surveys** The spatial distribution derived from redshift surveys like SDSS and 2dF show that there are no larger structures than $100 - 200h^{-1}Mpc$ (Yadav et al., 2005). Problems with biasing, evolution and K-corrections will limit the usability of these surveys.
2. **Galaxy Number Counts** Counting galaxies by magnitude show that the number of galaxies, for $z < 1$, scale as
$$N(m) \propto m^{0.6} \tag{1.2}$$
which is exactly what would be expected for a homogeneous universe.

3. **Projected Galaxy Clustering** The two-point correlation function of the projected galaxy distribution scales with depth of the galaxy sample as

$$\omega(\theta) \propto \frac{1}{D}\omega(\theta D). \tag{1.3}$$

The correlation function for deeper samples have a lower amplitude ($\frac{1}{D}$) and a smaller angular scale (θD) as expected.

4. **Peculiar Velocities** The velocity of the Local Group, inferred from the dipole in the CMB is approximate $620km/s$. Nearly all of this motion can be explained by the gravitational force exerted by matter within a distance $\leq 150h^{-1}Mpc$. This can be concluded from the convergence of the dipole (of galaxy light, which correlates with gravity). For a non-homogeneous universe the dipole would not converge. (Schmoldt et al., 1999)

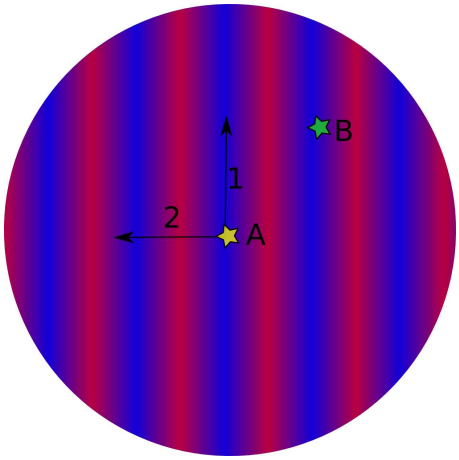

Figure 1.6: This 2 dimensional universe is homogeneous, but not isotropic. You cannot distinguish point A from point B, but direction 1 is very different from direction 2 or any directions in between.

Isotropy

Isotropy implies that the universe looks the same in all directions and there are no preferred directions. An isotropic universe which is not homogeneous is very unlikely, since that will place us in the only one place in the universe where isotropy holds. As long as there are two points where isotropy holds, the universe is homogeneous. On the very local scale the universe isn't isotropic at all, in some directions there appears to be much more matter then in others, but again when one looks further then $200h^{-1}Mpc$ the evidence for isotropy is overwhelming.

Evidence of isotropy of the Universe include:

1. **Cosmic Microwave Background** By far the most compelling evidence is the isotropy of the cosmic microwave background. The COBE data has a variation of $\frac{\Delta T}{T} = 10^{-5}$ on the scales of 10° (Wu et al., 1999; Smoot et al., 1991).

2. **Radio Sources** It is difficult to obtain distance information of radio sources, therefore they are hard to use as probes for homogeneity. However, surveys have given evidence for isotropy (Baleisis et al., 1998).

3. **X-ray Background** unresolved X-ray sources, probably AGNs, originate from objects with a very high redshift and are therefore a good probe for isotropy (Tikhomirova and Stern, 2000).

4. **Projected Galaxy Distribution** Galaxies are distributed isotropic.

5. **γ-ray Bursts** Gamma ray bursts are bright enough to see across the entire Universe and occur isotropic (Vavrek et al., 2004).

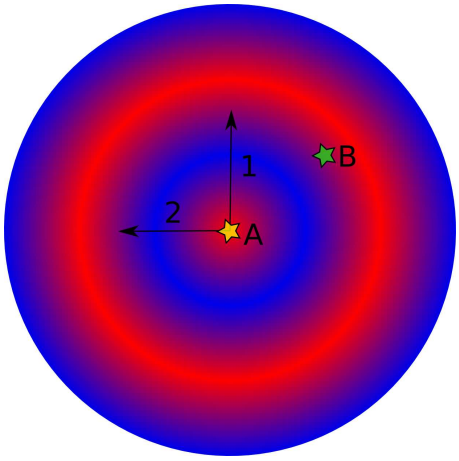

Figure 1.7: This 2 dimensional universe is homogeneous for the observer at point a (for scales about 1/20 of the picture). However it is only isotropic for that observer, for any other observer it is not isotropic. Evidently, it would be a great coincidence if we happen to be at such a point.

1.2.2 Least Constraints

The possibility of a curved space instead of the Euclidean geometry, which for so long has been dominant is an example of the rule that a priori we should put as least constraints as possible on our theory.

On the other hand, standard cosmology only teaches the possibility of trivial topologies. This is an artificial restriction, and therefore violates this principle. It is not based on physical evidence or experiment, nor the outcome of verified theories like general relativity. In this thesis we abandon this restriction and investigate the possibilities that this opens up.

However, some of the topologies we will propose for our universe will violate the classical global cosmological principle. In section 2.4.1 we will show that the classical cosmological principle is to constraining, and opt for a less restrictive version called the *local cosmological principle*.

1.3 Geometry

Geometry is the study of the local aspects of a 2 dimensional surface or 3 dimensional space. Geometry is mainly concerned with the local properties of space, in particular with its curvature. Up till now we have only considered a flat Euclidean geometry, but many more are possible.

The three main geometries we will discuss are spherical geometry, flat geometry and hyperbolic geometry, visualized in figure 1.1. These 3 geometries are the only ones that are both homogeneous and isotropic, therefore the only ones allowed by the cosmological principle.

Two important concepts in geometry, geodesics and parallelism, will be discussed before going into geometry.

1.3.1 Geodesics

A geodesic is an extension of the term *straight line* — which is only well defined in Euclidean space — to curved space. A geodesic is the locally shortest path between two points. The path length

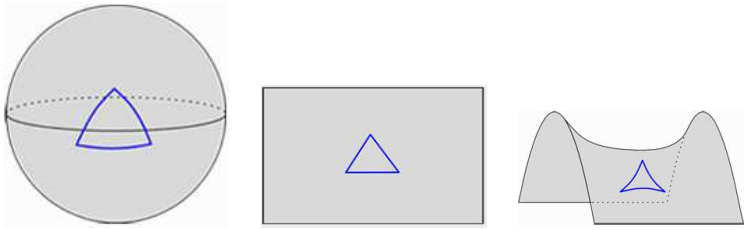

Spherical	Flat	Hyperbolic

Table 1.1: Triangles on the 3 geometries.

is a local minimum, a slight deviation of the path results in a longer path (figure 1.8). There can be more then one geodesic connecting two points, not necessary of equal length, however the true shortest distance is always a geodesic. In Euclidean space a geodesic is a regular straight line, in spherical space this is a great circle (figure 1.9).

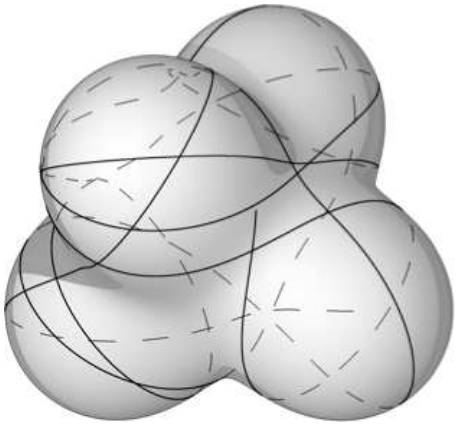

Figure 1.8: A geodesic over a very curved surface.

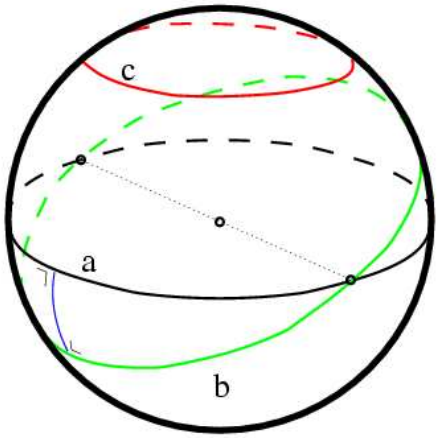

Figure 1.9: A spherical space. a and b are great circles, c is a small circle. b intersects a in two antipodal points and shares a common perpendicular. c is equidistant to a and also shares a common perpendicular with a (at every point) but is not a geodesic.

1.3.2 Parallelism

The concept of parallelism is important in geometry. The classical high school definitions of *parallel*, based upon Euclid's 5th postulate (section 1.3.5), are often ambiguous or even contradicting when applied to non-Euclidean geometry.

Given a geodesic ℓ and a point a not on that line there are 3 different kind of lines that are all identical to a parallel geodesic in Euclidean geometry (figure 1.10(a)). However, in a general geometry they are distinct. We distinguish

- *equidistant* lines: lines that are everywhere separated by the same distance (figure 1.10(b)),
- geodesics that share a common perpendicular (figure 1.10(c)) and [1]
- *parallel* geodesics: geodesics that intersect 'at infinity' (figure 1.10(d)).

Following this definition, a parallel geodesic can be constructed by taking an intersecting line through point a and move the point of intersection x along line l till the limit at infinity. There are two main reasons this definition of parallel is favorable above the other two. Firstly, we want parallel lines to be geodesics. In non-Euclidean geometries equidistant lines are usually no geodesics. Secondly, if a line m is parallel to a given line ℓ at *one point* a *on* m, *we want* m *to be parallel to* ℓ *at* every point on m. Geodesics sharing a common perpendicular in generally only do so at a specific point. The angle the parallel line m makes with the perpendicular from a to ℓ is called the *parallel angle* ϕ. In the Euclidean case the parallel angle is always $\frac{1}{2}\pi$. A geodesic is always parallel to itself.

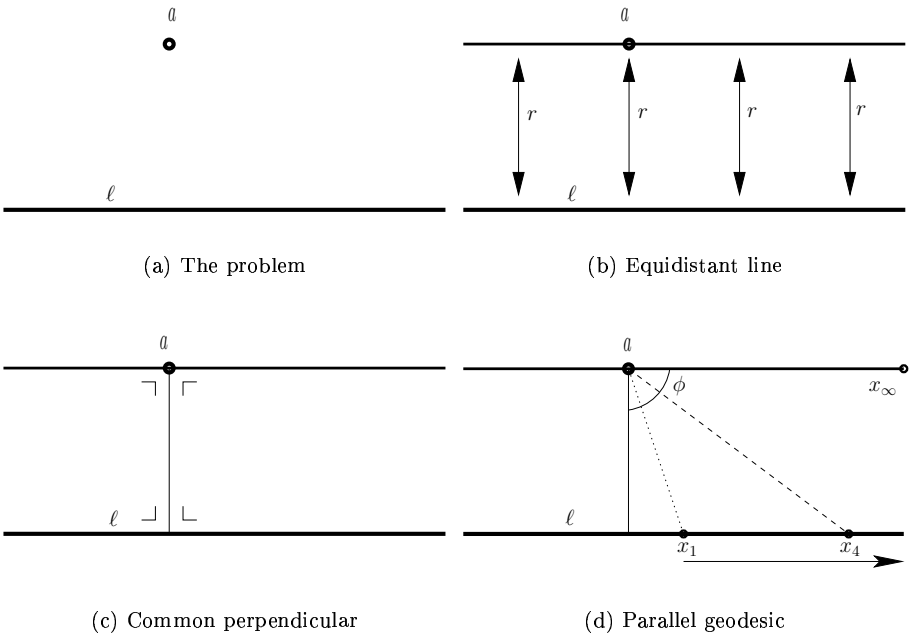

(a) The problem (b) Equidistant line

(c) Common perpendicular (d) Parallel geodesic

Figure 1.10: Parallel line creation in the Euclidean plane, 3 equivalent definitions.

Together with parallelism we consider 3 kinds of relation between two geodesics in the same plane. Two geodesics can either be

- *intersecting*: they have one or more points in common within the plane,

[1] Technically, it is enough that there exists a transversal geodesic that intersects both geodesics at the same angle. If this angle is $\frac{1}{4}\pi$ the transversal is a common perpendicular. If this angle is 0 the transversal coincides with one of the geodesics and the geodesics are parallel.

- *parallel*: they intersect 'at infinity', but nowhere within the plane or
- *ultra parallel*: they diverge in the limit of infinity

The point where parallel geodesics intersect, 'at infinity' is called an *affine point*. In general parallel lines intersect only in one direction. Parallel lines in the Euclidean plane are the exception, they intersect in the same affine point in both directions.

1.3.3 2 Dimensional Isotropic Geometries

There are infinitely many different geometries. Restricting ourselves by the cosmological principle to the geometries of homogeneous 2 dimensional spaces there are spherical geometry, flat geometry and hyperbolic geometry. Mathematically speaking, flat geometry is the limit between spherical and hyperbolic geometry and therefore should be listed between them. However since it is the most well known geometry it is listed first.

1. *Flat Geometry*
   - For a given point only one line exists parallel to a given line which does not contain that point. The flat Euclidean plane corresponds to an infinite flat surface, like a sheet of paper of infinite extent. Interestingly, also the surface of a cylinder is flat. Any surface that can be papered in a way that you only have to bend the paper, not stretch or cut it, is called flat. It may be 'bent', but it is not 'curved'.
   - The Euclidean plane is called $\mathbb{E}^2$.
2. *Spherical Geometry*
   - For a given point no geodesics exists parallel to a given line which does not contain that point.
   - The spherical plane is called $\mathbb{S}^2$.
   - Lines equidistant to a geodesic (a great circle) are small circles and are no geodesics (line c in figure 1.9).
   - A geodesic that shares a common perpendicular with another geodesic intersects that geodesic in two antipodal points (line b in figure 1.9).
3. *Hyperbolic Geometry*
   - For a given point an infinite amount of geodesics exist parallel to a given line which does not contain that point. There are two lines that meet the given line at infinity, and an infinite number that diverge, called ultra-parallel lines[2]. The hyperbolic plane is the hardest to visualize, this is because it cannot be displayed correctly in three dimensions. The hyperbolic plane is as infinite plane with a saddle point everywhere.
   - The hyperbolic plane is called $\mathbb{H}^2$.
   - A line equidistant to a geodesic is not a geodesic itself.
   - A geodesic sharing a common perpendicular is called a ultra parallel line (figure 1.12(c)).
   - The pseudo-sphere discovered by Beltrami is an object with two dimensional hyperbolic geometry, but it does not reflect its infiniteness and even has borders.

[2] Ultra parallel lines sometimes are called just parallel lines as well, by that (ambiguous) definition there are an infinite number of parallel lines. Lines that do intersect at infinity are usually called *limiting lines* or *critical parallels*.

The properties of the planes are summarized in table (1.2).

These 2 dimensional geometries have 3 dimensional equivalents and our Universe, which has 3 spatial dimensions, can posses one of these. On scales smaller than the radius of curvature most geometries look exactly like Euclidean geometry. That is why it took mankind so long to discover the Earth was not flat. Mathematicians like Gauss and Riemann showed the world that these geometries (and there are many) are just as real as the flat Euclidean geometry and can be extended to three or more dimensions.

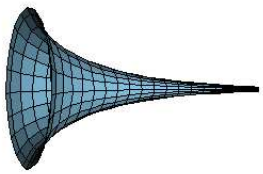

Figure 1.11: The pseudo sphere has hyperbolic geometry. It can be extended indefinitely to the right, but cannot be continued on the left. On the left it has a discrete boundary where its tangent is perpendicular to its axis of symmetry.

	Spherical	Euclidean / Flat	Hyperbolic plane
Symbol	$\mathbb{S}^2$	$\mathbb{E}^2$	$\mathbb{H}^2$
Intersecting Lines	∞	∞	∞
Parallel Lines	none	1	2
Ultra Parallel Lines	none	none	∞
Size	finite	infinite	infinite
Sum of angles	$< \pi$	$= \pi$	$> \pi$

Table 1.2: Properties of the 3 geometries.

1.3.4 Poincaré and Klein Disks

Unlike spherical geometry, hyperbolic geometry cannot be embedded isometrically in 3 dimensional Euclidean space, therefore non isometric representations are developed. Two of the more insightful representations of the hyperbolic plane are the Poincaré and Klein disks. Both are unit disks which represent the entire infinite hyperbolic plane in such a way that points on the boundary of the disk represent points infinitely far away from the origin but both with their own distance transformation. In figure (1.12) the Poincaré and Klein model of the hyperbolic plane are shown.

Poincaré Disk

If r' is the radial distance on the unit Poincaré disk then the hyperbolic distance is

$$r = \operatorname{arccosh}\left(1 + 2\frac{r'^2}{1 - r'^2}\right). \tag{1.4}$$

In the Poincaré model of the hyperbolic disk

- angles are preserved,
- geodesics are circle arcs perpendicular to the boundary of the disk,
- intersecting geodesics intersect in a point on the disk,
- parallel geodesics are tangent at an affine point on the boundary,

- ultra parallel geodesics do not intersect,
- circles are circles that do not cross the boundary and
- equidistant lines are circle arcs that intersect the boundary at any angle, they are equidistant to the geodesic passing through those intersections.

Klein Disk

If r' is the radial distance on the unit Klein disk then the hyperbolic distance is

$$r = \operatorname{arccosh}\left(\frac{1}{\sqrt{1-r'^2}}\right). \tag{1.5}$$

In the Klein model of the hyperbolic disk

- geodesics are straight lines,
- intersecting geodesics intersect in a point on the disk,
- parallel geodesics are intersect at an affine point on the boundary and
- ultra parallel geodesics intersect at an ultra affine point outside the disk.

Poincaré and Klein Combined

A pair of ultra parallel lines has a third geodesic as common perpendicular. The center of this perpendicular in the Poincaré disk is the intersection point of the two ultra parallel lines in the Klein disc. Any geodesic that intersect two other geodesics in the same ultra affine point also shares the perpendicular and vice-versa.

If u is the radial distance of a point on the Poincaré disk, then

$$s = \frac{2u}{1+u^2} \tag{1.6}$$

is the radial distance on the Klein disk. Conversely

$$u = \frac{s}{1+\sqrt{1-s^2}}. \tag{1.7}$$

1.3.5 History of Curved Space

Euclid was a Greek mathematician who wrote "The Elements" in the 3th century B.C in which he formulated the rules for flat geometry. The typical situation is that of an infinitely flat 2 dimensional or 3 dimensional space.

It is considered to be one of the major works in science and most successful textbooks ever written. It was one of the first books to go to print and it is the second most reprinted book next to the Bible (over a thousand editions). It is said to be the most widely read and studied book after the Bible. Up into the 20th century it was required for all students and considered a book that all educated people had read.

The Elements are based on 5 postulates.

1. A straight line segment can be drawn by joining any two points.
2. A straight line segment can be extended indefinitely to a straight line.
3. Given a straight line segment, a circle can be drawn using the segment as radius and one endpoint as center.

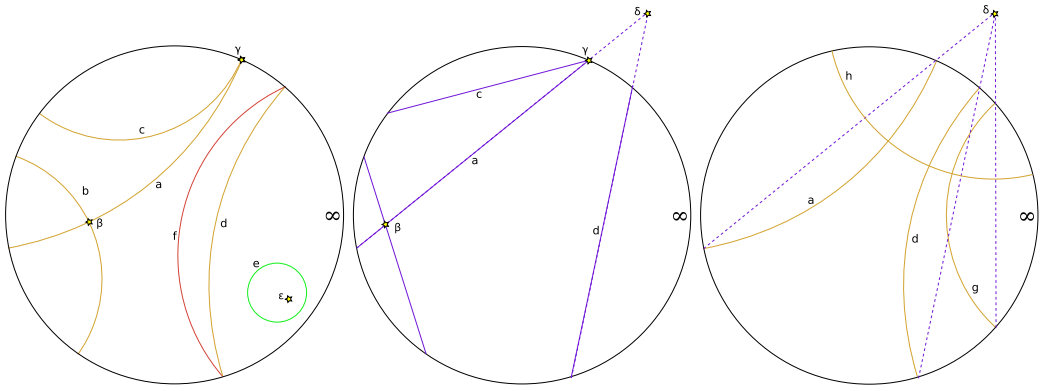

(a) Poincaré disk (b) Klein disk (c) Combined

Figure 1.12: The left disk is the *Poincaré Disk*, the middle disk the *Klein Disk*, the right a combination of both. **Poincaré Disk** Geodesic are brown (a,b,c,d), circles are green (e), equidistant lines are red (f). β and ϵ are regular points, γ is an affine point. Geodesic a is intersecting with geodesic b at point β which lies in the disc. Geodesic a is parallel to geodesic c, it touches c at affine point γ. Geodesic a and d are ultra parallel, they never intersect in or on the boundary of the disc. Equidistant line f is equidistant to geodesic d. **Klein Disk** Geodesics are purple (a,b,c,d). β is a regular point, γ an affine point and δ an ultra affine point. Geodesic a intersects with d in δ. **Combined** Geodesic h is the common perpendicular of a and d which intersect in affine point δ. Since geodesic g also goes through δ, h is also perpendicular to g.

4. All right angles are congruent.

5. Through any given point there is only one line parallel to a given line not through that point.

The famous 5th one is called the parallel postulate and is the basis for Euclidean 'flat' geometry. The definition of parallel is not unambiguous, but this form of the postulate is the most intuitive. As stated we will call two lines parallel if they lie in the same plane but do intersect only at infinity.

For two millennia this was the only geometry considered possible at all, so it was thought the Universe possessed it as well. There were ample attempts to prove the 5th postulate on the basis of the other 4 mostly by reductio ad absurdum, all of which failed. In 1829, the Russian Nikolai Ivanovich Lobachevsky published (in Russian) the first works on hyperbolic geometry (thus called Lobachevsky geometry). In 1832, János Bolyai included a description of hyperbolic geometry in an appendix in one of his father's books. Before publishing, Bolyai contacted Carl Friedrich Gauss, who claimed to have studied the subject more then 30 years earlier. Gauss never published his work because he thought it too be to controversial for the mathematical society at that time.

The study of smooth geometries was generalized by Riemann in 1854 into differential or Riemannian geometry. Although known for a long time in astronomy and navigation, Riemann is often credited with the discovery of elliptic geometry, a superset of spherical geometry. Finally, in 1868 Eugenio Beltrami proved that it is indeed impossible to proof Euclid's 5th postulate from the first 4 and that both Euclidean geometry and geometries that included a negation of Euclid's 5th postulate (i.e. spherical and hyperbolic geometry) were consistent.

1.4 Modern Cosmology

In the beginning of the 20th century it was Einstein who took the revolutionary step to prove that time and space each form an integral part of a 4-dimensional spacetime. No longer space and time

represented rigid external frames to a physical system. Up to Einstein's 1905 special relativity theory, time and space had been assumed to be strictly separated. He proved otherwise.

1.4.1 General Relativity

In 1905 Einstein wrote an article called 'Theory of the Transformation of Co-ordinates and Times from a Stationary System to another System in Uniform Motion of Translation Relatively to the Former' which describes *special relativity*. Special relativity tells us that time as well as space is relative — events simultaneous for one person might not be simultaneous for another — and that we should consider space and time interwoven, a 4 dimensional entity/fabric called space-time. In between 1905 and 1915 Einstein developed his General theory of Relativity, the theory dealing with accelerating bodies and thus implicitly including gravity.

Einstein equation

General relativity says that matter curves the structure of space and space influences the motion of mass. It is all encapsulated in one single central equation, the Einstein field equation (using Einstein notation for the tensors and geometric units, which put the speed of light c and the gravitational constant G at unity)

$$G_{\mu\nu} + \Lambda g_{\mu\nu} = 8\pi T_{\mu\nu}. \tag{1.8}$$

In this equation $G_{\mu\nu}$ is called the *Einstein tensor* and $g_{\mu\nu}$ the *metric*, which together encompasses the (localized) curvature of the Universe. $T_{\mu\nu}$ is called the *stress-energy tensor* which contains the matter/energy content of the Universe and Λ is the *cosmological constant*. The cosmological constant originates as a free integration parameter when the differential equations leading to equation 1.8 are solved. The cosmological constant can be moved algebraically to the other side of the equation where it can be seen as the vacuum contribution to the stress-energy tensor or as dark energy. Einstein used the cosmological constant to ensure a static Universe, a universe that does not expand.

Cosmological Consequences

The validity of General relativity has been demonstrated by many experiments. If matter curves the universe locally, it also curves it globally. One of the key questions in modern cosmology is whether the Universe is curved or flat. Locally this is difficult to determine, as it occurs to be nearly flat. Cosmic microwave background experiments like Boomerang and WMAP have shown convincingly the Universe to be nearly flat (Spergel et al., 2006).

Cosmological Constant

Traditionally, the cosmological constant, together with the (rest of the) energy momentum tensor, determines the curvature of the Universe. However, this can be turned the other way around. The Universe is embedded with a certain metric which manifests itself in a specific value for the cosmological constant: This is especially the case with non-trivial topological shapes, since they often dictate a specific geometry. The lack or excess of matter to account for the corresponding curvature will then be compensated by the cosmological constant which automatically will acquire the necessary strength.

In short, there are two possibilities:

- The cosmological constant (partly) defines the geometry of space, which in turn limits the possible topologies
- the topology of space determines the geometry, which then set the cosmological constant.

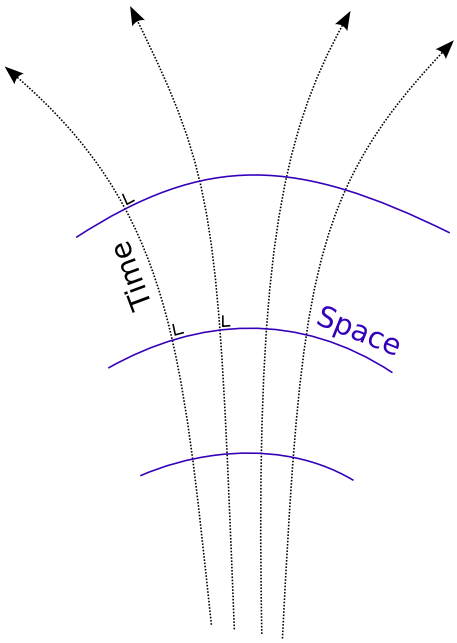

Figure 1.13: By the Weyl postulate it is always possible to define a surface in the space time manifold of 'equal time'. This is a surface that is everywhere perpendicular to the time direction.

A possible scenario for the latter is the following. The Universe began as a small, closed, quantum fluctuation with yet undetermined shape and geometry. When it expanded it collapsed into a specific topology, with a non isotropic and homogeneous metric. If the Universe is small enough to be entirely casually connected it will not only homogenize all energy, it will also become homogeneous in curvature since the energy of such a space is lower then a space with a non homogeneous metric.

Which of these two options is the case is beyond this thesis, but it is worthwhile to keep the latter option in mind. In both cases, measuring the exact value of the cosmological constant will be a strong indicator of possible topologies.

1.4.2 Cosmic Time: Weyl Postulate

The Weyl postulate states that, on a universal scale, the time direction space-time is everywhere perpendicular to its spacial dimensions. In other words, for all positions on the time dimension, measured as *universal time*, there exist a perpendicular 3 dimensional slice of our Universe which is its spatial section (figure 1.13). This hypothesis is not strictly necessary for all cosmological models, but most include it. In this thesis we accept the Weyl postulate. We will not consider the motion of observers and for most subjects ignore time altogether.

1.4.3 Robertson-Walker Metric

The cosmological principle applied to geometry gives rise to only the three different geometries of section (1.3), spherical, flat and hyperbolic space. They are described by the Robertson-Walker metric:

$$ds^2 = dt^2 - d\sigma^2 \tag{1.9}$$

$$d\sigma^2 = dr^2 + R^2 \sin\left(\frac{r}{R}\right)^2 d\Phi^2 \tag{1.10}$$

$$d\Phi^2 = d\theta^2 + \sin^2 d\phi^2 \tag{1.11}$$

where x, θ and ϕ are spherical coordinates and R is the radius of the Universe. R is positive for spherical space, infinite for flat space and purely imaginary for hyperbolic space. This is different from the classical cosmological schools which often teach that R is negative for hyperbolic spaces. This is mathematically incorrect, the hyperboloid is a sphere with imaginary radius. Also, traditionally cosmologists use different definitions of the radial coordinate depending on curvature. This discrepancy is unnecessary and confusing, and should be avoided. See appendix (A) for details.

1.4.4 Evolution of the Universe

Allowing only the Robertson-Walker metric, the Einstein field equations can be simplified. In a simply connected homogeneous isotropic universe the structure of space is given by only one parameter, its curvature. The evolution of the Universe is determined by a homogeneous energy/momentum distribution. The evolution is described by the Friedmann equations

$$H^2 = \left(\frac{\dot{a}}{a}\right) = \frac{8}{3}\pi\rho + \frac{\Lambda}{3} - \frac{k}{a^2} \tag{1.12}$$

$$\frac{\ddot{a}}{a} = -\frac{4}{3}\pi\left(\rho + 3p\right) + \frac{\Lambda}{3} \tag{1.13}$$

Geometrized units are used again. a is the dimensionless scale factor of the universe, which is usually normalized as unity at present $R = aR_0$. ρ is the energy/momentum density, p the pressure and Λ the cosmological constant. k relates to the curvature of the universe as

$$k = \begin{cases} 1 & \text{spherical} \\ 0 & \text{flat} \\ -1 & \text{hyperbolic} \end{cases} \tag{1.14}$$

The cosmological constant can be seen as a pure curvature term, or can be seen as a part of the content of the Universe and integrated into ρ. The pressure p relates to the density ρ through the equation of state $p = p(\rho) = \omega\rho$. The contents of the Universe can than be decomposed into three contributions, each with a different equation of state. The Universe consists of

- matter, which can be decomposed into baryonic matter and dark matter with $0 < \omega \ll 1$,
- radiation, with $\omega = \frac{1}{3}$ and
- dark energy, with $\omega < -\frac{1}{3}$

The cosmological constant corresponds to a dark energy with $\omega = -1$. At this moment the Universe contains approximately 4% baryons, 23% dark matter, 73% dark energy and 5×10^{-3}% radiation.

Integrating Λ into ρ it is possible to define a critical density ρ_c. If the density of the Universe is larger then ρ_c the Universe will be spherical, if it is smaller it will be hyperbolic and if $\rho = \rho_c$ the Universe will be flat. Usually this is represented with the dimensionless parameter

$$\Omega = \frac{\rho}{\rho_c} = \Omega_m + \Omega_r + \Omega_\Lambda \tag{1.15}$$

$$= \frac{k}{R^2H^2} + 1 \tag{1.16}$$

where Ω is split up into relatively its matter, radiation and dark energy component. Thus

$$k = R_0^2 H_0^2 \left(\Omega_0 - 1\right). \tag{1.17}$$

The evolution of the Universe is determined by these three parameters of Ω. There are three possibilities:

1. The Universe reaches a maximum size and collapses in the Big Crunch,

shape	k	ρ	Ω
spherical	1	$> \rho_c$	> 1
flat	0	$= \rho_c$	$= 1$
hyperbolic	-1	$< \rho_c$	< 1

2. the Universe expands forever since the Big Bang or

3. there was no Big Bang, in the past the Universe shrunk to a minimum size and is now expanding again.

The limit between the 2nd and 3th option is called a *loitering* Universe, which does not expand but is unstable. Einstein proposed this in 1917 before Hubble showed the Universe did expand. Figure 1.4.4 displays the evolution for five different Universes given in table 1.3.

Name	Ω	Ω_m	Ω_m	Ω_m
Concordance	1.00	0.27	4.6e-5	0.73
Loitering	2.01	0.30	0	1.713
Big Bounce	2.1	0.30	0	1.8
Big Crunch	2.0	2.0	0	0.0
Hyperbolic	0.3	0.3	0	0.0

Table 1.3: 5 different models for the contents of the Universe. The corresponding evolution of the scale factor is given in figure 1.4.4.

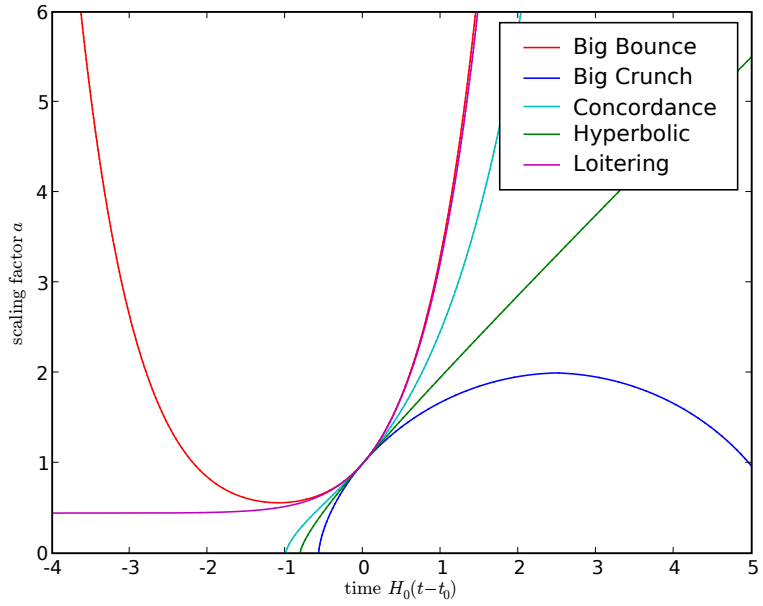

Figure 1.14: 5 different models for the expansion of the Universe. The corresponding parameters are given in table 1.3. Courtesy of Johan Hidding.

1.5 Cosmic Microwave Background

Undoubtedly the main source of information of our Universe is the Cosmic Microwave Background radiation (CMB). We receive the CMB radiation from the surface of last scattering (SLS), the region of space we observe at the time the Universe was 379.000 years old. It is nearly perfectly isotropic black body radiation at a temperature of 2.725K with fluctuations of 1 in 10^5 (with the exception of the dipole and foreground contamination).

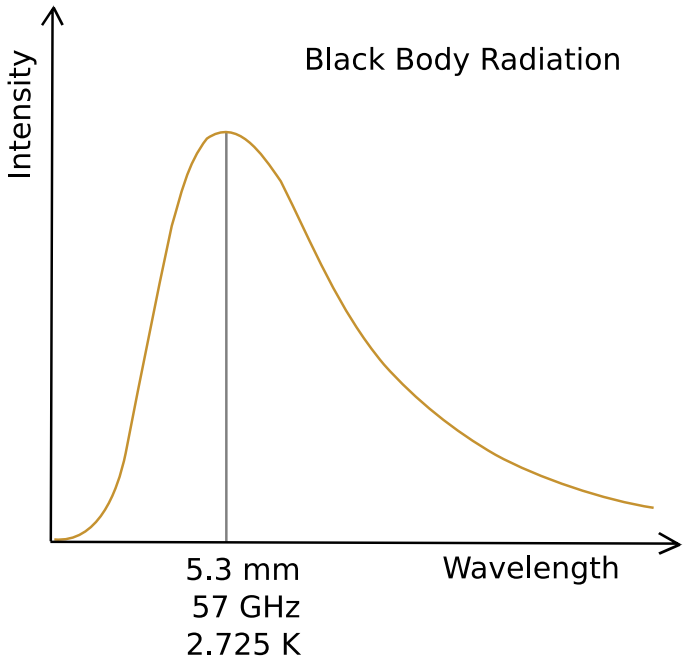

Figure 1.15: The black body spectrum of the CMB. The deviations are smaller then the width of the line.

1.5.1 Discovery and Observing of the CMB

The radiation was first predicted by Alpher et al. (1948), with a temperature of $10K$. The CMB was discovered by Penzias and Wilson in 1964, even though there had been, at hindsight, earlier detections. Their discovery was purely serendipitous. They tried to detect radio waves bouncing off balloon satellites but their measurements were disturbed by noise of which they could not find the source. The signal seemed to come from all directions. Robert Dicke and his group (Dicke, Peebles, Roll and Wilkinson) as well as Zel'dovich had deduced that if the Universe started with a hot dense phase, it would be possible to observe radiation from this epoch. Dicke predicted a signal of 20-40K and immediately told Penzias and Wilson he was looking for it. He had even build an antenna to detect just this radiation.

Over time the CMB has been measured very accurately by many different experiments on different scales and sensitivities. The COBE satellite (1989) has made the first full sky maps of the CMB, at a resolution of 7°. Several airborne experiments like BOOMERanG (2003, Antarctica) and MAXIMA (1999) have measured a smaller patch of the sky but up to a resolution of $10'$ and a sensitivity of $20\mu K$. The WMAP satellite (2001) has made detailed measurements of the full sky CMB down to degree scales. In 2007 the PLANCK satellite is planned for launch which will measure the full sky to even lower scales.

1.5.2 Angular Power Spectrum and Spherical Harmonics

The CMB is very isotropic, the deviation around the mean of 2.725 K is less then 1 in 100.000. The small perturbations are scale dependent, on different scales the perturbations have a different magnitude. The measure of this distribution is the angular power spectrum.

The sky distribution of the temperature fluctuations can be decomposed into spherical harmonics:

$$\frac{\Delta T\left(\Omega\right)}{T} = \sum_{\ell=0}^{\infty} \sum_{m=-\ell}^{\ell} a_{\ell m} Y_{\ell}^{m}\left(\Omega\right) \tag{1.18}$$

Spherical harmonics can best be seen as standing waves on a spherical surface.

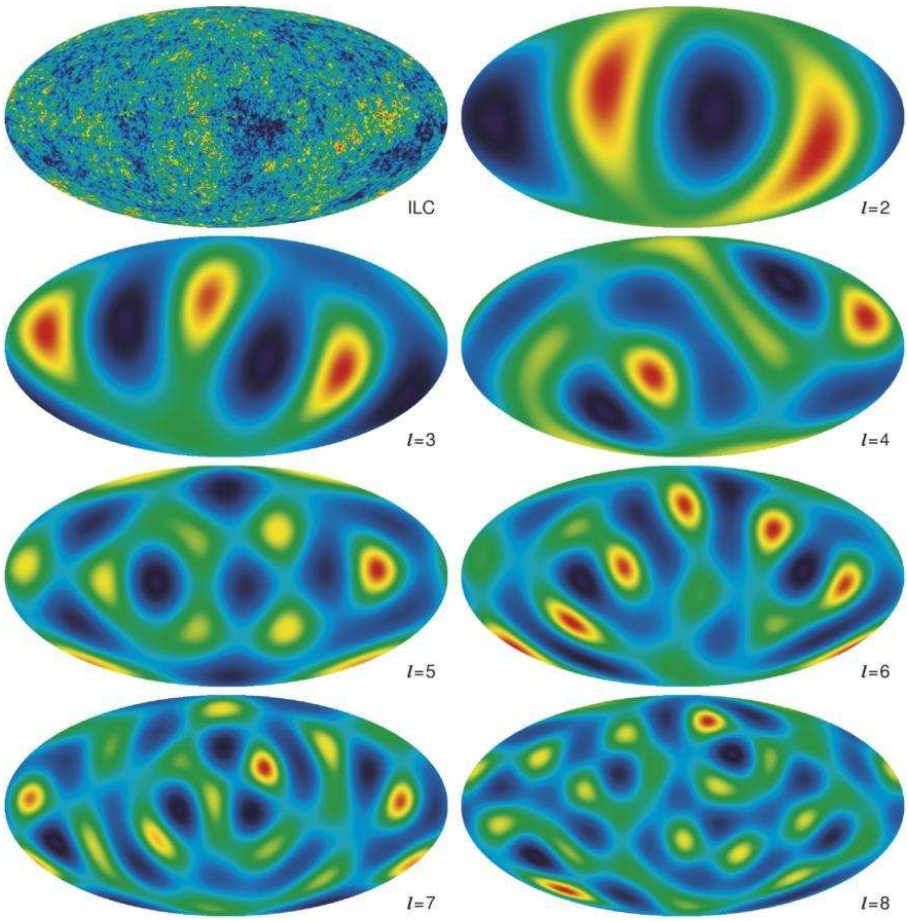

Figure 1.16: The cosmic microwave background as measured by WMAP, with its decomposition in spherical harmonics. The $\ell = 0$ monopole and $\ell = 1$ dipole are not shown (Verde, 2006).

With a general Gaussian field, the $a_{\ell m}$ of equation 1.18 are completely independent. In an isotropic real field, they are chosen from a Gaussian distribution based on ℓ. Because the density field has to be real the $a_{\ell m}$ also have to fulfill the reality equation

$$a_{\ell m} = (-1)^{\ell} a_{\ell -m}^{*}. \tag{1.19}$$

For a Gaussian density field the $a_{\ell m}$ for fixed ℓ are further uncorrelated and all information about

the CMB is contained in the power spectrum (figure 1.17)

$$C_\ell = \frac{1}{2\ell+1} \sum_{m=-\ell}^{\ell} a_{\ell m} a^*_{\ell m}. \tag{1.20}$$

Standard cosmology predicts for low ℓ a flat Harrison-Zel'dovich power spectrum as

$$P_\Phi(k) \propto k^{-3} \tag{1.21}$$

$$C_\ell \propto \frac{1}{\ell(\ell+1)}. \tag{1.22}$$

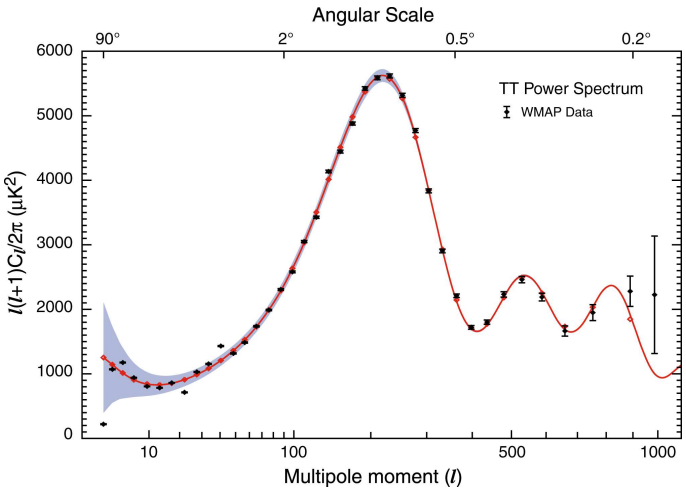

Figure 1.17: The power spectrum of the cosmic microwave background (WMAP Science Team, 2006). The cold dark matter model (solid line) matches the experimental data (diamonds) very well. The acoustic peaks are clearly visible.

1.5.3 Origin of the CMB

The structure of the CMB can be understood by examining its origin. The exact times and sizes of events differ between the various cosmological models. Without going into model specific details we describe in short the important events that led to the CMB.

Big Bang

The Universe came into existence as a singularity called the *Big Bang*. Since the Universe includes all time and space, there is no such thing as 'before the Big Bang'. The theory of the big bang was first developed by Lemaître in 1927. The term was coined sarcastically by Hoyle to parody Lemaître's theory in favor of his own *steady state theory* which proclaims an infinite (in time) Universe.

The Universe was full of energy, which — due to the extreme density and temperature — was not yet condensed into matter. This energy density did not have to be homogeneous at creation. In the short while before inflation started the Universe had time to relax within scale lengths smaller then the horizon radius. This made the Universe within those scales very homogeneous and isotropic.

Inflation

Shortly after the Big Bang, approximating between $t = 10^{-36}s$ and $t = 10^{-34}s$, the Universe went in an exponential expansion called *inflation*. During inflation the quantum fluctuations in the Universe expanded 10^{60} to 10^{100} times. Due to the expansion being exponential the horizon shrunk with respect to the scaling factor of the Universe. While these fluctuations, after inflation on superhorizon scales, enter the horizon they produce the scalefree Harrison-Zel'dovich spectrum.

At the end stage of this phase the latent heat of inflation is converted into radiation, baryons, dark matter and anti-matter. Due to CP-violation[3] slightly more matter was formed than anti-matter. The following annihilation of the anti-matter created most photons of the CMB.

Radiation Dominated Era

After inflation the dynamics of the Universe was dominated by radiation. The Universe expanded polynomial as

$$a \propto t^{\frac{1}{2}}. \tag{1.23}$$

The energy of radiation is given by $E = h\nu = h\frac{c}{\lambda}$. The wavelength λ of the radiation redshifts with expansion, $\lambda \propto a^{-1}$. Therefore the energy density of the radiation drops as $\rho_r \propto a^{-3}a^{-1} = a^{-4}$. The energy of matter, which moves non-relativistic, is given by its rest mass $E = mc^2$ which is not dependent on expansion. Therefore the energy density of matter drops of as $\rho_m \propto a^{-3}$.

Because radiation density drops faster than the matter density, the matter density becomes higher than the radiation density at a certain point in time. This is called radiation-matter equality, and happened at $z = 3570$, $T = 9730K$, $t = 0.047Myr = 1.4 \times 10^{12}s$.

Matter Dominated Era

In the matter dominated era, the Universe expanded faster as

$$a \propto t^{\frac{2}{3}}. \tag{1.24}$$

Since the dark matter is much more abundant then the baryons, the gravitational potential is dominated by the dark matter. For the development of the CMB the two relevant components of the Universe are

- the (cold) dark matter, responsible for the major share of gravity and
- the photon-baryon gas, responsible for pressure.

The photons are very energetic are coupled to the less abundant electrons, they are in thermal equilibrium. The electrons in turn are coupled to the protons and other baryons. Therefore they act as a single gas. This has two effects:

- Because the mean free path of a photon is short the Universe is opaque and
- protons (and helium nuclei) cannot bind with the electrons: any atom formed will be immediately ionized by the photons.

The dark matter interacts with the photon-baryon gas only by means of the weak interaction and furthermore by gravity. Therefore it will not be not be hindered by the photon-baryon gas and collapse and enhance features in the potential. However, when the photon-baryon gas falls into a gravitational well its pressure increases. When the pressure is high enough, it becomes stronger than the gravitational pull and the gas starts to expand again. This expansion lasts until the pressure is low enough for the gravity to take over again and make the region contract again, and so on. These equilibria are called *acoustic waves* because of their similarity to standing waves in musical instruments.

[3] CP-violation is the violation of tho product of the symmetries Charge conjugation and Parity. It was discovered in 1964 in the decays of neutral kaon by Cronin and Fitchs.

Recombination

Due to the expansion of the Universe the photons redshift to lower energies. When the energy of a photon becomes lower then the ionization energy of a hydrogen atom ($13.6eV$), the photon can no longer ionize hydrogen atoms. Since less and less photons are able to do so in the course of time, more and more hydrogen nuclei combine with electrons, this is called *recombination* (although the protons and electrons have never been combined before). The time of recombination is usually defined as the moment when only half of the hydrogen atoms are still ionized, at $t_{rec} = 324000yr = 1.0 \times 10^{13}s$ and redshift $z = 1370$.

Since the baryonic matter in the Universe is $1/4$ helium this should be taken into account. Helium has lower ionisation energy, so the time of (full) recombination is later than in a universe with only hydrogen. Also, because the number of photons greatly outnumber the number of electrons – 2 billion photons for each baryon – and because the thermal black body distribution of the energies of the photons has an exponential tail towards the high energies, the average photon energy at recombination is much less than $13.6eV$. The effective average photon energy was $0.87eV$, with a temperature of $T = 3740K$.

Last Scattering and Photon Decoupling

As the Universe expands, the mean free path length of the photons increase and the amount of photon-electron interactions reduce until the photons and the baryons are not in thermal equilibrium anymore and cannot be considered a single gas, this is called *photon decoupling*. The moment of photon decoupling is the moment when the mean free path length λ is longer then the Hubble distance c/H. After photon decoupling the Universe is transparent.

Once electrons have combined with protons to hydrogen atoms, Thomson scattering ceases to be effective and there comes a moment when a photon scatters for the last time. The photons can move freely and the photons reaching us just now form the CMB. The places where these photons originate from form a surface, the spherical boundary of our visible Universe called the *surface of last scattering* (SLS). Since not every last scattering of a photon happens at the exact same time this is more like a last scattering region than a surface.

Since after decoupling the probability of a photon scattering of an electron drops very rapidly, the time of last scattering and the time of recombination are roughly the same at $t = 379000yr = 1.2 \times 10^{13}s$ and redshift $z = 1100$. As the Universe expands, the electromagnetic waves that travel through it expand as well. The wavelength of the radiation at last scattering is about $5\mu m$. Due to the expansion it is stretched to $5mm$, which corresponds to a gas with a temperature of 2.7K. This is why it is called cosmic *microwave* background.

Structure Formation

After decoupling the acoustic oscillations of the now only baryon gas stops and its features freeze. In the subsequent history of the Universe these density excesses will grow. As the horizon expands larger fluctuations enter the horizon and join this growth. Eventually stars, galaxies and ultimately galaxy clusters and superclusters will be formed.

1.5.4 Sachs-Wolfe Effect

CMB photons originating from regions with a minimum in the gravitational potential (a 'potential well') have to climb out of the minimum. This causes them to loose energy due to gravitational redshift and time dilation. Photons from a region in a potential maximum (a 'potential hill') fall into a potential well, gaining energy, thus blueshift. This is the main contribution to the visual fluctuations in the CMB. The energy difference is

$$\frac{\Delta T}{T} = \frac{1}{3}\frac{\Delta \Phi}{c^2}. \tag{1.25}$$

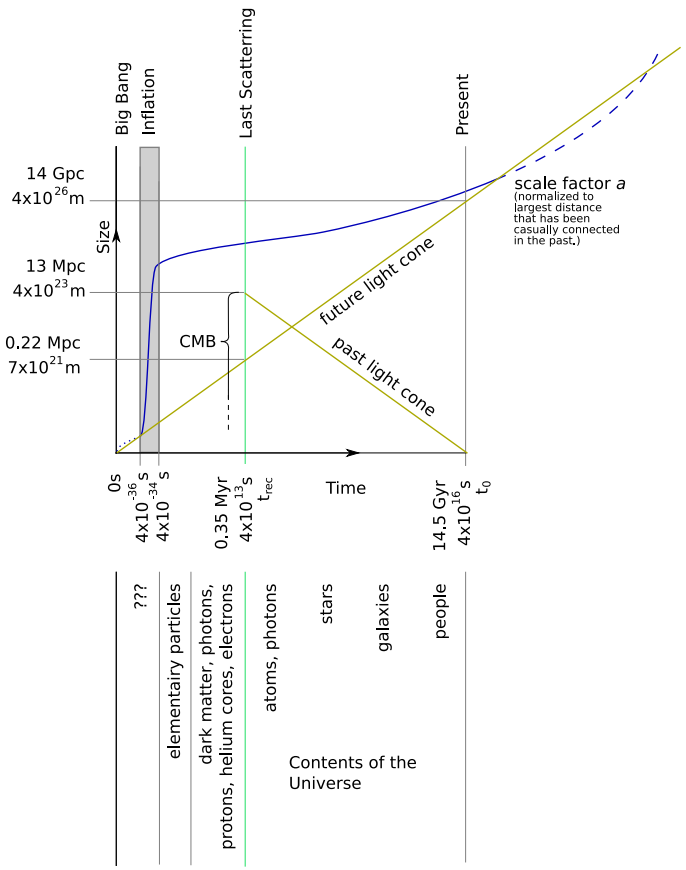

Figure 1.18: Schematic history of the Universe. The future light cone is the light cone for an position at $t = 0$, objects within it are casually connected at that time. The past light cone is our light cone for $t = t_0$, all events within it that can have influenced us. The blue solid line represents the maximum radius that has been casually connected in the past, at the moment inflation began. It is proportional to the scale factor a. The dotted and solid blue lines are a continuation of the solid line in the past and future. Our past lightcone is larger than the future lightcone of $t = 0$ at the time of last scattering. Therefore not the entire CMB could have been casually connected at $t = t_{rec}$. However, since the entire CMB falls within the blue line, it has been casually connected in the past, before inflation.

With a flat Harrison-Zel'dovich the Sachs-Wolfe effect results in a horizontal power spectrum at large angular scales.

Integrated Sachs-Wolfe Effect

During their travel from the surface of last scattering to Earth the photons pass a large number of potential wells, the accumulated effect of these wells is called the *integrated Sachs-Wolfe effect* (ISW effect). In general these contributions even out.

In a Universe with a large ρ_Λ the fluctuations in the gravitational potential get suppressed by the expansion of the Universe due to dark energy. This causes the so-called late ISW effect. For small scale fluctuations this evens out because the photon travels through many potential hills and wells. For large scale fluctuations there are only a few hills and wells so this does not happen. This results in the slight declining slope of the power spectrum at $l < 10$. Measuring the exact effect of the late ISW effect can provide constraints on the dark energy equation of state and its

time variation (Cooray et al., 2004).

1.5.5 Isotropy and low ℓ fluctuations

Before the theory of inflation was introduced, the isotropy of the CMB posed a worrisome fine-tuning problem. The horizon, i.e. the radius within which objects are casually connected, was smaller in the past. A measure for the horizon size is the Hubble length

$$r_H = \frac{c}{H_t}. \tag{1.26}$$

In a matter dominated Universe we can use

$$\frac{H^2}{H_0^2} = \frac{\Omega_{m,0}}{a^3} \tag{1.27}$$

to estimate the Hubble parameter (with $\Omega_{m,0} = 0.3$) as

$$H(z) = 1.24 \times 10^{-18} s^{-1} (1+z)^{\frac{3}{2}}. \tag{1.28}$$

This gives a horizon size at last scattering as $r_{H_{ls}} = 0.22 Mpc$. With the use of the *angular-diameter distance* d_A it is possible to determine the angular size of the horizon at t_{sls}

$$\delta\theta = \frac{l}{d_A} \tag{1.29}$$

$$d_A = \frac{d_{hor}(t_0)}{z} = \frac{14000 Mpc}{1100} = 13 Mpc \tag{1.30}$$

$$\delta\theta = \frac{0.22 Mpc}{13 Mpc} \approx 1^\circ \tag{1.31}$$

where $d_{hor}(t_0)$ is the horizon diameter at current time. So only 1 degree of the CMB was casually connected at the time of last scattering. The fact that the CMB is isotropic anyway can be explained with inflation in the sense that before inflation, the entire CMB *was* casually connected (figure 1.18).

The horizon size at $t = t_{sls}$ of 1 degree is the dividing line between subhorizon acoustic fluctuations and superhorizon fluctuations marked by Sachs-Wolfe only. Because the Universe was only casually connected within 1 degree , density fluctuations beyond that scale could not have exchanged information (photons or matter). Therefore they could not have evolved and still are what they were at the end of inflation, i.e. a slight downward slope due to the late ISW effect.

Cosmic Variance

In figure (1.17) the theoretical model allows a large deviation (purple) from average (red), this is due to *cosmic variance*. The densities fluctuations follow a Gaussian, i.e. random, distribution. On small scale (high ℓ) there are many realisations of these fluctuations, evening out any deviation from the mean. For large scale fluctuations there are only a few realisations, therefore they can fluctuate more beyond the mean. Note that most observational dots fit within the allowed variance level, but the quadrupole does not.

1.5.6 Anisotropy and high ℓ fluctuations

As the horizon grew, larger and large fluctuations became casually connected. These fluctuations started oscillating as acoustic waves, with an oscillation speed proportional to their size. After decoupling, the photon pressure drops and all oscillations stop. Oscillations that just reached a phase of maximum amplitude at the time of decoupling have over and under dense regions and show as peaks in the power spectrum, called *acoustic peaks*.

The oscillation giving rise to thefirst peak is at maximum compression at its potential minima. The second peak is caused by a fluctuation at maximum rarefaction at the potential minima, thus at maximum compression at the potential maxima, and so on for all peaks. If the oscillation would not be driven by gravity both phases would be equivalent. However, gravity enhances the effects of odd numbered peaks and reduces the effects of even numbered peaks. Therefore the second peak is significantly lower than the first peak.

At higher ℓ the strength of the peaks quickly diminishes because the perturbations are washed out due to random scatter of the photons. When the average path length a photon travels in the gas becomes of the same order as the size of the perturbation, the perturbation gets washed away by the photons. This is called Silk damping.

1.5.7 Non-Trivial Topologies

Although the structure of the CMB is very well understood, there are two problems with the CMB that prompt us for the investigation of non-trivial topologies for the Universe.

Low Quadrupole

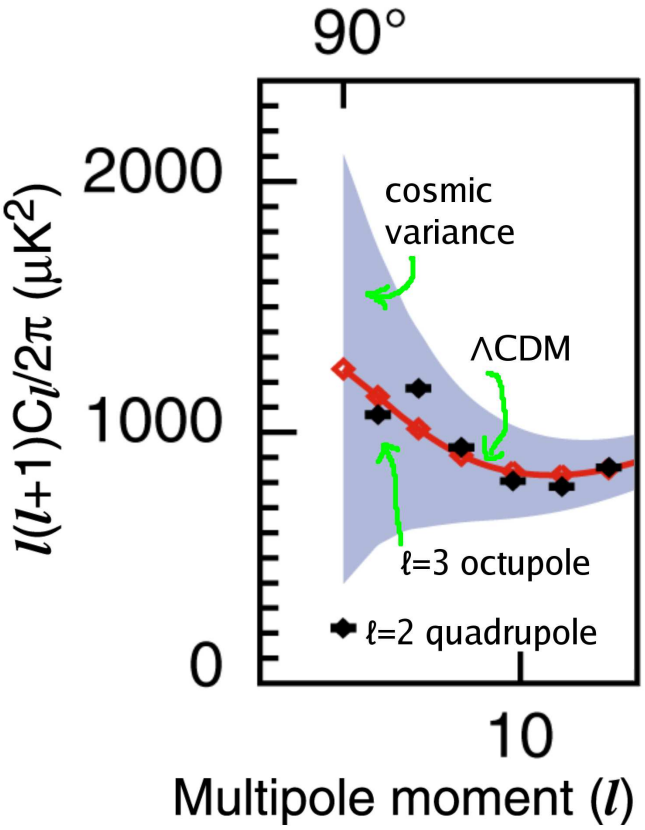

Figure 1.19: Close up of the power spectrum. A cosmological model with a large dark energy density component and cold (slowly moving) dark matter (ΛCDM) fits most of the measurements. The quadrupole moment $\ell = 2$ however does not fall within the allowed cosmic variance deviation.

The power spectrum can be fitted very well with a ΛCDM cosmological model, however the measured quadrupole is much lower then expected (figure 1.19). This might be explained as a

data error, or as the result of a yet unknown physical effect. However it can also be explained with a non-trivial topology, without having to alter the physics behind the cosmological model. A non-trivial topology imposes a limit on the size of the Universe and therefore on the size of the large scale fluctuations. This can suppress the low ℓ moments.

Axis of Evil

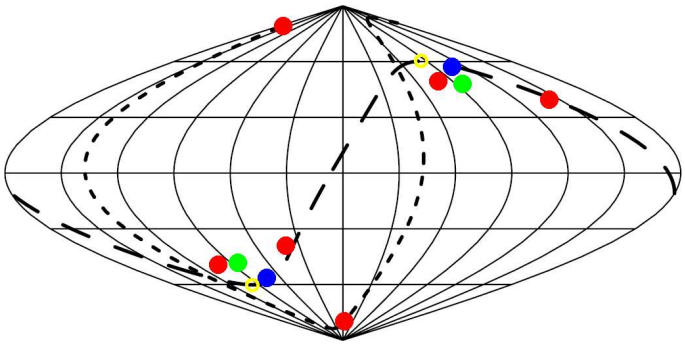

Figure 1.20: A representation of the axis of evil by Schwarz et al. (2004). Green is the dipole, blue represents the quadrupole and red the octupole, yellow are the equinoxes. The long dashed line is the ecliptic, the short dashed line is the super galactic plane. The vectors are related to, but not equal to, the multipole vectors.

Although the CMB is nearly isotropic, several searches for anisotropies have been performed. A very remarkable result is that there appears to be a preferred direction of the CMB (figure 1.20), dubbed by Land and Magueijo (2005) the 'Axis of Evil'. Almost all Universes with a non-trivial topology have intrinsic special directions. A preferred direction on the CMB like the axis of evil might be correlated with one or more of these special directions inherently in the Universe.

Non-Trivial Topologies

When the $a_{\ell m}$ are independent of m, an universe with trivial topology, the power spectrum as given in figure (1.17) contains all the information of the structure of the cosmic microwave background radiation. In a Universe with Gaussian fluctuations but a non-trivial topology, the $a_{\ell m}$ are not independent anymore and need to be studied in full to infer statistical information about the CMB.

In this thesis we investigate what possible topological shapes the Universe might have, what the effects of a non trivial topology are and how we might detect them. In particular we examine special directions of non-trivial topological universes in simulated CMBs by the use of *multipole vectors* developed by (Copi et al., 2004) which take into account all degrees of freedom of the $a_{\ell m}$ and thus of the CMB.

Chapter 2

Cosmic Topology: Concepts

2.1 Cosmology vs Topology

Cosmology deals with the largest entity we know, the Universe itself. To do so it needs to describe the geometry as well as the topology of the Universe. In current form cosmology indeed determines physics to the largest known distances, but in essence it is a theory based upon differential equations and therefore still a local theory. Cosmology is able to define the curvature of spacetime at any specific place. However it does not make a firm statement on its global structure. This concerns in particular the topology of space.

Topology deals with the global structure of objects, in particular with its shape. Topology does not take into account any local attributes of the object. In order to describe (the largest scales of) the universe knowledge of geometry is also crucial. As this is encapsulated in the cosmology, we have synthesized this in the name Cosmotopology.

For further reference, many of the concepts of this chapter can be found in Lachièze-Rey and Luminet (1995).

2.2 Topology

Topology is most easily described as the science of shapes. If two objects can be transformed into another by molding, but without cutting and pasting, topologists consider the two to be equivalent. They do not care about what the shape exactly is, or what exactly the curvature of the object is. So a ball is topologically the same as a bowl, you can push a 'pit' in the ball (without going trough the bottom) and you have a bowl. You cannot mold it into, say a coffee cup with ear, since in order to make the ear you have to punch a hole all the way through, which counts as cutting. You can however transform a coffee cup into a donut, which is the most classic example of topology.

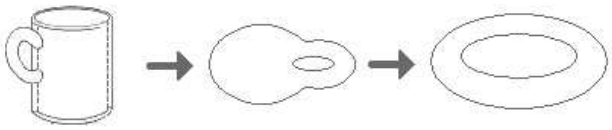

Figure 2.1: The coffee cup transforms into a donut.

2.2.1 Manifolds

All that exists in topology is the surface of these objects, not their interior or the space where they resides in. In the previous examples the surfaces were all 2 dimensional, the surface of a

ball is just like the surface of a coffee cup 2 dimensional. Topology, however, concerns itself with surfaces in any dimension. A circle for example can be seen as a 1 dimensional surface, and a 3 dimensional space such as our universe can be seen as a 3 dimensional surface. These 2 or higher dimensional surfaces are called *manifolds*.

Embedding

If you visualize the manifold as the surface of an object, like seeing the sphere as a real surface of a ball it is called embedding. A 2 dimensional sphere can be embedded isometrically in a 3 dimensional flat space, i.e. without having to stretch it. Others can not. An example is the Klein bottle (see section 3.1.1). In general an n dimensional manifold can always be embedded in a $2n+1$ dimensional flat space.

Size

Manifolds do not have to be of finite size but can also be infinite. Infinite spaces are called *open* like the Euclidean plane which is a flat surface. Finite surfaces are called *closed* like a sphere. An example of a semi closed manifold in which a fraction of its dimensions are closed while the others are open, is an infinite cylinder.

2.2.2 Geometry

The local shape of a manifold is determined by its geometry. Geometries of more then 2 dimensional manifolds can be very hard to describe directly, it is usually more insightful to concentrate on their 2 dimensional cross sections. Here we will only consider 3 dimensional manifolds with constant curvature (see section 2.4.2), they correspond to their 2 dimensional equivalents from section (1.3.3). The 3 dimensional geometries corresponding to the spherical plane, the flat plane and the hyperbolic plane are the spherical space $\mathbb{S}^3$, flat space $\mathbb{E}^3$ and hyperbolic space $\mathbb{H}^3$. All possible 1, 2 and 3 dimensional homogeneous geometries (each corresponding to a simply connected homogeneous manifold) are listed in table (2.1).

	geometries							
	isotropic			non-isotropic				
3D	$\mathbb{S}^3$	$\mathbb{E}^3$	$\mathbb{H}^3$	$\mathbb{S}^2 \times \mathbb{E}^1$	$\mathbb{H}^2 \times \mathbb{E}^1$	$\widetilde{SL2R}$	Nil	Sol
2D	$\mathbb{S}^2$	$\mathbb{E}^2$	$\mathbb{H}^2$					
1D		$\mathbb{E}^1$						

Table 2.1: All 1,2 and 3 dimensional homogeneous geometries. The number of possible configurations increases as the number of dimensions increases. We will only consider isotropic spaces, although for completeness we will list also the non-isotropic ones.

2.3 Multi Connected Topologies

For a proper understanding of non-trivial topologies of the Universe some concepts of topology and group theory need to be introduced.

2.3.1 Isometries

An isometry Λ is a transformation that moves every point x of a manifold to another point on the manifold while preserving distances between points.

$$\Lambda : x \mapsto \Lambda(x) \tag{2.1}$$

$$dist(x,y) = dist(\Lambda(x), \Lambda(y)) \tag{2.2}$$

Examples of isometries of the Euclidean plane (see section 3.1.1) are

- translations,
- rotations,
- reflections and
- glide reflections.

These all transform the Euclidean plane into the Euclidean plane, while the distances between all points stay intact. Note that the center of a rotation keeps its position after applying the isometry. In case of a reflection this is a line of points. These points are called fixed points of the isometry.

Examples of isometries of the 2-sphere are

- rotations (along an axis through two antipodal points) and
- reflections in a great circle.

2.3.2 Isometry Group

The set of isometries of a manifold is a group, called the *isometry group* of that manifold. See appendix B for a short introduction of group theory. E.g. in the Euclidean plane 2 translations yield another translation. The identity element I of the isometry group is just the 0-translation, a translation with a distance of 0. In chapter 3 we will explain that all the isometry groups of the 2 dimensional simply connected homogeneous spaces can be generated by the set of reflections. The isometry group is not Abelian, e.g. a rotation around the x axis followed by a rotation around the y axis is different from first a rotation around the y axis and then a rotation around the x axis.

A special subgroup of the isometry group are the Clifford transformations. With a Clifford transformation Λ_C the distance between each point x and its image is the same for all points.

$$dist(x, \Lambda_C(x)) = dist(y, \Lambda_C(y)) \tag{2.3}$$

A translation is a Clifford isometry, but a rotation is not. In the Euclidean plane/space most isometries are Clifford isometries, but in the spherical or hyperbolic space most are not.

2.3.3 Multi Connectedness

One way to distinguish objects in topology is by comparing their connectedness. There are two classes of objects, simply connected and multi connected. On simply connected manifolds, a circle can be contracted until it gets arbitrarily small to a point. On a multi connected manifold this is not possible for all circles. There can be several classes of circles that can be isomorphically transformed into each other, but not into circles of other classes. For example, on a torus a loop around the 'hole' cannot be transformed into a loop around the 'tube', see figure (2.2).

We will use the terms simply connected and multi connected to distinguish between the well known shapes of space and the ones that we are interested in and fold back into themselves.

2.3.4 Identification

A multi connected manifold can be constructed from another (often simply connected) manifold by choosing a subgroup from the isometry group of that manifold and *identifying* every point on the manifold with the points that can be reached by applying these isometries to that point. The 'parent' manifold is called the *covering space*. When the covering space is simply connected it is called the *universal covering space* of the multi connected space. A manifold can have multiple covering spaces, but only one universal covering space. The subgroup is called the *holonomy group* (figure 2.3). E.g. the torus can be created by using the Euclidean plane as covering space and choosing two non-parallel translations as the generators of the holonomy group (section 2.3.8).

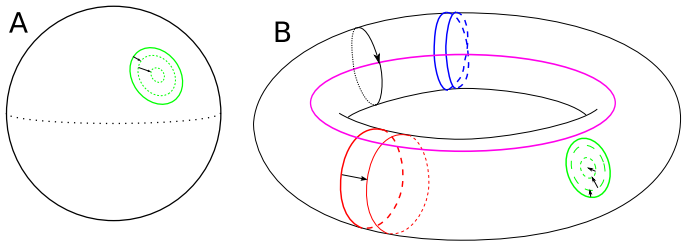

Figure 2.2: The green circle on ball A can be contracted to a point. This can be done for all loops on the ball: the ball is simply connected. On the torus B only the green loop can be contracted to a point, the red loop can be moved around, but not contracted, because such circles exist we call the torus multi connected. The blue loop (which crosses itself) cannot be contracted to a point either. Nonetheless it is of a different class then the red loop because they cannot be continuously transformed into one another.

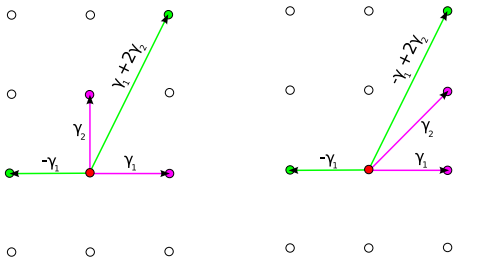

(a) Generators γ_1 and γ_2 are perpendicular.

(b) Generators γ_1 and γ_2 are not perpendicular but still linearly independent.

Figure 2.3: Some elements from the holonomy group of the torus. Two choices for the generators γ_1 and γ_2 are shown. Every circle can be reached from every other circle by an isometry composed of an integer, possibly negative, amount of the generators.

Physically, identifying two points means that one states that the points are the exact same location in space. An object at a certain point also is at all the points identified with that point since those are merely other instances of the same point. Mathematically it means you divide the full isometry group of the manifold by the holonomy group, resulting in a new (smaller) isometry group of the new manifold. Usually the full isometry group is denoted as $\widetilde{\mathcal{M}}$ and the holonomy group as Γ with its generators as $\gamma_0, \ldots, \gamma_n$. The multi connected manifold is called the *quotient space* who's isometry group is $\mathcal{M} = \widetilde{\mathcal{M}}/\Gamma$. Identification is similar to *compactification* in string theory. Identification by a isometry group often reduces the number of infinite dimensions of the covering space.

Technically, the isometries in $\mathcal{M}$ are different isometries than the isometries in $\widetilde{\mathcal{M}}$ since they belong to different manifolds. However, for all practical purposes the isometries in $\mathcal{M}$ can be seen as the isometries in $\widetilde{\mathcal{M}}$ that are periodic in the isometries in Γ. If there are non trivial isometries left in $\mathcal{M}$ the resulting manifold can still be further compactified by choosing a new holonomy group as subgroup of $\mathcal{M}$. The manifold corresponding to $\mathcal{M}$ is then called just *covering space*. E.g this allows the torus to be constructed by first dividing out a group generated by one translation — resulting in a cylinder — and then further compactify by dividing out a group generated by a translation in another direction.

The multi connected spaces can be classified by determining which sets of isometries can be used as generators of a holonomy group that, when divided out of the full isometry group, result in a physical possible space.

2.3.5 Ghost Copies

From the perspective of someone living in a multi connected universe the world looks just like the universal covering space corresponding to the multi connected space. Nonetheless, the space is not infinite. Mapping this universe one will notice that objects will appear multiple times. These copies are in fact different instances of the same object: they are located at points in the universal covering space that are identified by the holonomy group of the multi connected space. We call these apparent copies *ghost copies*.

Methods of detecting our Universe is multi connected all rely explicitly or implicitly on the existence and detectability of ghost copies of objects in our visible universe. The fact that we did not encounter any objects twice on our maps of the Universe can mean three things:

1. the Universe is not multi connected,
2. the scale on which it is multi connected is beyond the size of our maps,
3. we do not recognize the duplicate objects.

In this thesis we investigate the latter. The CMB is the best probe for detecting such reproductions.

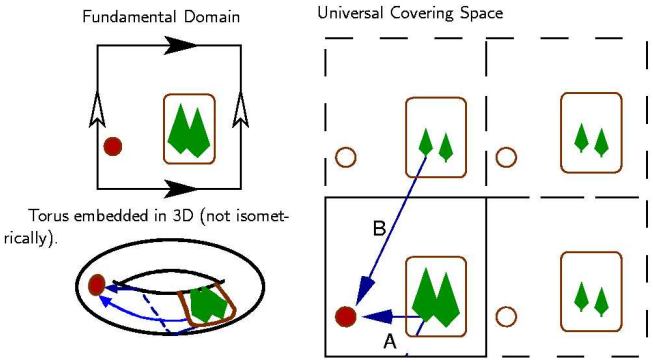

Figure 2.4: Three ways to visualize the torus. In the upper left is the fundamental domain (section 2.3.6), in this case a square which contains all the contents of the universe. The sides that have to be identified (section 2.3.4) are labeled with arrows. On the right is the universal covering space (section 2.3.4), this is how the torus looks like for an observer living on the torus. In this case it is the Euclidean plane. The most useful and compact way to visualize a multi connected space is by use of the fundamental domain.

2.3.6 Fundamental Domain

If you inflate a perfect sphere in a multi connected closed universe you will not be able to expand it indefinitely. Since your ghost copies will inflate the same sphere, your sphere will contact theirs and will form a face where they touch. At certain time every part of the sphere will touch another part and it cannot expand any more. The sphere will be transformed into a polytope (a polygon in 2 dimension, a polyhedron in 3 dimensions) which tessellates the entire universal covering space. Every point within the polygon is closer to you then to any of your ghost copies. This polygon is called the *fundamental domain* (FD). This tessellation is a special case of a *Voronoi Tessellation*. Every fundamental domain is a Voronoi cell and the observer forms the center of each cell.

In spherical and hyperbolic space the polytope will have resp. spherical and hyperbolic faces. This means that in the spherical space it is possible to have *digons* and *dihedrons*, polytopes with only two sides. In a semi open universe, the fundamental domain is semi open as well. The fundamental domain of a chimney space (figure 3.5(k)) is a cuboid extending indefinitely in one dimension.

Note that the FD can be different for different observers in the same multi connected space (see section 2.4.1). Technically, a better term for fundamental domain is *Dirichlet domain*. Any polytope that contains all the contents of the Universe exactly once which tessellates the universal covering space can be called a fundamental domain. A Dirichlet domain has to have the properties of a Voronoi cell.

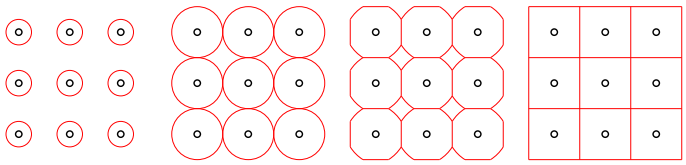

Figure 2.5: The small black circles represent several copies of an observer in a toroidal universe, the thinner red circles represent balloons they are inflating. When the balloon gets large enough it touches itself (2nd image). At the points where the balloon touches it forms faces (3th image) all the way until the whole space is filled by the balloon (4th image). In this case the Voronoi tessellation is degenerate because there are 4 cells adjacent to each vertex. In general there are only 3 in a 2 dimensional space.

Where the sphere touches the sphere of the neighboring ghost copy it essentially touches itself at two different locations. Therefore it will form two congruential faces. These faces represent identical points in space and are thus identified. There is an isometry in the holonomy group that transform the face into its corresponding twin.

All multi connected spaces which we will discuss can be represented with a fundamental domain with a specific set of identifications of its sides. In general all polytopes with identifications of its sides form a space, but not all of them are suitable for our universe. A way of searching for possible shapes of the universe is examining which shapes tessellate the universal covering space one supposes the universe has. In the rest of this thesis multi connected spaces will often be represented by its fundamental domain.

Besides the selection of pairs one should also distinguish the orientation of the sides which are identified. The sides may have to be rotated or even mirrored before being identified. It is also possible to identify a face with itself, these are unphysical (section 2.4.3). All fundamental domain with identification set correspond to one specific space, but the opposite is not true.

2.3.7 Sizes

While discussing the topology of the Universe there are six important length scales or radii to address (figure 2.6):

- R the curvature radius: the parameter of curvature,
- r_{SLS} the radius of the visible universe (section 1.5.3),
- r_{in} the radius of the *insphere* or *incircle* of the fundamental domain,
- r_{circum} the radius of the *circumsphere* or *circumcircle* of the fundamental domain,
- r_- the smallest radius of r_{in} among all possible observers.
- r_+ the largest radius of r_{in} among all possible observers.

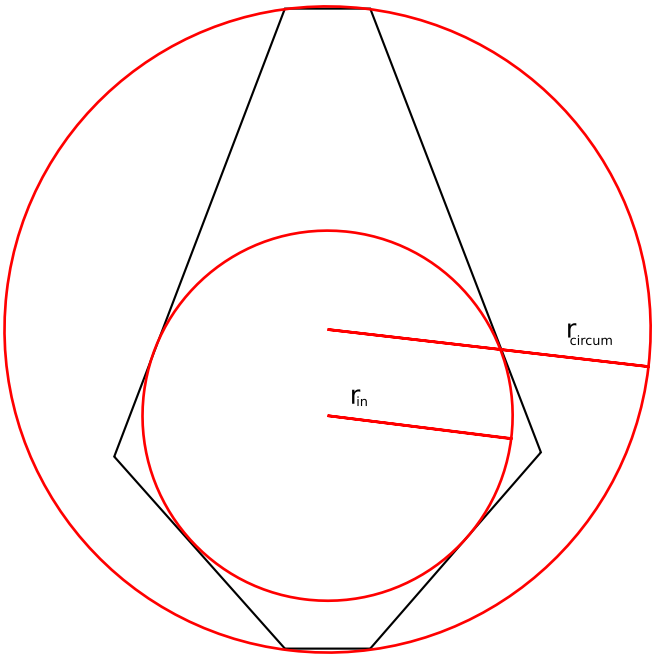

Figure 2.6: The different radii of a compact space.

If our visible universe, r_{SLS}, is smaller then r_{in} there will be no ghost copies of objects visible which makes it very hard — if not impossible — to determine the topology of the Universe. However, our results show that there might be a significant deviation from Gaussianity in the cosmic microwave background detectable even than. Inhomogeneity arguments (section 2.4.1) show that r_{in} is at least 200Gpc for us. If the visible universe is larger then r_{circum} we can see ghost copies of every object in the universe (provided we can recognize them).

In a spherical or hyperbolic Universe the latter four topological distances directly relate to the curvature radius R. All fundamental domains are rigid with respect to the curvature radius. If R is measured accurately it might be possible then to exclude certain topological shapes by observationally providing evidence for minimum values for r_{in}. The flat case is scaleless, $R = \infty$, therefore the latter four radii can take any value and it will be impossible to exclude any of the flat non-trivial topologies by size arguments alone.

Since a priori we do not know what position in a non-trivial topology we will have, we cannot know our fundamental domain and our value of r_{in} for a proposed model. Therefore spaces with a low value of r_+ are often examined since they will be most easily detected for all positions. Non-trivial topological spaces are often sorted on size, either by r_+ directly or by volume V (with respect to R), which more or less is an indicator for r_+.

All spherical manifolds have a maximum size, the size of the (hyper)sphere with radius R but no minimum size: lens spaces (section 3.2.2) can be arbitrarily small. Therefore it is always possible to consider spherical spaces which can be detected at any curvature R. Hyperbolic manifolds on the other hand have a lower bound. There exists a yet undiscovered compact hyperbolic manifold with minimum size which is shown to be greater then 0.2815 (where $R = 1$) (Przeworski, 2003). The current list of smallest compact manifolds is maintained by Weeks (2002).

2.3.8 Example: Torus

The torus is the simplest shape suitable as reference for investigation of multi connected spaces. It shows most of the features specific to a multi connected space and is illustrative for the various pitfalls that may beset us when studying topology.

In this work we refer to the true flat torus, with zero curvature instead of the well-known donut shaped body. The donut shaped torus has different curvature at different points, on the 'outside' it has positive curvature, and on the 'inside' it has negative curvature. The flat torus has zero curvature everywhere (hence the name). The problem is that it is not possible to embed the flat 2 dimensional torus (2-torus) *isometrically* in 3 dimensions, that is, without stretching and/or compressing certain portions of the torus.

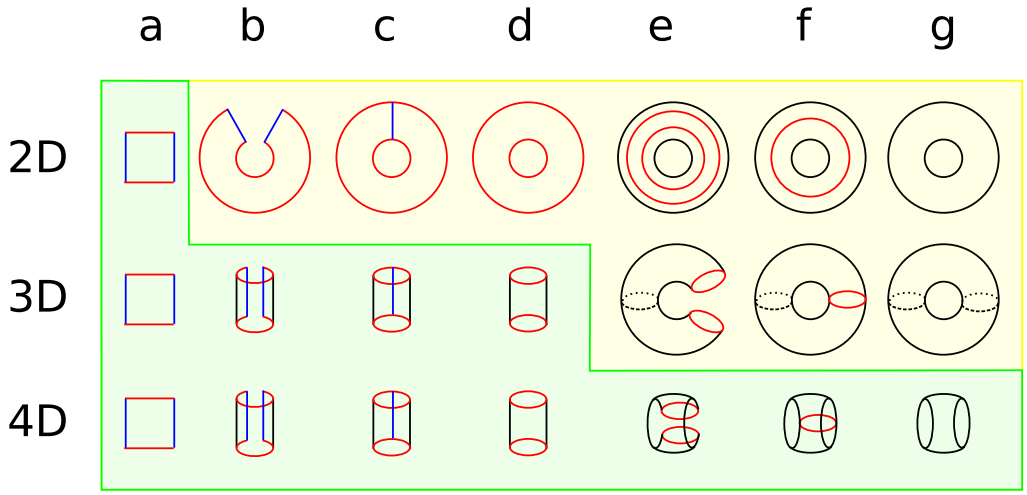

Figure 2.7: Creating the torus by gluing together ('identifying') its sides in 2,3 and 4 dimensions. Figures in green can be made isometrically, figures in yellow (upper right section) cannot. The most intuitive way of doing this is shown in the 3D way in the middle. The creation of a cylinder (a-d) can be done isometrically, i.e. without having to stretch the paper. The creation of the actual torus (d-g) cannot be done isometrically in 3D, one has to stretch some pieces of the cylinder. These last steps can be compared to the first steps of the 2D way. It is impossible to even make a cylinder in 2D without stretching the paper. What can be seen in (2D-d) would not even be called a cylinder by most people. However, it is just as much a cylinder in 2D as the torus in (3D-g) is a torus in 3D. A true flat torus can be created in 4D without having to stretch the paper at all! In (4D e-g) it looks like the cylinder crosses itself, that is just perspective. For someone not trained in seeing 3D the steps (3D b-d) seems to imply intersections as well while most people understand it does not.

The usual way to create the torus is by taking a square or rectangular piece of paper or rubber as a substitute for space and connect the sides across. Intuitively we are limited to 3 dimensions, this cannot be done without stretching the paper. If we remove that restriction and assume we can use 4 or more dimensions, we can make one without stretching the paper and bend it. The process is outlined in figure (2.7). In a similar fashion it would be possible to make a flat 3 dimensional torus by connecting together the opposite sides of a cube when resorting to more (6) dimensions. In general this is always possible if we allow bending in a sufficiently high dimension. Note that our figures are usually only 2 or 3 dimensional. This is mainly for illustrative purposes, to embed them correctly we need more dimensions.

2.4 A Priori Constraints

In principle there are infinitely many simply connected spaces to use as covering spaces both in 2 and 3 dimensional universes. Even more multi connected space can be formed from them. However, we can impose some heavy constraints on them. With the exception of the constraint concerning orientability all constraints are based upon an altered form of the cosmological principle, the *local*

cosmological principle.

2.4.1 Local Cosmological Principle

The cosmological principle is the most important principle in cosmology, we have to take it into account in our investigation of the shape of the Universe. Repeated from section 1.2.1 the principle states that the Universe is:

1. Homogeneous
2. Isotropic
3. Uniformly Expanding

This constraint is too strict. In order to have suitable solutions for cosmotopology, we should consider the less stringent *local cosmological principle*, the Universe is:

1. Locally Homogeneous
2. Locally Isotropic
3. Uniformly Expanding

The principle says that around every point in space one can create a sufficiently small ball in which the universe is homogeneous and isotropic. This ball should have a minimum radius. In other words, between any 2 points there exist an isomorphism that transforms the surroundings of one point to the surroundings of the other. The two spheres are indistinguishable.

This sphere will have a maximum size, the size of the inscribing sphere of the fundamental domain, of radius r_{in}. It may very well be that our entire visible universe is within this sphere, implying perfect homogeneity and isotropy.

Homogeneity

Some multi connected universes are homogeneous, but many are not. The fundamental domain of these universes is not the same for all observers.

Examples of multi connected spaces that are globally homogeneous are the tori $\mathbb{T}^2$ and $\mathbb{T}^3$. On the other hand, spaces for which reflections and rotations are isometries which are divided out are not homogeneous (figure 2.8).

However, in most manifolds *local homogeneity* does hold. If at every point on the manifold it is possible to create a ball of non-zero size in which the manifold appear homogeneous it is locally homogeneous (figure 2.9).

Isotropy

We restrict our universe to posses an isotropic geometry. However this does not mean the multi connected spaces that can be formed from them have no preferred directions (figure 2.10(a)). In fact, all multi connected spaces, with the exception of the projective plane $\mathbb{P}^2$ or space $\mathbb{P}^3$, are globally anisotropic.

On local scales however, on scales smaller than the size of the fundamental domain, they are isotropic (figure 2.10(b)). In a ball with a radius smaller than the inscribed sphere of the fundamental domain there is no way to distinguish the anisotropic multi connected space from its isotropic covering space. Therefore *local isotropy* holds, but global isotropy might not.

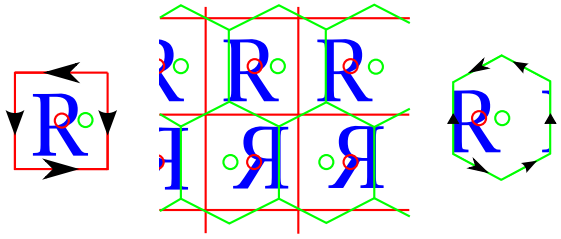

Figure 2.8: Homogeneity in a Klein Bottle. The center shows the covering space for the Klein bottle. The 'R's are imprinted in it to clarify the reflections. For both observers, the red circle on the R and the green circle next to it, the fundamental domain looks different. The red fundamental domain (on the left) is a square, while the green fundamental domain is a hexagon. As can be seen in the center image, both fundamental domains tile the covering space. Because different observers see different fundamental domains, the space is not globally homogeneous.

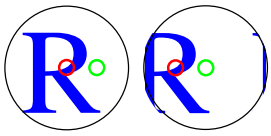

Figure 2.9: Locally, that is within a sphere of a certain radius, the two observers cannot distinguish their positions. The Klein bottle is locally homogeneous.

Local Cosmological Principle

Most multi connected spaces are not globally homogeneous and isotropic. However, this does not contradict standard cosmology. In cosmology the cosmological principle is used only for determining the geometry of space. Therefore there is no theoretical reason to substitute the local cosmological principle for the classic cosmological principle. The classic cosmological principle was only meant to address the issue of geometry, at the time of its formulation only simply connected spaces were deemed relevant for cosmology.

What we do have to concern are the philosophical arguments behind the cosmological principle, that there should be no special positions or directions in the universe and certainly that we are not in such a position or aligned with such a direction. It would be very coincidental if we would live in a special place in the universe, or that our Milky Way would be aligned exactly along (or perpendicular to) one of the major axes of our universe. Note, however, that we cannot assume that a special location does not exist. Therefore we will assume that special places and directions might exist in our universe, but that we will not be in or aligned with one of them.

This being said, it is much easier to simulate special cases of the universe in which we *are* in a special position. Therefore in our simulations, we will often investigate what happens when we are special.

2.4.2 Constraints on Geometry

The local cosmological principle influences our choice of geometry in the same way as the classical cosmological principle.

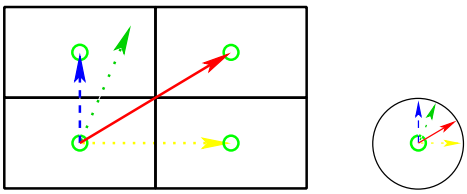

(a) Global anisotropy (b) Local isotropy

Figure 2.10: Isotropy in a toroidal universe. Globally (a), this universe clearly isn't equal in different directions. In the directions perpendicular to the edges of the fundamental domain (sides of the rectangle) the universe is smaller, also, in some directions one can see oneself, but in some not. Locally (b), the observer is unable to distinguish any of the directions. The torus is locally isotropic.

Homogeneity

In the context of geometry homogeneity means that we assume that the curvature of the universe is the same everywhere. While there are local variations due to the presence of mass concentrations on a sufficiently large scale these are supposed to even out. This excludes almost all manifolds. In fact it is known that only a few simply connected manifolds in low dimensions with the same curvature at every place.

In 2 dimensions there are only 3 homogeneous simply connected manifolds. In 3 dimensions there are only 8, which were first classified by Bianchi. They are summarized in table (2.1). Any cross section of the 3 dimensional spaces will have the curvature of one of the 2 dimensional planes, however these cross sections do not have to be simply connected themselves (just like the cross section of a 2-sphere is a (1 dimensional) circle which is also not simply connected).

Isotropy

In the context of geometry isotropy means that the curvature of space is the same in each direction. Curvature can only be measured to a single number in a plane. If a space is isotropic and the curvature of a cross section through a point has a certain value, every cross section through that point has the same value as curvature. In case of homogeneity this also means that every cross section of another point has that same curvature.

The 2 dimensional homogeneous simply connected spaces are all isotropic. Of the 3 dimensional spaces only the first 3 are isotropic:

- $\mathbb{S}^3$ the 3-sphere
- $\mathbb{E}^3$ the Euclidean space and
- $\mathbb{H}^3$ the hyperbolic plane.

The other 5 can have cross sections that are not the same, e.g. the cross section of $\mathbb{H}^2 \times \mathbb{E}$ can be an flat Euclidean plane or negatively curved hyperbolic plane. Because our universe appears to be isotropic we will only consider the first 3. However, we have to keep in mind that the other 5 spaces are possible in case the Universe is homogeneous but not isotropic.

2.4.3 Constraints on Topology

The local cosmological principle has a profound effect on which isometries can be chosen for the holonomy group.

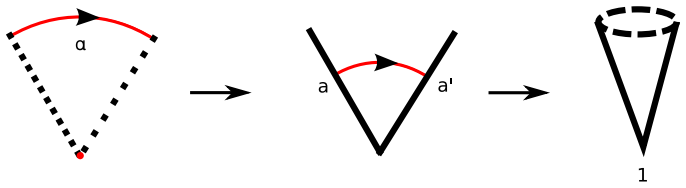

(a) A (clockwise) rotation (on the Euclidean plane) of angle α results in (semi-infinite) line a being identified with line a'. The resulting (2 dimensional) flat space embedded in 3 dimensions will look like a cone (of infinite 'height'). At every point the cone has flat geometry, except at point 1, there the cone has a singular point. In a real space such a point would be very peculiar: a 2 dimensional being traveling along the cone up to the point would get stuck.

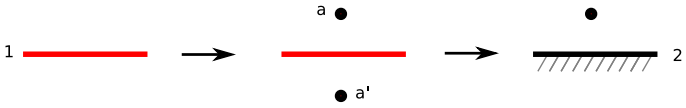

(b) A reflection (on the Euclidean plane) in line 1 identifies point a with a'. This causes the resulting space to have a line in it which literally looks like a mirror. If the observer at point a tries to reach line 2, it will walk into itself.

Figure 2.11: Fixed Points

Manifolds vs. Orbifolds

Some isometries transform every point to another point, like the translations in the Euclidean space but some keep some points fixed, these are called fixed point isometries. An example of a fixed point isometry is a reflection, all the points on the reflecting plane (in 3D) or line (in 2D) stay at the same position. Another example is a rotation, every point rotates around a certain center, this center point does not move at all.

If the isometries are used to identify points, these fixed point isometries identify one or several points with themselves. This leads to strange situations, like spaces with points where you can meet yourself (reflections, figure 2.11(b)) or where there is less space than at other points (rotations, figure 2.11(a)). The spaces that are created by identification with such a fixed point isometry are not called manifolds but orbifolds. Manifolds must be differential ('smooth'), orbifolds have singular points or lines.

Because they create orbifolds we will not include fixed point isometries as allowed isometries for our identifications. Note that this does not mean we should disregard them: Combinations of fixed point isometries can be fixed point free. A translation followed by a rotation is fixed point free. Two reflections can result in a translation. In fact on the three 2 dimensional planes every isometry can be generated by the combination of several reflections.

Fixed Affine Points

It is possible to create a semi-closed space that becomes infinitely small in the open direction. The pseudo-sphere is an example of this. It is possible to create the pseudo sphere by identifying two parallel lines in the hyperbolic plane. We must take care not to allow fixed affine points.

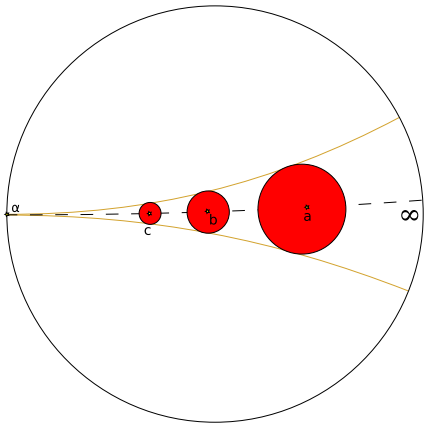

Figure 2.12: The pseudo sphere on the Poincaré disc. The two orange lines are parallel lines intersecting at affine point α. The dashed line in between is the bisector of angle α. The two parallel lines are identified with each other. The circles of isotropy — the inner radius of the fundamental domain — for several points on the middle line is drawn. Towards the left, the distance between the two parallel lines limits to 0 and so does the radius of the circle of local isotropy. Since in this case there is no lower limit on the radius within homogeneity isotropy holds this space is not locally isotropic.

Discrete

Our universal covering space is 3 dimensional, therefore the fundamental domain should be 3 dimensional as well. However, some isometries will reduce the number of dimensions of the fundamental domain. These isometries are called *non-discrete*.

Non discrete means that the distance between two identified points becomes infinitesimally small after applying the isometry infinite times which has as effect that one of the dimensions of the manifolds disappears. We illustrate the concept by a rotation on the Euclidean plane. A rotation by an angle that fits an integer (or rational) times in the full circle (2π), say n times, is called discrete because it divides the circle into n equal segments. The resulting space would be one of these slices with both sides identified with the other. When we connect the sides we get a cone (figure 2.13(a)).

A rotation by a transcendent factor of 2π does not divide the plane into a finite set of slices of a certain angle, but to infinite slices of zero angle. The resulting space is a half-infinite line (a 'ray'), which should be identified with itself (figure 2.13(b)). This space is 1 dimensional. Two parallel translations (which are fixed-point free) with transcendent ratio of their lengths have a similar effect. Because we do not want to lower the amount of dimensions we have we do not include (sets of) isometries that are not discrete.

Orientability

There are two kinds of manifolds, orientable and non-orientable. The difference between an orientable manifold and a non-orientable manifold is that a non-orientable surface has only one side, for example the Möbius strip is a non-orientable surface (figure 2.14). If you would live on such a surface and you would travel around it you would find yourself mirrored. There is no distinction between left and right. If it is possible to define 2 distinct orientations a manifold is called *orientable*, if this is not possible the manifold is *non-orientable*.

Several of the possible manifolds are non-orientable, and we will have to decide whether we

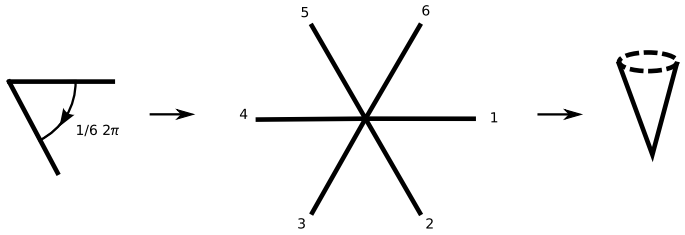

(a) When the rotation angle is exactly a fractional part of 2π (in this case $\frac{1}{6}2\pi$ then each point will be identified with a finite number of other points. In this case line 1 is identified with line 2 to 6, line 7 would be line 1 again. The (Euclidean) plane will be divided in a finite number of slices. The resulting space would be a 2 dimensional cone.

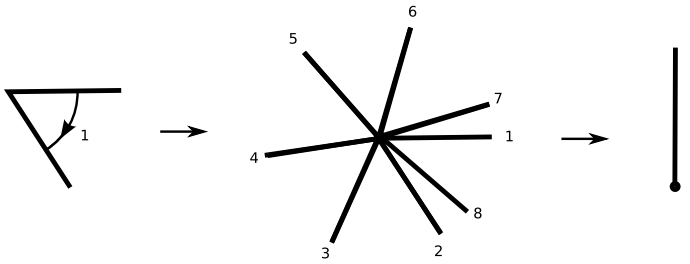

(b) When the rotation angle is a transcendental part of 2π (in this case 1) then each point will be identified with an infinite number of points and the distance between them becomes infinitely small. Line 1 is identified with line 2 to 9 and beyond, there will never be a line that coincides with line 1 again. The resulting space would be a 1 dimensional semi infinite line (infinite in only one direction).

Figure 2.13: 2 rotations, a discrete and non-discrete one. Every line should be extended indefinitely into the open directions.

include those as a possible model for our universe. While there might be physical reasons[1] to disregard non-orientable manifolds, there does not seem to be a cosmological reason for discarding them as possible models for our universe. Therefore we will include them in our research, however we will not select them for our simulations.

[1] Until the second half of the 20th century orientability did not seem to be a problem, but then parity violation was proved by experiment by Lee and Yang in 1957. Most of the laws of physics are based on underlying symmetries. The most important one is the one from which the word symmetry originates, the indifference between left and right. Nature seemed to make no difference in orientation. Every law of physics appeared to be the same if the universe would be mirrored, this is called Parity. This however is not the case, the weak force (responsible for beta-decay) is not symmetric. Experiments show that atoms with their spin aligned in a magnetic field do decay in favorable directions, which indicates that the universe is not indifferent in left and right. This is what physicists call 'parity violation'. There are so many consequences of parity violation that the so called 'standard model' of elementary particles will not hold if the universe is not orientable. For example, there are particles like neutrino's that are not even supposed to have a mirror image.

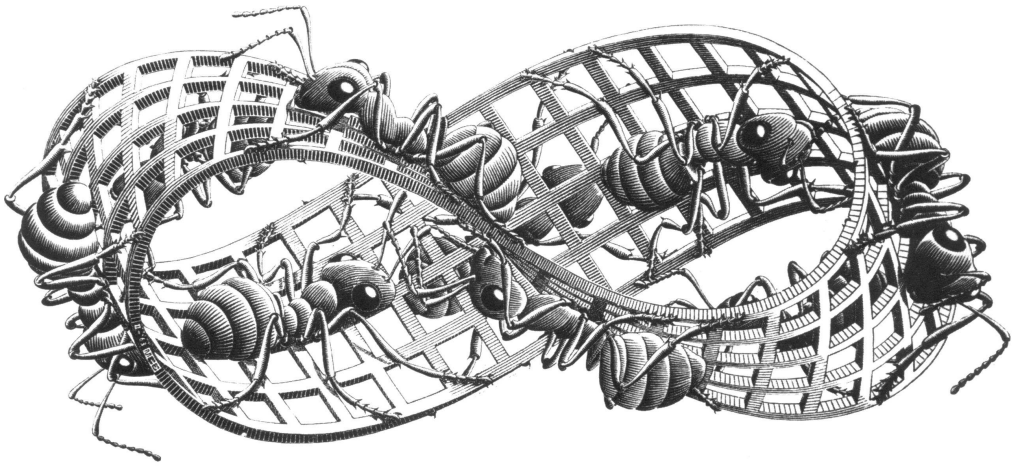

Figure 2.14: The Möbius strip by Escher. The Möbius strip is not orientable. It has only 1 side as you can see by following the ants. This would not be suitable for a real (2 dimensional) universe, since it does have an edge. Either the width of the strip should be infinite yielding the flat infinite Möbius band, or the edge should be contracted to a point (the edge is a circle), to create the spherical projective plane ($\mathbb{P}^2$).

Chapter 3

Cosmic Topology: Surfaces in 2D and 3D

In this chapter we will investigate all possible 2 and 3 dimensional manifolds that fulfill our local cosmological principle and the other a priori constraints. We consider all 3 geometries:

- flat: $\mathbb{E}^2$ and $\mathbb{E}^3$,
- spherical: $\mathbb{S}^2$ and $\mathbb{S}^3$ and
- hyperbolic: $\mathbb{H}^2$ and $\mathbb{H}^3$.

We list their corresponding isometry groups and determine what (semi-)closed manifolds can be created from them. Although mathematics would dictate us to go spherical to flat to hyperbolic (or the other way around) we will start with flat space because it is conceptually the easiest to understand.

3.1 2D

3.1.1 Flat

The full isometry group of the Euclidean plane $\mathbb{E}^2$ is called $E(2)$. It consists of (figure 3.1):

- translations,
- reflections,
- rotations and
- glide reflections.

A glide reflection is a translation with a reflection along a line parallel to the translation.

The isometry group of $\mathbb{E}^2$ can be generated by using only reflections. Two non-parallel reflections become a rotation about their crossing point. Two parallel reflections become a translation. The more you are away from the center of a rotation, the more the rotation (if small) becomes to look like a translation. In fact, one can consider a translation as a rotation about an affine point (i.e. a point "at infinity", section 1.3.2). At the basis of this definition of a affine point rotations and translations are fully equivalent. The group structure is summarized in table (3.1). The unity element I keeps all the points at the same place like a translation of length 0.

From this isometry group $X = E(2)$ we will choose the holonomy group Γ which will be divided out. The resulting fundamental domain will have isometry group $M = X/\Gamma$. On this subgroup Γ we have to impose the constraints of section 2.4.3, in order to let M still be a 2

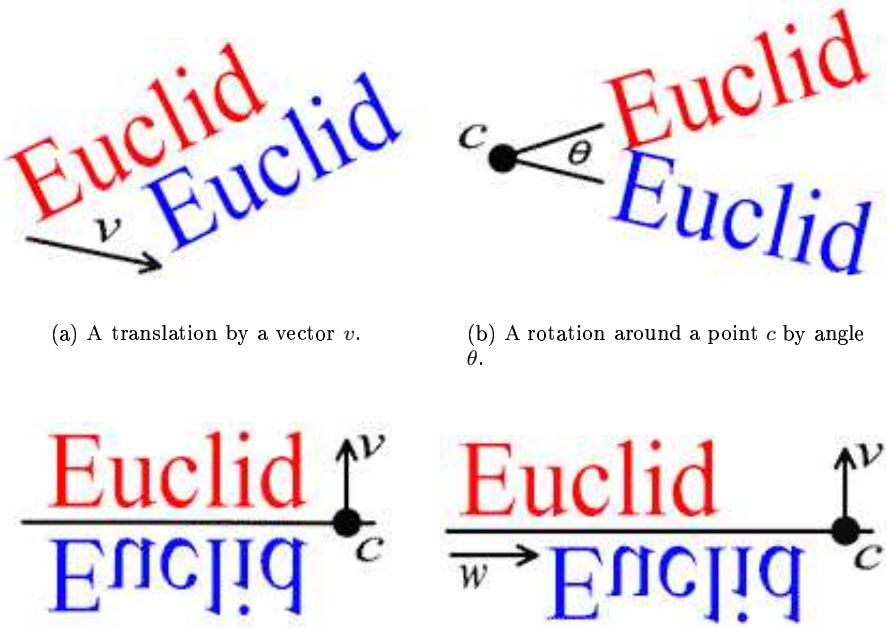

(a) A translation by a vector v.

(b) A rotation around a point c by angle θ.

(c) A reflection is identified by a point c and a unit vector v.

(d) A glide reflection is identified by a reflection and a translation along w perpendicular on v.

Figure 3.1: The 4 isometries of the Euclidean plane.

	I	R/T	Ref	G-R
I	I	R/T	Ref	G-R
R/T	R/T	R/T	G-R	R/T
Ref	Ref	G-R	R/T	G-R
G-R	G-R	R/T	G-R	R/T

Table 3.1: The group structure of the Isometry group of the Euclidean plane. I is the identity, R/T is a rotation or a translation. Ref is a reflection. $G-R$ is a glide reflection.

dimensional manifold. We do not want fixed point isometries, nor non-discrete (combinations of) isometries. In this case this means that we disregard all rotations, which leaves us with only 1 or 2 translations, one of them possibly combined with a reflection. We are not allowed to take the two translations/glide reflections parallel to each other, because this will either create a fixed point subset or a subset generated by only one translation/glide reflection. Two glide reflections do not give a manifold, it results in an orbifold with 2 singular points, since 2 glide reflections will result in a rotation. There are only 5 possibilities, summarized in table (3.2).

3.1.2 Spherical

The isometry group of the 2-sphere is isomorph with $O(3)$, all orthogonal 3×3 matrices with the absolute value of the determinant equal to one. The isometry group is again generated by reflections. A reflection is a transformation determined by a geodesic which in the case of spherical geometry is a great circle. All reflections therefore reflect in a great circle and leaves the points on that circle fixed. Just like in the Euclidean plane, 2 (non-trivial) reflections generate a rotation (around a particular axis when embedded in $\mathbb{E}^3$). In spherical space a rotation fixes two (antipodal) points.

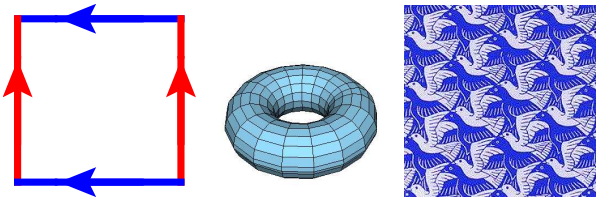

Torus

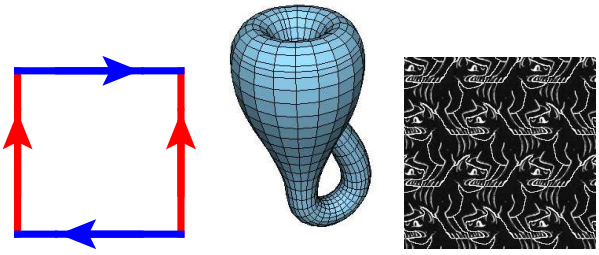

Klein Bottle

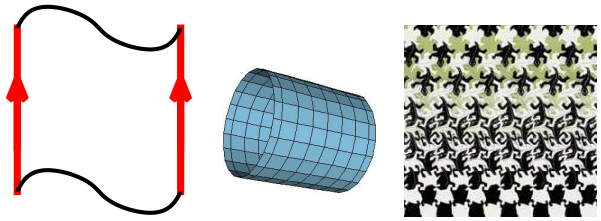

Annulus

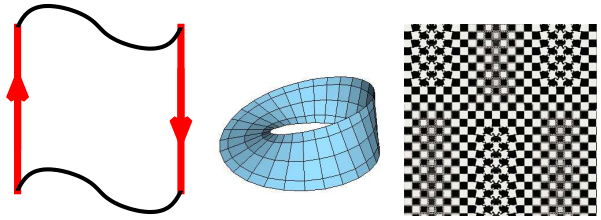

Möbius Band

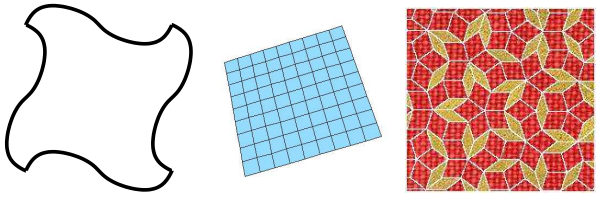

Euclidian Plane

Figure 3.2: All 5 2 dimensional homogeneous isotropic flat spaces. The first column shows the fundamental domain. The second column shows a representation of the manifold embedded in 3D. Only the annulus and Euclidean plane are embedded isometrically. The third column shows an impression of how the universal covering space looks like by M.C. Escher. The last tiling is a piece of a Penrose tiling. Penrose tilings are non-periodic.

Isometries	Name	Compact Dimensions	Orientable
2 Translations	2-torus	2	Yes
1 Translation, 1 Glide Reflection	Klein Bottle	2	No
1 Translations	Annulus	1	Yes
1 Glide Reflection	Möbius Band	1	No
None	Euclidean Plane	0	Yes

Table 3.2: Classification of the 5 2-dimensional flat spaces.

Unlike the Euclidean plane, two distinct straight lines (two great circles), will always intersect. There is no such thing as a parallel line on the spherical plane. There are smaller circles that at every point have the same distance to a great circle, like on Earth the circle of points with the same latitude to the equator. However, these lines are not straight, we call these lines *equidistant lines* (see section 1.3.2)

Because there are no parallel lines on the sphere, there are no translations either. Just reflections, rotations or a rotation followed by a reflection perpendicular to the rotational axis (and the identity). All of these have fixed points, except for the special case of a rotation of $\frac{1}{2}2\pi$ followed by a reflection (equivalent to 3 reflections in 3 mutually perpendicular great circles). This results in the only other spherical 2-manifold; the projective plane $\mathbb{P}^2$.

Isometries	Name	Compact Dimensions	Orientable
Point Reflection in 0	Projective Plane $\mathbb{P}^2$	2	No
None	Sphere $\mathbb{S}^2$	2	Yes

Table 3.3: Classification of the 2 2-dimensional spherical spaces.

3.1.3 Hyperbolic

The isometry group corresponding to the infinite hyperbolic plane (the hyperboloid) is $PSL(2,\mathbb{R}) = SL(2,\mathbb{R})/\mathbb{Z}_2$ with $SL(2,\mathbb{R})$ the Lorentz group of real 2×2 matrices with unit determinant. Thas (2002) describes the full isometry group of the hyperbolic plane.

The isometry group of the hyperboloid is also generated by reflections. On the sphere we had only 1 possibility for the combination of two reflections: a rotation. On the Euclidean plane we had 2: a rotation or translation. The translation could be seen as a rotation about an affine point 'at infinity' where two parallel lines intersect. In hyperbolic geometry we can go one step further. On the hyperboloid, ultra parallel lines are said to cross in an *ultra affine point* 'beyond infinity'.

When two reflections are defined by two straight lines that intersect at a regular point, the combined action of the two is just a regular rotation called a 'spherical isometry'. When the two lines intersect at an affine point the isometry is called 'parabolic' and when they intersect at an ultra affine point the combined isometry is said to be 'hyperbolic'. Spherical isometries fix the center point of the rotation. A parabolic isometry fixes its affine point and a hyperbolic isometry fixes 2 affine points. Since the latter two only fix affine points (at infinity), and these points are not part of the hyperbolic plane itself, these isometries are fixed point free.

Determining what multi connected spaces can be created from this isometry group is not very easy. In fact all 2 and 3 dimensional multi connected spaces have been discovered and cataloged except the hyperbolic ones. The most easiest way to talk about them is by their fundamental domain. Escher has made several pictures of tilings of the hyperbolic plane.

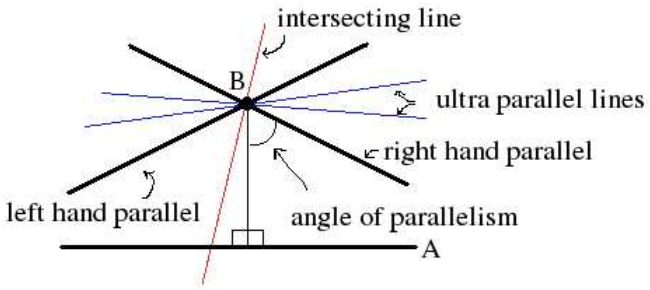

Figure 3.3: On the hyperbolic plane there are two parallel lines to line A through point B. The parallel lines have an angle of parallelism less then π with the perpendicular from B to A. They intersect at an affine point at infinity. There are an infinite number of ultra parallel lines that do not intersect on the plane either. They intersect at an ultra affine point 'beyond' infinity. There are also an infinite amount of lines through point B that do intersect with line A.

3.2 3D

3.2.1 Flat

All flat 3 dimensional manifolds have been known for a long time. Motivated by the study of crystallography Novacki (1934) completed the categorisation 1934. The isometries of the Euclidean space that are fixed point free are translations, translations followed by a rotation around the axis of translation (*screw operation*), and translations followed by a reflection in a plane parallel to the axes of translation (*glide plane operation*).

There are 18 different flat manifolds, one of which is simply connected and fully open ($\mathbb{R}^3$), 7 half open and 10 closed. These are summarized in figure (3.4). In figure (3.5) a possible fundamental domain for each of the spaces (except the simply connected one) is shown, with proper identifications of the sides.

3.2.2 Spherical

A spherical universe has positive curvature everywhere with $\mathbb{S}^3$ as covering space. This means that its spatial volume is necessarily finite. However it can be infinite in time if the cosmological constant is high enough. If the cosmological constant is low enough the universe will get to a maximum size and then contract again till a singularity (within finite time).

The isometry group of the spherical space $\mathbb{S}^3$ is isomorph with $SO(4)$, all 4 dimensional (Euclidean) rotations about the origin and reflections in spaces through the origin. It goes beyond the scope of this document to classify all the finite subsets of $SO(4)$, so we will list only a few of them. For the full classification we refer to Gausmann et al. (2001)

Lens Spaces

Just like it is possible to peel the skin of an orange (a 2-sphere) into parts (digons), you can cut the 3-sphere into lens shaped objects (see figure 3.7). A lens is a spherical polyhedron with two sides, a dihedron. The only way to tessellate the 2-sphere with digons is by identifying both sides, this creates a hosohedron with fixed points (figure 3.6). In 3 dimensions the 3-sphere can be tessellated by analogy into a hosochoron, but unlike the 2 dimensional case they can be rotated to prevent the creation of fixed points. A lens space is denoted by $L(p,q)$. p is the (integer) amount of lenses that tessellate the 3-sphere, every dihedron is rotated an angle of $\frac{q}{p}2\pi$ (counterclockwise when looking from the first lens to the second). The edges of a digon are half great circles. The surfaces

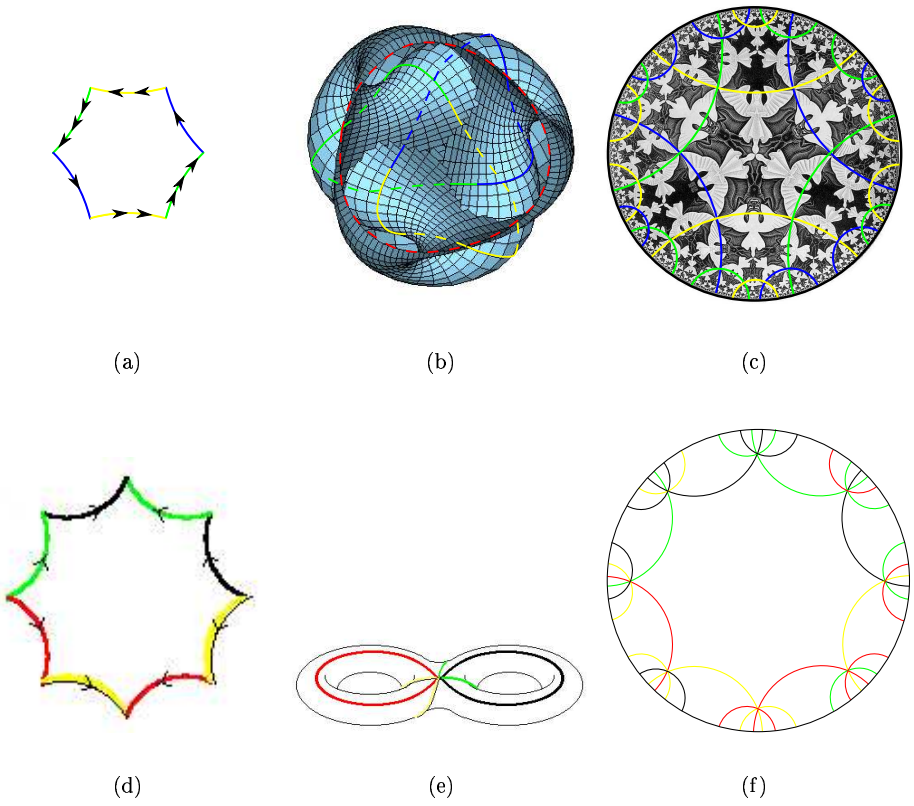

Figure 3.4: Examples of a hyperbolic 2 dimensional manifold. The left column shows the Fundamental domain, the middle column the manifold embedded in 3 dimensions in a non-isometrical fashion. The third column shows the Universal Covering Space on a Poincare disc. The dutch artist M.C. Escher has made several paintings of tessellations of the hyperbolic plane. Shown in 3.4(c) is Circle Limit IV, which corresponds to a universe with a hexagonal fundamental domain. However, the image does not resemble a physical universe. The vertices are singular points. All images from the circle limit series have this defect. A physical 2 dimensional multi connected universe is shown in image (3.4(d)) to (3.4(f)), the two holed torus. Note that 3.4(b) shows Boy's surface, the red line denotes a circular cut so it is possible to see 'inside' the surface. The Boy's surface is (also) representation of the projective plane. The projective plane can be embedded with all three geometries.

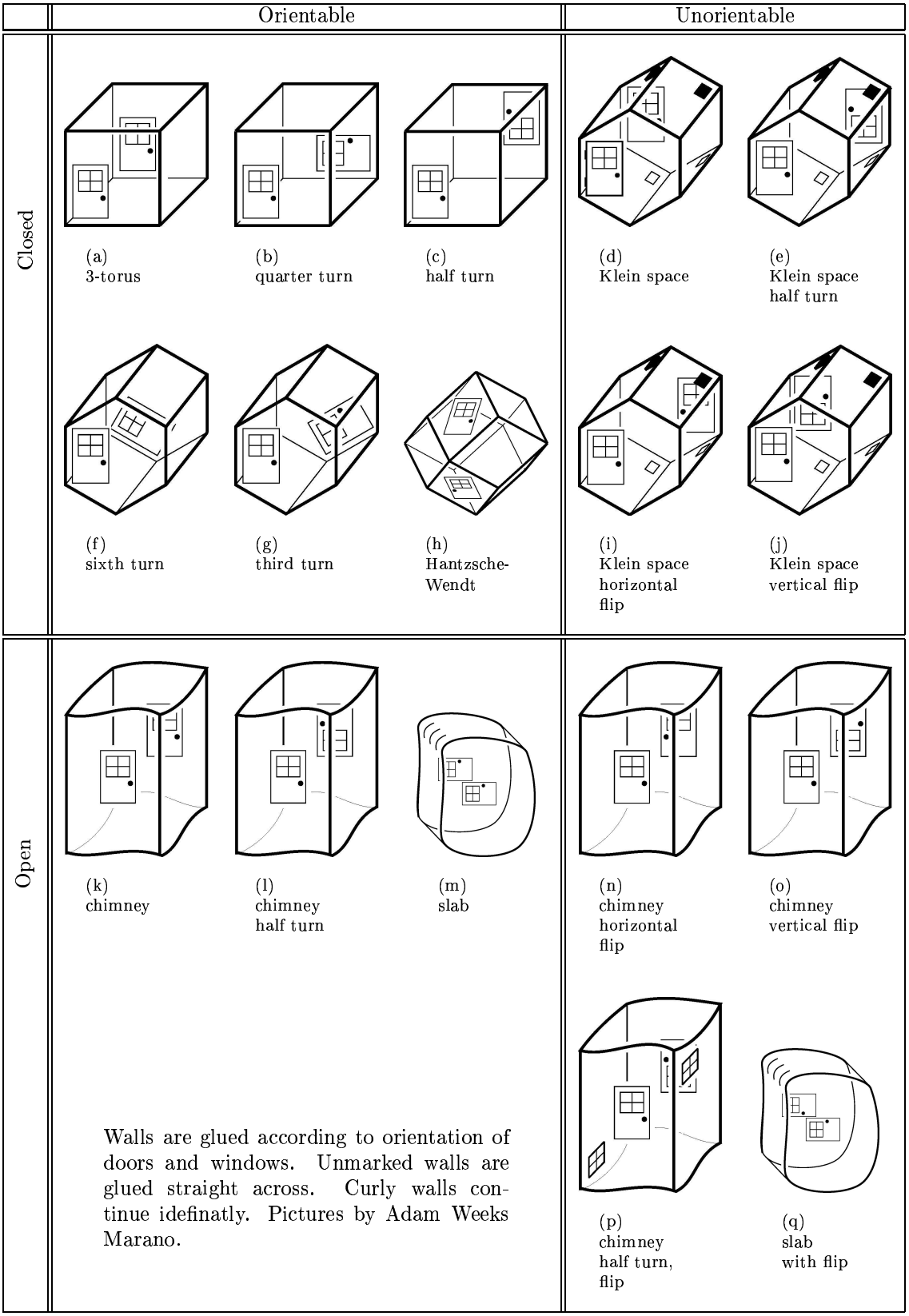

Figure 3.5: 3 dimensional flat spaces

Symbol	Name	Compact Directions	Orientable
E_1	3-torus	3	Yes
E_2	half turn space	3	Yes
E_3	quarter turn space	3	Yes
E_4	third turn space	3	Yes
E_5	sixth turn space	3	Yes
E_6	Hantzsche-Wendt space	3	Yes
E_7	Klein space	3	No
E_8	Klein space vertical flip	3	No
E_9	Klein space horizontal flip	3	No
E_{10}	Klein space with half turn	3	No
E_{11}	chimney space	2	Yes
E_{12}	chimney space with half turn	2	Yes
E_{13}	chimney space with vertical flip	2	No
E_{14}	chimney space with horizontal flip	2	No
E_{15}	chimney space with half turn and flip	2	No
E_{16}	slab space	1	Yes
E_{17}	slab space with flip	1	No
E_{18}	Euclidean space	0	Yes

Table 3.4: Classification of the 18 3-dimensional flat spaces.

of the dihedron are half great spheres. Although these surfaces appear curved in Euclidean space, they are straight in spherical space.

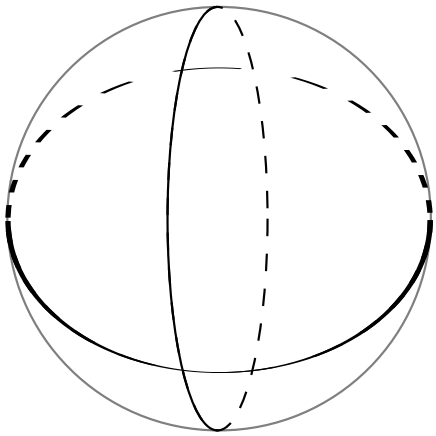

Figure 3.6: A tetragonal hosohedron created from 4 digons. There are two singular points.

Projective Space

The division of the 3-sphere into 2 dihedral lenses was first described by Dante in his "Divina Comedia" (Peterson, 1979) in the early 14th century. He visualizes the 3-sphere as two solid 2-spheres (2-balls) glued together on the surface. This is analogous with the projection of the 2-sphere on 2 solid circles. The two surfaces of the dihedron would be tangent to each other on their circle of intersection, therefore the surface of the entire dihedron is indeed a 2-sphere. In the case

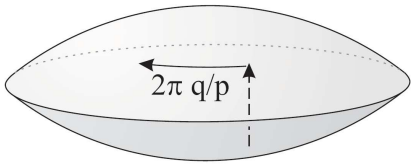

Figure 3.7: The construction of a lens space (Gausmann et al., 2001).

of a true lens space the two solid 2-spheres would be the same and would require the only possible rotation of a half circle ($\frac{1}{2}2\pi$) to create a manifold. This manifold is called the projective space ($\mathbb{P}^3$). In contrast with the projective plane, the projective space is orientable. The projective space (also called elliptic space) has often been called more natural or more simple then the 3-sphere itself because the 3-sphere violates Euclid's first postulate. Euclid's first postulate can be read as "two points define a line", which is true in the Euclidean space, but not in the spherical space (or plane). Through two antipodal points an infinite amount of lines (great circles) can be drawn, like meridians on the Earth's surface. In the projective space two antipodal points are identified with each other, therefore every two points define a single line.

Regular Polyhedron

The isometry groups of the orientation-preserving symmetries of the Platonic solids are related to tessellations of the spherical plane by (semi-)regular polyhedrons. The 3-sphere can be tessellated by 24 octahedrons, 48 truncated cubes or 120 dodecahedrons. The opposite faces are identified after appropriate rotation (figure 3.8, table 3.5).

A dodecahedral space is proposed by Luminet et al. (2003) because it can explain the low quadrupole and octupole in the WMAP data from the CMB (see section 1.5.7).

Symmetry Group	Order	Fundamental Domain
T_d	24	octahedron
O_h	48	truncated cube
I_h	120	dodecahedron

Table 3.5: The three (semi-)regular fundamental domains.

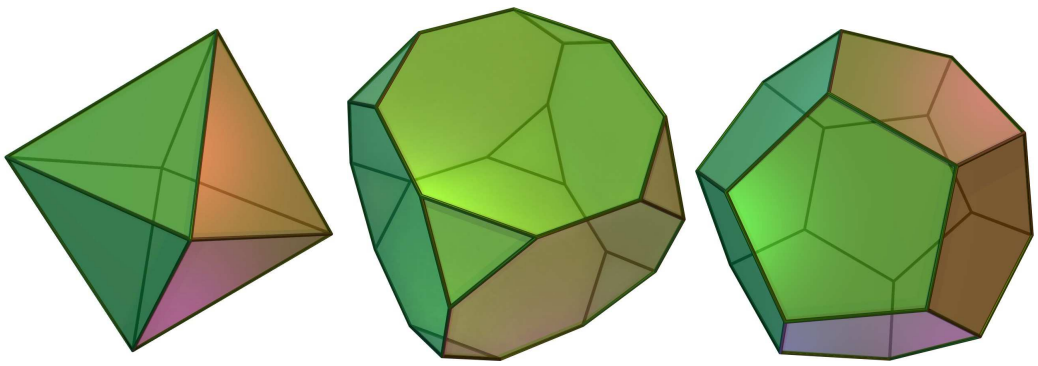

(a) Octahedron (b) Truncated Cube (c) Dodecahedron

Figure 3.8: The three (semi-)regular fundamental domains (Cyp).

3.2.3 Hyperbolic

The hyperbolic multi connected manifolds are not yet fully classified. Unlike the spherical manifolds, the hyperbolic manifolds have a lower limit in volume instead of an upper limit. This lower limit is important, because it determines what the minimum size is which our visible universe must have (in terms of curvature radii) in order to let any effects of a possible multi connected hyperbolic space be detectable.

In the beginning of the 20th century only a very few closed hyperbolic 3-manifolds were known, but in the last 50 years a lot more were found. In the 1970's Thurston showed that most closed 3-manifolds admit a hyperbolic geometry. Unlike the flat 3-manifolds, all hyperbolic 3-manifolds are rigid. There is only 1 degree of freedom, the curvature radius. Also, no hyperbolic 3-manifold is globally homogeneous, the fundamental domain always depends on the position of its base point. Every finite group can occur as the symmetry group of a closed hyperbolic 3-manifold, so the possibilities are endless.

Chapter 4

Cosmic Topology: Observational Imprint

In the last decades a lot of research has been dedicated towards determining whether we live in a multi connected universe, and if so, in what kind of multi connected universe. Here we will describe various methods which were proposed to infer whether the Universe is multi connected. All techniques are based on the principle that if a multi connected universe is small enough one should see various copies of the same features. Such features might be concrete objects like galaxies or clusters of galaxies. Arguably the best candidate for detection is offered by features on the surface of last scattering.

We make a distinction between 2-dimensional and 3-dimensional methods. In addition, we distinguish between statistical and concrete methods. The 2D methods only deal with the CMB (which is a 2 dimensional surface) and the 3D methods with everything that's closer by, distributed in 3 dimensions. Concrete methods try to identify ghost copies of discrete sources, like another copy of the Galaxy. Statistical methods use statistics from a large number of sources to find evidence for a multi connected space. A review of early attempts to detect the topology of the Universe is given by Luminet and Roukema (1999).

The new method we apply in the upcoming chapters is based on statistical analyses of the cosmic microwave background with the use of multipole vectors.

4.1 3D Concrete methods: Ghost Hunting

In a multi connected universe every object can be seen several times if the universe is small enough. If the radius of the visible universe is larger than the radius of the inscribed sphere of the fundamental domain (r_{in}) there are several sections of space that are at least two times within our visible range. Objects in those sections might be detectable twice. Lachièze-Rey and Luminet Lachièze-Rey and Luminet (1995) describe several methods to detect the topology using ghost images.

Since these objects can exist at various distances and directions in the sky there are certain criteria that the objects that are studied have to meet. The objects should

- not evolve significantly over the age of the universe,
- be detectable up to very high redshift in every direction,
- emit isotropically,
- have near zero three-dimensional peculiar velocity.

Due to these constraints it is far from trivial to find good candidates. Most objects evolve rapidly in time or look different from different angles (e.g. quasars). This is especially true for non-statistical methods. Examples of studies of non-statistical research include the search for our own galaxy as a quasar, detection of copies of the Coma cluster and even multiple instances of large scale structures on scales of $50 - 150h^{-1}Mpc$ such as walls and voids.

These concrete studies have not been very successful since it is to hard to determine whether two objects that are so far apart (in space and time) really are the same physical object. Results do show that the injectivity radius (r_{in}) of our fundamental domain must be larger than $100h^{-1}Mpc$ and probably even larger than $200h^{-1}Mpc$.

4.2 3D Statistical methods

The most important statistical 3 dimensional method for the detection of the topology of the universe is *Cosmic Crystallography* (CC). This name is given in by the analogy with techniques used in normal crystallography (Lehoucq et al., 1996). In a multi connected space, some isometries translate every element of the fundamental domain by a fixed distance. These fixed distances result in spikes in a *Pair Separation Histograms* (PSH). A PSH is a histogram that shows how often certain distances between two objects occur. All the distances of sources in a catalog are squared, normalized, binned and then plotted as a histogram. Every topology has a theoretically expected shape of the PSH, the *Expected Pair Separation Histogram* Gomero et al. (2002).

We illustrate the method with the simplest case, the 3-torus. The 3-torus has 3 distinct length scales, λ_1, λ_2 and λ_3 corresponding to the generators of its holonomy group. Each isometry translates the fundamental domain along an integer number of these generators and we can express the distance Λ_i of the isometry i in terms of λ_k:

$$\Lambda_i^2 = n_1^2\lambda_1^2 + n_2^2\lambda_2^2 + n_3^2\lambda_3^2 \tag{4.1}$$

$$V = \lambda_1\lambda_2\lambda_3 \tag{4.2}$$

where n_i corresponds to the (integer) times the holonomy of length λ_i is in the isometry. V is the volume of the fundamental domain. We can rewrite equation (4.1) to volume-normalized distance as

$$\frac{\Lambda_i^2}{V^{\frac{2}{3}}} = n_1^2 + n_2^2 + n_3^2 \tag{4.3}$$

Equation (4.3) is valid for all flat manifolds, not just the 3-torus, but needs adjustment for curvature in the spherical or hyperbolic case. The frequency of the volume-normalized distances is plotted in the histogram. Distances corresponding to integer values of the isometries (right side of equation (4.3)) will show up as spikes. Figure (4.1) shows a PSH for a simulated toroidal universe with equal lengths of the sides of the fundamental domains.

The equal sided 3-torus is the most promising scenario, because all generators of the holonomy group are translations of equal length. Only isometries that translate every element of the fundamental domain by the same length, the Clifford translations, contribute to spikes in PSHs. All other flat manifolds result in PSH with similar spikes, be it they will be less pronounced (Gomero et al., 2000). The hyperbolic and spherical manifolds do not show these spikes at all (Lehoucq et al., 1999) since none of their isometries translate every point by the same distance. A few of such spaces are exceptional, in that they do as e.g. spherical projective space. It remains to be seen whether cosmic crystallography will be a suitable method for the detection of the topology of our universe. Lehoucq et al. (2000) discuss the limits of cosmic crystallography and also propose some modifications to successfully detect hyperbolic and elliptic universes using cosmic crystallography.

4.3 2D Concrete methods

When looking for ghost images, one wants to look as far as possible in order to cover a larger part of the visible universe and thus a larger amount of fundamental domain cells. The ultimate

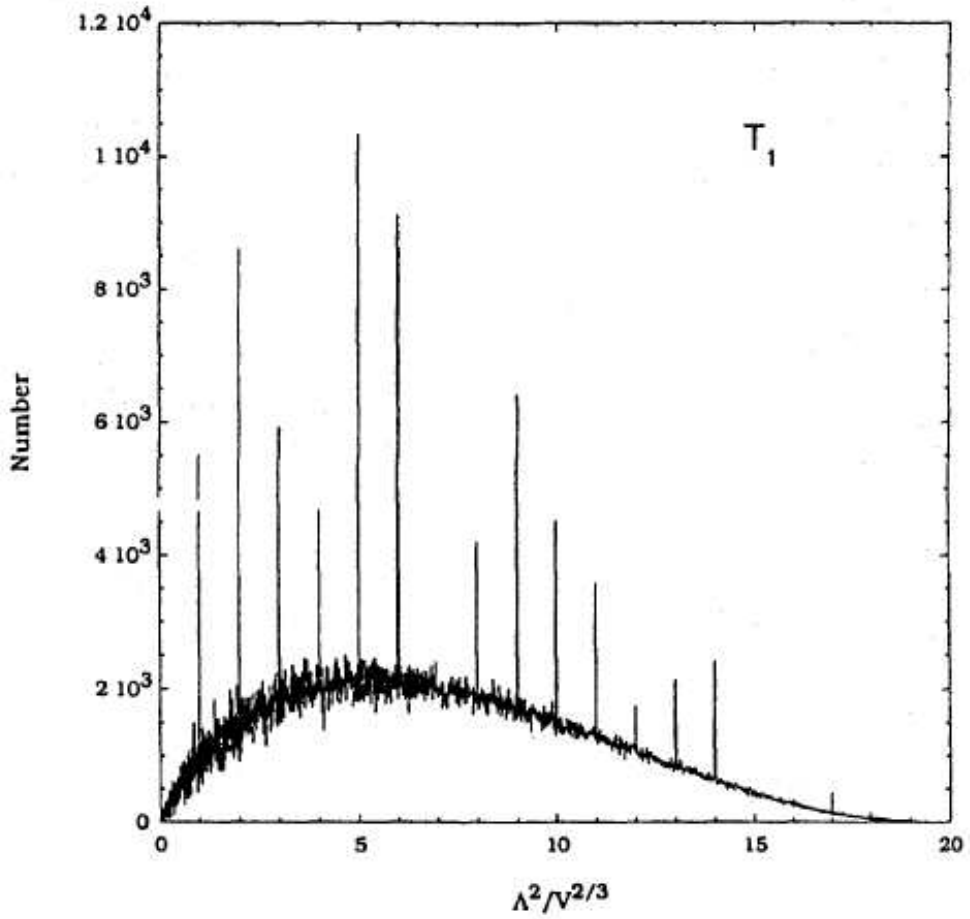

Figure 4.1: Pair Separation Histogram of a simulated 3-torus universe with equal lengths. About 45 copies of the fundamental domain exist in the universe (Lehoucq et al., 1996).

test probe is therefore the cosmic microwave background, which originates from the surface of last scattering — the edge of the visible Universe. A multi connected universe affects the cosmic microwave background in subtle but measurable ways.

If the radius of the surface of last scattering is larger than the inner radius of the fundamental domain (r_{in}) then the surface of last scattering will intersects with itself. This means that the temperature of certain points on the CMB are the same as the temperature of certain other points, because physically the are the same set of points in space. The fact that all of the SLS is at the same distance (r_{SLS}) assures that any ghost images will be of the same age, therefore there will be no difference in evolution unlike with 3D concrete methods. This will enlarge the possibility of detecting them significantly.

The non-statistical circle method tries to detect these ghost images (which are circles in 3D) directly.

Circles

The intersection of the last scattering surface is a circle. This circle can be seen from both sides, and will therefore appear in two directions on the CMB. In principle one can scan the CMB for such identical circles and from there reconstruct the isometries that define the fundamental domain.

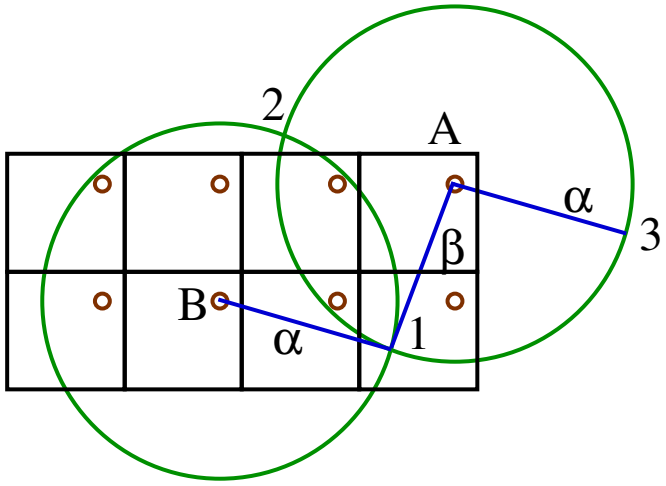

Figure 4.2: The surface of last scattering in a 2 dimensional toroidal universe. The observer is in the small brown circles. The surface of last scattering for two of them is shown as the green circle. At two places the green circles intersect, at point 1 and 2. The observer at B sees a spot 1 in direction α, the observer at point A sees it in direction β. But since the both observers are the same, the observer sees point 1 in both directions. In 3 dimensions these points will be circles.

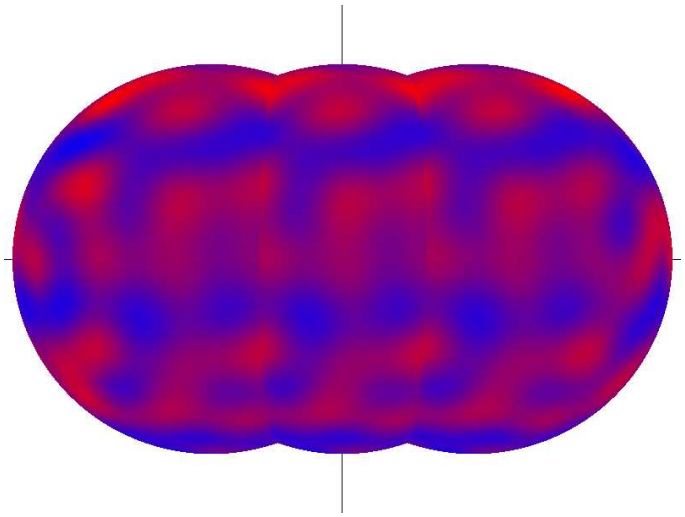

Figure 4.3: This figure is the 3 dimensional analog of figure (4.2). Instead of two circles of last scattering, we have here 3 spheres of last scattering. The observer (us) is in the center of all three spheres. The CMB of the middle observer intersects the CMB of the left observer. Therefore he will see the same circle on the CMB also in the exact opposite direction (in this case of a toroidal universe).

Because this method is model independent, it can provide direct conclusions about the topology of any universe. If matched circles are found, it is possible to reconstruct the topology of space (Weeks, 1998). However, finding all possible intersection circles is computational highly demanding. This method is therefore mainly used to verify a certain proposed candidate manifold. A particular example is the search for antipodal circles, i.e. identical circles exactly at opposite positions on the CMB. These are expected to exist for manifolds made with identifications corresponding to translations. Most flat models are an example of this. These however have not been found conclusively, so more difficult manifolds might have to be proposed.

Cornish et al. (2004) have found no evidence for back-to-back matching circles within the range of $25° - 90°$. However, Luminet et al. (2003) claim there are pairs of matching circles of $11°$ radius, consistent with a binary dodecahedral space.

4.4 2D Statistical methods: non-Gaussian CMB signatures

The (discrete) search for circles in the CMB has been proven hard, and no conclusive evidence can be derived from it. More promising are statistical methods.

Inflation theory suggests an statistically isotropic Gaussian random distribution of the temperature of the CMB at scales larger then $1°$. However, this is only true for a universe large enough. If we live in a small multi connected universe the CMB would assume a distinctly non-Gaussian character. The spatial distribution of temperature fluctuations of the primordial soup will still be Gaussian but its spherical projection as the CMB will not. Since the CMB might contain several sections of space several times, the temperature fluctuations on the CMB are non-Gaussian.

In classical cosmology the $a_{\ell m}$ in the spherical harmonics decomposition of the CMB

$$\frac{\Delta T(\Omega)}{T} = \sum_{\ell=0}^{\infty} \sum_{m=-\ell}^{\ell} a_{\ell m} Y_{\ell}^{m}(\Omega) \tag{4.4}$$

are drawn from a Gaussian distribution based on ℓ with a power spectrum

$$C_{\ell} = \frac{1}{2\ell+1} \sum_{m=-\ell}^{\ell} a_{\ell m} a_{\ell m}^{*} \tag{4.5}$$

with C_l predicted by the adopted cosmological theory. All the information about the CMB is then contained in the C_ℓ, for fixed ℓ the $a_{\ell m}$ are uncorrelated. However, if the universe is multi-connected the $a_{\ell m}$ will be correlated and the C_ℓ alone does not define the CMB. All statistical 2D methods for determining the topology of the universe are based on this fact.

Studies of the WMAP data show that there might indeed be anisotropies and non Gaussianities in the CMB (Park, 2004; Hajian and Souradeep, 2003; Hajian et al., 2005; Eriksen et al., 2004). Possibly they can be explained with a multi connected universe (Scannapieco et al., 1999; Levin et al., 1998; Rocha et al., 2004; Dineen et al., 2005). For a comprehensive review of statistical methods of topological effects on the CMB see Levin (2002).

By only calculating the power spectrum, ignoring the possible m dependence of the a_{lm} we can still get valuable information about the topology of the universe. Experiments show that the C_l for low l, the quadrupole and octupole moments, are smaller then expected from standard cosmological models. This can be explained by a multi connected universe. If the universe has a limited size in certain directions, then one does not expect large density fluctuations at larger scales. In most universes with a fundamental domain with each primary direction about the same size (i.e. the inscribed sphere is about the same size as the circumscribed sphere) the low l moments get suppressed. When the sizes of the fundamental domain are not comparable however, (like with a 3-torus with one size much smaller then the other two) it might also be that the large l moments get suppressed (Weeks et al., 2004). Gundermann (2005) shows that a spherical binary polyhedral space may explain the low quadrupole.

4.5 Multipole Vectors

Recently, Copi et al. (2004) developed a new statistical method for studying the CMB using multipole vectors. The method comprises the decomposition of the CMB into spherical harmonics, and connects headless vectors, called *multipole vectors*, to the spherical harmonics. In a simply connected universe following standard cosmology, these vectors are nearly independent and oriented randomly. The only information a specific cosmological model adds is the size of the vectors. A multi connected universe might have both an effect on the direction and the size of these vectors. Figure 4.4 shows examples of multipole vectors of a simulated CMB.

4.5.1 Degrees of Freedom

The usual spherical decomposition of the CMB is given by equation 1.18. Because the coefficients $a_{\ell m}$ have to fulfill the reality condition from equation 1.19 the set of coefficients with fixed ℓ contains $2\ell + 1$ degrees of freedom.

Usually the only statistic considered is C_ℓ of the power spectrum (equation 1.20) which is only one degree of freedom. The multipole vector decomposition takes all $2\ell+1$ degrees of freedom into account and therefore offers more room for statistical tests. For every ℓ value there are ℓ headless multipole vectors giving rise to 2ℓ degrees of freedom. The last degree of freedom is a scalar that can be seen as the size of the vectors. This scalar corresponds to the C_ℓ of the power spectrum.

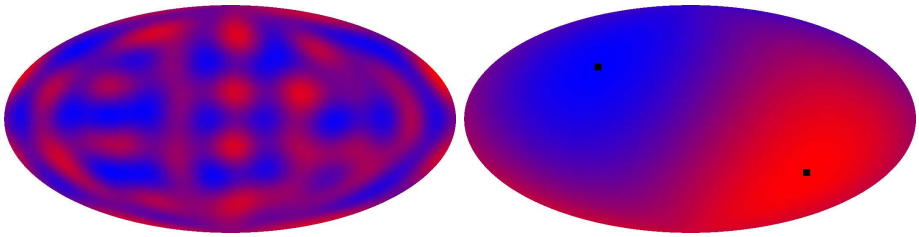

(a) CMB up to $\ell = 10$ (b) Dipole

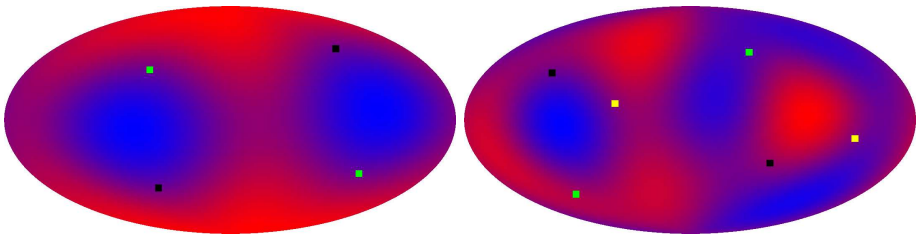

(c) Quadrupole (d) Octupole

Figure 4.4: Multipole vectors for a simulated CMB.

4.5.2 Construction

The principle behind the method is that the decomposition of the CMB in spherical harmonics can be converted into a vector decomposition

$$\sum_{m=-\ell}^{\ell} a_{\ell,m} Y_{\ell,m}(\hat{e}) = A^\ell \left(\hat{v}^{1,\ell} \cdot \hat{e}\right) \left(\hat{v}^{2,\ell} \cdot \hat{e}\right) \ldots \left(\hat{v}^{\ell,\ell} \cdot \hat{e}\right). \tag{4.6}$$

The multipole vectors are denoted by $\hat{v}^{i,\ell}$, i ranging between 1 and ℓ. The scalar is denoted by A^ℓ. The $\hat{e}$ is a unit vector. In general this conversion is not possible because the product on the right hand side will contain terms of lower ℓ, but because the CMB is a real vector field it is.

For the proof of 4.6 and full conversion of the $a_{\ell m}$ we refer to Copi et al. (2004). Katz and Weeks (2004) give a mathematically more rigorous polynomial interpretation of multipole vectors.

4.5.3 Dipole

That the decomposition in equation 4.6 is possible for the dipole can be easily seen. The dipole directly define a vector in space, along the direction in which the dipole lies. The direction of the dipole can be inferred from the directions corresponding to the $\ell = 1$ spherical harmonics:

$$Y_{1,0} \to \hat{z}, \qquad Y_{1,\pm 1} \to \mp \frac{1}{\sqrt{2}} \left(\hat{x} \pm i\hat{y}\right). \tag{4.7}$$

For a real valued density field $v^{1,1}$ is given by

$$v^{1,1} = \begin{pmatrix} -\sqrt{2}a^{\mathrm{re}}_{1,1} \\ \sqrt{2}a^{\mathrm{im}}_{1,1} \\ a_{1,0} \end{pmatrix} \tag{4.8}$$

and $A^1 = |v|$.

In fact the dipole in the CMB is mostly caused by the motion of the Earth. With respect of the surface of last scattering we travel with about 600km/s, which results in a (apparent) dipole in the CMB which is orders of magnitude higher then the primordial dipole. Therefore we are unable to see the primordial dipole in the CMB at all.

4.5.4 Statistics

In this thesis we will decompose simulated CMBs of multi connected spaces into multipole vectors and their directional dependency of will be investigated.We have used the sample code from Copi et al. (2004) for the computation of the multipole vectors. Comparing our simulated results with physical CMB data might give an indication whether we live in a multi connected universe and which one it might be.

The WMAP data has been decomposed into multipole vectors by Copi et al. (2004) and Copi et al. (2005). Their findings are that the low multipole vectors ($\ell = 2$ and $\ell = 3$) align with each other, it even shows an alignment with the plane of the solar system, which is statistically infeasible for standard cosmology. There appears to be a preferred direction in the CMB, which means it is anisotropic. In a multi connected space this is to be expected. On a universal scale the universe is not isotropic but has preferred direction, e.g. a toroidal universe has 3 major axes. It is not unlikely that the low multipole vectors align with or perpendicular to these directions.

Chapter 5

Cosmic Microwave Background Simulations

In this chapter we will describe the mathematics behind our simulations. The model is a two step process:

- Decomposition of eigenmodes of the multi connected space into toroidal (planar) eigenmodes.
- Projection of planar eigenmodes into spherical eigenmodes.

5.1 Conversion between linear eigenmodes to spherical

Research of the fluctuations in the Cosmic Microwave Background (CMB) radiation seems to be the best way to look for signatures of the topology of our universe (see section 4.4). The COBE and WMAP data has a high resolution, yet several attempts to detect traces of topology have been in vain. This might be because the available CMB data still are not good enough. We may also not have a good idea of what we are looking for and, finally, the intended effects are to small to measure. Evidence is accumulating that there is still a lot of foreground noise in the data. More definite conclusions may have have to wait for the PLANCK satellite to be launched.

It is useful to determine how and how much we might detect from a topological signal in the CMB. It is useful, and arguably necessary, that we can make accurate simulations of the CMB in a multi connected universe. Here we describe how several of the flat multi connected spaces can be simulated by a method developed by Riazuelo et al. (2004). We limit ourselves to the orientable flat manifolds. However this technique can be easily extended to all manifolds if the eigenmodes are known (Lehoucq et al., 2002).

As in section 2.3.4, we denote the multi connected space M as a quotient of the universal covering space $\widetilde{M}$ by the holonomy group Γ: $M = \widetilde{M}/\Gamma$. The (primordial) density field of the universe can be decomposed into eigenmodes Υ_k^Γ of the quotient space. These eigenmodes form a subgroup of the group of eigenmodes of the covering space, therefore their eigenvalues will be the same ($-k^2$ in the flat case). This also means that we can write any eigenmode of the multi connected space as a superposition of a basis of eigenmodes of the simply connected space, although the elements of this basis are in general not eigenmodes of the multi connected space itself.

The principle as outlined above will be the basis of this section. The eigenmodes of the multi connected spaces will be calculated as a superposition of the eigenmodes of the torus. Thereafter they will be rewritten as a superposition of the spherical eigenmodes of the universal covering space. These can then be used directly to calculate the CMB. We will assume a static density field, i.e. a field which has not evolved in the course of time. This may be regarded a valid assumption since we are only concerned in the low multipoles ($\ell < 50$). The physical scale corresponding to these multipoles are far larger than the horizon at the decoupling epoch and still reside in the regime of linear growth.

5.1.1 Linear Eigenmodes

The most natural eigenmode basis of a flat space are the planar waves:

$$\Upsilon_{\mathbf{k}}(\mathbf{x}) = e^{i\mathbf{k}\mathbf{x}} \tag{5.1}$$

which is normalized as:

$$\int_{\mathbb{R}^3} \Upsilon_{\mathbf{k}}(\mathbf{x})\Upsilon^*_{\mathbf{k}'}(\mathbf{x})\frac{d^3\mathbf{x}}{(2\pi)^3} = \delta^3(\mathbf{k}-\mathbf{k}') \tag{5.2}$$

Where $\mathbf{x}$ is the 3 dimensional coordinate-space parameter, usually written as $\mathbf{x} = (x, y, z)$ and $\mathbf{k}$ is the 3 dimensional phase-space parameter, usually written as $\mathbf{k} = (k_x, k_y, k_z)$.

Using linear eigenmodes, any complex field (including the real primordial density field) can be written as:

$$\phi(\mathbf{x}, t) = \int \frac{d^3k}{(2\pi)^{\frac{3}{2}}}\phi_{\mathbf{k}}(t)\Upsilon_{\mathbf{k}}(\mathbf{x})\hat{e}_{\mathbf{k}} \tag{5.3}$$

where $\hat{e}_{\mathbf{k}}$ is a complex variable, which is usually a random Gaussian satisfying

$$\langle \hat{e}_{\mathbf{k}}\hat{e}^\star_{\mathbf{k}'}\rangle = \delta^D(\mathbf{k}-\mathbf{k}') \tag{5.4}$$

$\phi_{\mathbf{k}}(t)$ can be written as

$$\phi_{\mathbf{k}}(t) = \phi_k(t)e^{i\theta_{\mathbf{k}}}. \tag{5.5}$$

Since the exponential part can be absorbed into the random variable $e_{\mathbf{k}}$ we can choose ϕ_k to be a real function of k only. This gives rise to the reality equation

$$\hat{e}^\star_{\mathbf{k}} = \hat{e}_{-\mathbf{k}}. \tag{5.6}$$

This relation does not hold for all multi connected spaces, it's equivalent is shown for all spaces.

If we consider a static field, the time dependence of $\phi_k(t)$ can be scraped:

$$\phi(\mathbf{x}) = \int \frac{d^3k}{(2\pi)^{\frac{3}{2}}}\Upsilon_{\mathbf{k}}(\mathbf{x})\phi_k\hat{e}_{\mathbf{k}} \tag{5.7}$$

In this context ϕ_k is a measure for the magnitude of the density fluctuations at scale k. It is determined by the initial conditions one assumes, we leave this unspecified for the moment. For practical applications we can substitute the integral with a summation, taking $dk = \frac{2\pi}{L}$ for some limiting length value L, so $d^3\mathbf{k} = \frac{(2\pi)^3}{V}$. V is the volume of the box (in an approximate calculation) or of the fundamental domain (in a multi connected universe). If the resolution of the simulation is smaller then $d\mathbf{x} = 1/V$ there will be a loss of information. The only artificial thing about the summation is that an upper limit of k has to be chosen. In the compact case, the summation is in fact natural, so expression (5.7) can be written as:

$$\phi(\mathbf{x}) = \frac{(2\pi)^3}{V}\sum_{\mathbf{k}}\Upsilon_{\mathbf{k}}(\mathbf{x})\phi_k\hat{e}_{\mathbf{k}} \tag{5.8}$$

where the summation goes over all (allowed) values of $\mathbf{k}$. In the compact case, the $\hat{e}_{\mathbf{k}}$ need to be normalized by volume as

$$\langle \hat{e}_{\mathbf{k}}\hat{e}^\star_{\mathbf{k}'}\rangle = \frac{V}{(2\pi)^3}\delta_{\mathbf{k}\mathbf{k}'}. \tag{5.9}$$

5.1.2 Spherical Eigenmodes

In situations were we describe the sky, it is usually more appropriate to use spherical harmonics, i.e. they are particularly useful when looking at the projection of the density field on the sky.

$$\mathcal{Y}_{k\ell m}(\mathbf{x}) = \sqrt{\frac{4}{2\pi}}(2\pi)^{\frac{3}{2}}\, j_\ell(kr)\, Y^m_\ell(\Omega) \tag{5.10}$$

where the Y_ℓ^m are spherical harmonics and the j_ℓ are Bessel functions. The spherical eigenmodes are normalized as:

$$\int_{\mathbb{R}^3} \mathcal{Y}_{k\ell m}(\mathbf{x})\mathcal{Y}^*_{k'\ell'm'}(\mathbf{x})\frac{x^2 dx d\Omega}{(2\pi)^3} = \frac{1}{k^2}\delta(k-k')\delta_{\ell\ell'}\delta_{mm'} \tag{5.11}$$

where r is the radial component of $\mathbf{x}$, $r = |\mathbf{x}|$ and Ω the angular component of $\mathbf{x}$, usually written in spherical coordinates (θ, ϕ). The wavenumber k in the spherical decomposition is the same as the absolute value of the wave vector $\mathbf{k}$ in the linear decomposition.

5.1.3 Converting Linear Eigenmodes to Spherical

Linear eigenmodes can be converted to a linear combination of spherical eigenmodes and visa versa. For details see appendix (C.1). The projection of a linear eigenmode onto spherical eigenmodes is given by:

$$\Upsilon_{\mathbf{k}}(\mathbf{x}) = \sum_{\ell=0}^{\infty}\sum_{m=-\ell}^{\ell}\left(i^\ell Y_\ell^{m*}\right)\mathcal{Y}_{k\ell m} \tag{5.12}$$

Using this, equation (5.8) can be written in spherical waves as

$$\phi(\mathbf{x}) = \frac{(2\pi)^3}{V}\sum_{\mathbf{k}}\sum_{\ell=0}^{\infty}\sum_{m=-\ell}^{\ell}\left(i^\ell Y_\ell^{m*}(\hat{k})\right)\mathcal{Y}_{k\ell m}\phi_k\hat{e}_{\mathbf{k}} \tag{5.13}$$

Presently we can only see the primordial density field in the surface of last scattering (SLS). Therefore we are only interested in the field at $|\mathbf{x}| = r = r_{SLS} = x_0$.

$$\phi(\Omega) = \sum_{\ell=0}^{\infty}\sum_{m=-\ell}^{\ell} a_{\ell m}Y_\ell^m(\Omega) \tag{5.14}$$

$$a_{\ell m} = \frac{(2\pi)^3}{V}i^\ell\sum_{\mathbf{k}}\left(\left(Y_\ell^{m*}(\hat{k})\right)j_\ell(kx_0)\phi_k\hat{e}_{\mathbf{k}}\right) \tag{5.15}$$

5.1.4 Implementing Topology

In the next section we shall see that every eigenmode of the compact space $\left(\Upsilon^\Gamma_{\mathbf{k}}\right)$ can be written as a linear combination of linear eigenmodes of the universal covering space $(\Upsilon_{\mathbf{k}})$:

$$\Upsilon^\Gamma_{\mathbf{k}} = \sum_r \chi_r \Upsilon_{\mathbf{k}_r} \tag{5.16}$$

for certain real values of χ_r. The $\mathbf{k}$ are defined using a unitary matrix M as:

$$\mathbf{k}_r = \mathbf{k}M^r \tag{5.17}$$

$\mathbf{k}_0 = \mathbf{k}$ and because M is unitary, every $\mathbf{k}_r$ has the same magnitude k. The χ_r and matrix M will be determined in the next section, for now we will assume there exists such a decomposition. This allows us to write the density field of the multi connected space as:

$$\phi(\mathbf{x}) = \frac{(2\pi)^3}{V}\sum_{\mathbf{k}}\Upsilon^\Gamma_{\mathbf{k}}(\mathbf{x})\phi_k\hat{e}_{\mathbf{k}} \tag{5.18}$$

$$= \frac{(2\pi)^3}{V}\sum_{\mathbf{k}}\sum_r \chi_r\Upsilon_{\mathbf{k}_r}(\mathbf{x})\phi_k\hat{e}_{\mathbf{k}} \tag{5.19}$$

Using equation (5.12) and the fact that all $\mathbf{k}_r$ share the same magnitude we can calculate the $a_{\ell m}$:

$$a_{\ell m} = \frac{(2\pi)^3}{V}4\pi i^\ell\sum_{\mathbf{k}}\sum_r \chi_r\left(\left(Y_\ell^{m*}(\hat{k_r})\right)j_\ell(k_r x_0)\phi_k\hat{e}_{\mathbf{k}}\right) \tag{5.20}$$

To calculate the $a_{\ell m}$ for our CMB simulations we determine the allowed eigenmodes (values of $\mathbf{k}$), in combination with the values for the corresponding χ_r and M_r.

5.2 Eigenmodes of Flat Spaces

In this section the eigenmodes for all flat closed orientable manifolds will be calculated. The spaces are treated in the order

- 3-Torus
- Half Turn Space
- Quarter Turn Space
- Third Turn Space
- Sixth Turn Space
- Hantzsche-Wendt Space

Every flat multi connected space can be seen as a quotient space $M = \mathbb{E}^3/\Gamma$, where Γ is the holonomy group. In order to get a plausible physical space (see section 2.4.1 about the cosmological principle), Γ has to be discrete and fixed point free. This means that eigenmode Υ of the quotient space corresponds to an eigenmode of the Euclidean space $\mathbb{E}^3$ that is periodic in the isometries of the holonomy group, this reduces the problem to finding these periodic eigenmodes.

The group of planar waves form a complete basis of eigenmodes of $\mathbb{E}^3$, therefore the subgroup of the planar waves that is periodic in the isometries from the holonomy group is a complete basis of the quotient space. Every discrete fixed point free isometry of $\mathbb{E}^3$ is composed of a rotation/reflection and/or a translation. Therefore each isometry Λ takes $\mathbf{x}$ to $\mathbf{x}'$ as follows:

$$\Lambda : \mathbf{x} \mapsto M\mathbf{x} + T \tag{5.21}$$

where M is the rotation/reflection matrix and T the translation vector. These isometries take every planar wave Υ to another planar wave:

$$\begin{aligned} \Lambda : \Upsilon_{\mathbf{k}}(\mathbf{x}) &\mapsto e^{i\mathbf{k}(M\mathbf{x}+T)} \\ &= e^{i\mathbf{k}M\mathbf{x}} e^{\mathbf{k}T} \\ &= e^{i\mathbf{k}T} \Upsilon_{\mathbf{k}M}(\mathbf{x}) \end{aligned} \tag{5.22}$$

For the planar wave to be periodic in Λ the conditions $M = \mathbb{1}$ and $e^{i\mathbf{k}T} = 1$ must be met. This restricts the choice of isometries greatly. However there exists a subgroup of planar waves that has lesser restrictions:

$$\{\Upsilon_{(\mathbf{k})}, \Upsilon_{(\mathbf{k}M)}, \Upsilon_{(\mathbf{k}M^2)}, \ldots, \Upsilon_{(\mathbf{k}M^{n-1})}\} \tag{5.23}$$

with n the lowest integer that fulfills $M^n = \mathbb{1}$. Under the action of the isometry, this subgroup maps to itself. There exist an integer value of n since we assume the transformation is discrete, usually merely the order of the matrix M. This basis fixes a specific eigenmode:

$$\Upsilon^{\Lambda}_{\mathbf{k}} = a_0 \Upsilon_{\mathbf{k}} + a_1 \Upsilon_{\mathbf{kM^1}} + \ldots + a_{n-1} \Upsilon_{\mathbf{k}M^{n-1}} \tag{5.24}$$

$$a_{j+1} = e^{i\mathbf{k}M^j T} a_j \tag{5.25}$$

This element will therefore be periodic in $\mathbb{E}^3$ by the isometry Λ since every term maps to another term:

$$\begin{aligned} \Lambda : a_j \Upsilon_{\mathbf{kM^j}} &\mapsto a_j e^{i\mathbf{k}M^j T} \Upsilon_{\mathbf{k}M^{j+1}}(\mathbf{x}) \\ &= a_{j+1} \Upsilon_{\mathbf{kM^{j+1}}} \end{aligned} \tag{5.26}$$

$$\begin{aligned} \Lambda : a_{n-1} \Upsilon_{\mathbf{kM^{n-1}}} &\mapsto a_{n-1} e^{i\mathbf{k}M^{n-1}T} \Upsilon_{\mathbf{k}M^n}(\mathbf{x}) \\ &= a_n \Upsilon_{\mathbf{k}} \\ &= a_0 \Upsilon_{\mathbf{k}} \end{aligned} \tag{5.27}$$

If we find an eigenmode which is periodic in all isometries of the holonomy group then we have found an eigenmode which is also an eigenmode of the quotient space. We will show that just like all isometries of a general flat quotient space form a subgroup of the Euclidean space, the isometries of any flat compact space other then the torus form a subgroup of the isometries of a torus. This means that it is mathematically much easier to find all possibilities then was previously expected.

5.2.1 Eigenmodes of the 3-Torus

The 3-Torus is the most simple case and will function as a basis for most other spaces we will investigate. The generators of the holonomy group of 3-torus are 3 translations so $M = \mathbb{1}$, this means that $n = 1$ as well and all the eigenmodes need to fulfill is:

$$e^{i\mathbf{k}T} = 1 \tag{5.28}$$

for all T. This means that $\mathbf{k}T_1 = n_1 2\pi$, $\mathbf{k}T_2 = n_2 2\pi$ and $\mathbf{k}T_3 = n_3 2\pi$. In general the three translations span a parallelepiped:

$$T_1 = \begin{pmatrix} L_{1x} \\ L_{1y} \\ L_{1z} \end{pmatrix}, T_2 = \begin{pmatrix} L_{2x} \\ L_{2y} \\ L_{2z} \end{pmatrix}, T_3 = \begin{pmatrix} L_{3x} \\ L_{3y} \\ L_{3z} \end{pmatrix} \tag{5.29}$$

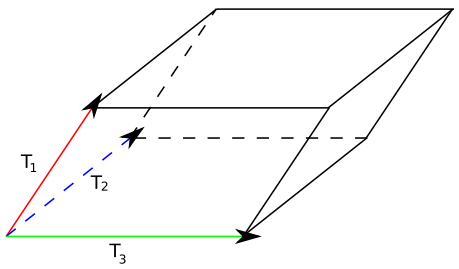

Figure 5.1: The three generators of the holonomy group of the torus span a parallelepiped.

In general this parallelepiped forms a fundamental domain that is not a Dirichlet domain. All parallelepipeds can be transformed in a hexagonal prism which is a Dirichlet domain. Since these are easier to visualise these will be used. A cuboid is simply a hexagonal prism with one of it's lengths 0. For simplicity we will limit ourselves here to cuboids and regular hexagonal prisms but the principle works for all parallelepipeds. Limiting to cuboids we have:

$$T_1 = \begin{pmatrix} L_x \\ 0 \\ 0 \end{pmatrix}, T_2 = \begin{pmatrix} 0 \\ L_y \\ 0 \end{pmatrix}, T_3 = \begin{pmatrix} 0 \\ 0 \\ L_z \end{pmatrix} \tag{5.30}$$

this gives us allowed $\mathbf{k}$ values of

$$\mathbf{k} = \left(\frac{n_x}{L_x}, \frac{n_y}{L_y}, \frac{n_z}{L_z} \right) 2\pi \tag{5.31}$$

Equation (5.8) can be rewritten as

$$\phi(\mathbf{x}) = \frac{(2\pi)^3}{L_x L_y L_z} \sum_{\mathbf{k}} e^{i\mathbf{k}\mathbf{x}} \hat{e}_{\mathbf{k}} \tag{5.32}$$

Since this has to be real for every $\mathbf{x}$, all parts within the sum with the same k should sum up to a real value as well:

$$e^{i\mathbf{kx}}\hat{e}_{\mathbf{k}} + e^{-i\mathbf{kx}}\hat{e}_{-\mathbf{k}} = e^{-i\mathbf{kx}}\hat{e}^*_{\mathbf{k}} + e^{i\mathbf{kx}}\hat{e}^*_{-\mathbf{k}} \quad (5.33)$$

$$\hat{e}_{\mathbf{k}} = \hat{e}^*_{-\mathbf{k}} \quad (5.34)$$

Note the above bears striking similarity to the classical Fast Fourier Transform (FFT). However, the design of the FFT imposes its own conditions on the allowed wave vectors. In this case they are the same as these imposed by the topological shape. In general they will not be compatible, and the use of a FFT would limit the scope of the simulation to tori. In the following we will introduce a new basis for the 3-torus not compatible with the FFT.

Hexagonal Torus

One can also choose a hexagon as base for the fundamental domain. The transformation corresponding to a hexagonal torus are

$$T_1 = \begin{pmatrix} L \\ 0 \\ 0 \end{pmatrix}, T_2 = \begin{pmatrix} -\frac{1}{2}L \\ +\frac{\sqrt{3}}{2}L \\ 0 \end{pmatrix}, T_3 = \begin{pmatrix} -\frac{1}{2}L \\ -\frac{\sqrt{3}}{2}L \\ 0 \end{pmatrix}, T_4 = \begin{pmatrix} 0 \\ 0 \\ L_z \end{pmatrix} \quad (5.35)$$

The first 3 of these combined result in the unit transformation, so we can eliminate 1 of these if we want. Following the same line of reasoning as above we derive the allowed wave vectors $\mathbf{k}$:

$$\mathbf{k} = \left(\frac{n_1}{L}, \frac{2n_1 - n_2}{\sqrt{3}L}, \frac{n_3}{L_z}\right) 2\pi \quad (5.36)$$

The restrictions on $\hat{e}_{\mathbf{k}}$ are the same.

It is not possible to use any fast Fourier transform algorithm to calculate the CMB for a universe with a hexagonal prism as a fundamental domain because the wave vectors $\mathbf{k}$ are all transcendental. A FFT needs rational equidistant wave vectors.

5.2.2 Quotients of the Torus

We will show that any of the other flat compact spaces are quotient spaces of one of the representations of the torus. We know by construction that every isometry we have is discrete and fixed point free. This means that there exist an n which is the lowest integer that fulfills $M^n = \mathbb{1}$. By applying the action of the isometry n times on a point $\mathbf{x}$, we get $\mathbf{x} + T'$ where T' is just a translation. Therefore every isometry is also periodic in that translation.

5.2.3 Half Turn Space

The half turn space is constructed by the isometries of the 3-torus and a half turn corkscrew motion in half the length of one of the axes:

$$\Lambda_1(\mathbf{x}) = (\mathbf{x}) + \begin{pmatrix} L_x \\ 0 \\ 0 \end{pmatrix} \quad (5.37)$$

$$\Lambda_2(\mathbf{x}) = (\mathbf{x}) + \begin{pmatrix} 0 \\ L_y \\ 0 \end{pmatrix} \quad (5.38)$$

$$\Lambda_3(\mathbf{x}) = (\mathbf{x}) + \begin{pmatrix} 0 \\ 0 \\ L_z \end{pmatrix} \quad (5.39)$$

$$\Lambda_4(\mathbf{x}) = \begin{pmatrix} -1 & 0 & 0 \\ 0 & -1 & 0 \\ 0 & 0 & 1 \end{pmatrix} (\mathbf{x}) + \begin{pmatrix} 0 \\ 0 \\ L_z/2 \end{pmatrix} \quad (5.40)$$

We can eliminate Λ_3 since it is the same as Λ_4 applied twice. It would also be suitable if we used twice the length for the z-axes, $L'_z = 2L_z$, we choose L_z as the size of the covering torus in which the isometry is periodic. We already know what subspace of flat eigenmodes are preserved by the first 3 isometries, we have to find out which of these are also preserved by the 4th isometry. We can find these by applying equations (5.24) and (5.25). The subgroup that is preserved when starting from Υ_{k_x,k_y,k_z} ($\mathbf{k} = 2\pi(n_x/L_x, n_y/L_y, n_z/L_z)$)is

$$\left\{\Upsilon_{k_x,k_y,k_z}, \Upsilon_{-k_x,-k_y,k_z}\right\} \tag{5.41}$$

It should be noted that this subgroup is the same as the subgroup generated by $\Upsilon_{-k_x,-k_y,k_z}$. Hence we must choose one of the half planes covered by k_x and k_y. We choose that either k_x is positive, or $k_x = 0$ and k_y is positive or the special case when both $k_x = 0$ and $k_y = 0$.

Equation (5.24) is applied to determine the preserved element. When both $k_x \neq 0$ and $k_z \neq 0$ the element is

$$\Upsilon^{\Lambda}_{\mathbf{k}} = \Upsilon_{k_x,k_y,k_z} + (-1)^{n_z}\Upsilon_{-k_x,-k_y,k_z}, \tag{5.42}$$

when k_z is even

$$\Upsilon^{\Lambda}_{0,0,k_z} = 2\Upsilon_{0,0,k_z} \tag{5.43}$$

Table (5.1) lists the χ_r values for the half turn space.

r	0	1	conditions
χ_r	$\frac{1}{\sqrt{2}}$	$\frac{(-1)^{n_z}}{\sqrt{2}}$	for $(n_x > 0)$
	1	0	for $(n_x = n_y = 0, n_z = 2\mathbb{Z})$

Table 5.1: χ_r values for the half turn space

In order to be sure the field will be real a different condition is needed than in case of the torus. By accumulating all terms with the same $\mathbf{k}$ values and require that to be real we get

$$\hat{e}^*_{k_x,k_z,k_z} = (-1)^{n_z}\hat{e}_{k_x,k_y,-k_z} \tag{5.44}$$

5.2.4 Quarter Turn Space

The quarter turn space is very similar to the half turn space, except that it is turned 4 times before being aligned in the same way again. Therefore we add a quarter turn corkscrew motion to the torus (we leave away the 3 torus isometries):

$$\Lambda_4(\mathbf{x}) = \begin{pmatrix} 0 & -1 & 0 \\ 1 & 0 & 0 \\ 0 & 0 & 1 \end{pmatrix}(\mathbf{x}) + \begin{pmatrix} 0 \\ 0 \\ L_z/4 \end{pmatrix} \tag{5.45}$$

This implies that $L_x = L_y$ because the sides have to match when the fundamental domain is turned a quarter circle. We can again remove the third isometry from the torus since it is the same as applying Λ_4 4 times. If we again take $\Upsilon_{\mathbf{k}}$ as a element we see that the preserved subgroup corresponding with it is

$$\left\{\Upsilon_{k_x,k_y,k_z}, \Upsilon_{-k_y,k_x,k_z}, \Upsilon_{-k_x,-k_y,k_z}, \Upsilon_{k_y,-k_x,k_z}\right\} \tag{5.46}$$

Since the group is symmetric in k_x and k_y, the groups generated by Υ_{k_x,k_y,k_z} is also generated by the Υ_{k_y,k_x,k_z}, therefore we should exclude the subgroups generated by Υ_{k_x,k_y,k_z} with negative k_x or k_y, and take care when handling the special cases when either one of them or both are 0. The corresponding preserved eigenmodes are

$$\Upsilon^{\Lambda}_{k_x,k_y,k_z} = \Upsilon_{k_x,k_y,k_z} + i^{n_z}\Upsilon_{-k_y,k_x,k_z} + i^{2n_z}\Upsilon_{-k_x,-k_y,k_z} + i^{3n_z}\Upsilon_{k_y,-k_x,k_z} \tag{5.47}$$

r	0	1	2	3	condition
χ_r	$\frac{1}{2}$	$\frac{i^{n_z}}{2}$	$\frac{i^{2n_z}}{2}$	$\frac{i^{3n_z}}{2}$	for $(n_x \in \mathbb{Z}^+, n_y \in \mathbb{Z}^a \cup 0, n_z \in \mathbb{Z})$
	1	0	0	0	for $(n_x = n_y = 0, n_z \in 4\mathbb{Z})$

Table 5.2: χ_r coefficients for the half turn space.

In the special case that $n_x = n_y = 0$ the set reduces to $\{\Upsilon_{0,0,k_z}\}$ and $\Upsilon_{0,0,k_z}$ will be preserved when $n_z \in 4\mathbb{Z}$. The full set of χ_r for the quarter turn space are given in table(5.2).

The restrictions on $\hat{e}_{\mathbf{k}}$ are the same as at the half turn space: When $k_z \neq 0$, k_z is a complex random variable fulfilling

$$\hat{e}^*_{k_x,k_z,k_z} = (-1)^{n_z} \hat{e}_{k_x,k_y,-k_z} \tag{5.48}$$

and when $k_z = 0$, $\hat{e}_k$ is a real variable.

5.2.5 Third Turn Space

The third turn space can be best described as a quotient of the hexagonal representation of the torus. Together with the 4 known isometries of the hexagonal torus we also add a third turn corkscrew motion.

$$\Lambda_1(\mathbf{x}) = (\mathbf{x}) + \begin{pmatrix} L \\ 0 \\ 0 \end{pmatrix} \tag{5.49}$$

$$\Lambda_2(\mathbf{x}) = (\mathbf{x}) + \begin{pmatrix} -\frac{1}{2}L \\ +\frac{\sqrt{3}}{2}L \\ 0 \end{pmatrix} \tag{5.50}$$

$$\Lambda_3(\mathbf{x}) = (\mathbf{x}) + \begin{pmatrix} -\frac{1}{2}L \\ -\frac{\sqrt{3}}{2}L \\ 0 \end{pmatrix} \tag{5.51}$$

$$\Lambda_4(\mathbf{x}) = (\mathbf{x}) + \begin{pmatrix} 0 \\ 0 \\ L_z \end{pmatrix} \tag{5.52}$$

$$\Lambda_5(\mathbf{x}) = \begin{pmatrix} -\frac{1}{2} & -\frac{\sqrt{3}}{2} & 0 \\ \frac{\sqrt{3}}{2} & -\frac{1}{2} & 0 \\ 0 & 0 & 1 \end{pmatrix} (\mathbf{x}) + \begin{pmatrix} 0 \\ 0 \\ \frac{1}{2}L_z \end{pmatrix} \tag{5.53}$$

As above, we can eliminate any of the first 3 isometries by linear combination of the latter 2. The 4th isometry is also a linear superposition of the 5th. This fixes the element

$$\Upsilon_{\mathbf{k}} + e^{\frac{1}{3}i2\pi}\Upsilon_{\mathbf{k}M} + e^{\frac{2}{3}i2\pi}\Upsilon_{\mathbf{k}M^2}. \tag{5.54}$$

Where the $\mathbf{k}M$ are given by

$$\mathbf{k} = 2\pi\left(\frac{-n_2}{L}, \frac{2n_1 - n_2}{\sqrt{3}L}, \frac{n_3}{L_z}\right) \tag{5.55}$$

$$\mathbf{k}M = 2\pi\left(\frac{n_1}{L}, \frac{2n_2 - n_1}{\sqrt{3}L}, \frac{n_3}{L_z}\right) \tag{5.56}$$

$$\mathbf{k}M^2 = 2\pi\left(\frac{n_2 - n_1}{L}, \frac{-n_1 - n_2}{\sqrt{3}L}, \frac{n_3}{L_z}\right) \tag{5.57}$$

By the same line of reasoning as above we can calculate the χ_r values given in table (5.3). The corresponding constraints on $\hat{e}_{\mathbf{k}}$ are

$$\hat{e}^*_{n_1,n_2,n_3} = \begin{cases} e^{\frac{2n_3}{3}2\pi i}\hat{e}_{n_2,n_2-n_1,-n_3} & \text{when } n_2 > n_1, \\ e^{\frac{n_3}{3}2\pi i}\hat{e}_{n_1-n_2,n_1,-n_3} & \text{when } n_2 \leq n_1. \end{cases} \tag{5.58}$$

r	0	1	2	condition
χ_r	$\frac{1}{\sqrt{3}}$	$\frac{e^{\frac{1}{3}i2\pi}}{\sqrt{3}}$	$\frac{e^{\frac{2}{3}i2\pi}}{\sqrt{3}}$	for $(n_1 \in \mathbb{Z}^+, n_2 \in \mathbb{Z}^+ \cup 0, n_z \in \mathbb{Z})$
	1	0	0	for $(n_1 = n_2 = 0, n_3 \in 3\mathbb{Z})$

Table 5.3: χ_r coefficients for the third turn space.

5.2.6 Sixth Turn Space

The procedure for the sixth turn space is very similar to the third turn space, except we add a sixth turn corkscrew motion instead of a third turn:

$$\Lambda_5(\mathbf{x}) = \begin{pmatrix} \frac{1}{2} & -\frac{\sqrt{3}}{2} & 0 \\ \frac{\sqrt{3}}{2} & \frac{1}{2} & 0 \\ 0 & 0 & 1 \end{pmatrix}(\mathbf{x}) + \begin{pmatrix} 0 \\ 0 \\ \frac{1}{6}L_z \end{pmatrix} \tag{5.59}$$

the fixed eigenmodes is

$$\frac{1}{\sqrt{6}}\left(\Upsilon_{\mathbf{k}} + \zeta^{n_3}\Upsilon_{\mathbf{k}M} + \zeta^{2n_3}\Upsilon_{\mathbf{k}M^2} + \zeta^{3n_3}\Upsilon_{\mathbf{k}M^3} + \zeta^{4n_3}\Upsilon_{\mathbf{k}M^4} + \zeta^{5n_3}\Upsilon_{\mathbf{k}M^5}\right) \tag{5.60}$$

where ζ is a sixth root unit vector $\zeta = e^{\frac{i}{6}2\pi}$. When $n_1 = n_2 = 0$ this is reduced to just $\Upsilon_{0,0,k_3}$ for $k_3 \in 3\mathbb{Z}$. The χ_r are given in table (5.4). The corresponding $\mathbf{k}$ vectors are

r	0	1	2	3	4	5	condition
χ_r	$\frac{1}{\sqrt{6}}$	$\frac{\zeta^{n_3}}{\sqrt{6}}$	$\frac{\zeta^{2n_3}}{\sqrt{6}}$	$\frac{\zeta^{3n_3}}{\sqrt{6}}$	$\frac{\zeta^{4n_3}}{\sqrt{6}}$	$\frac{\zeta^{5n_3}}{\sqrt{6}}$	for $(n_1 \in \mathbb{Z}^+, n_2 \in \mathbb{Z}^+ \cup 0, n_2 < n_1, n_z \in \mathbb{Z})$
	1	0	0	0	0	0	for $(n_1 = n_2 = 0, n_3 \in 6\mathbb{Z})$

Table 5.4: χ_r coefficients for the sixth turn space.

$$\mathbf{k} = 2\pi\left(\frac{-n_2}{L}, \frac{2n_1 - n_2}{\sqrt{3}L}, \frac{n_3}{L_z}\right), \tag{5.61}$$

$$\mathbf{k}M^1 = 2\pi\left(\frac{n_1 - n_2}{L}, \frac{n_1 + n_2}{\sqrt{3}L}, \frac{n_3}{L_z}\right), \tag{5.62}$$

$$\mathbf{k}M^2 = 2\pi\left(\frac{n_1}{L}, \frac{-n_1 + 2n_2}{\sqrt{3}L}, \frac{n_3}{L_z}\right), \tag{5.63}$$

$$\mathbf{k}M^3 = 2\pi\left(\frac{n_2}{L}, \frac{-2n_1 + n_2}{\sqrt{3}L}, \frac{n_3}{L_z}\right), \tag{5.64}$$

$$\mathbf{k}M^4 = 2\pi\left(\frac{-n_1 + n_2}{L}, \frac{-n_1 - n_2}{\sqrt{3}L}, \frac{n_3}{L_z}\right), \tag{5.65}$$

$$\mathbf{k}M^5 = 2\pi\left(\frac{-n_1}{L}, \frac{n_1 - 2n_2}{\sqrt{3}L}, \frac{n_3}{L_z}\right). \tag{5.66}$$

The constrained on $\hat{e}_{\mathbf{k}}$ is

$$\hat{e}^*_{n_1,n_2,n_3} = \begin{cases} (-1)^{n_3}\hat{e}_{n_1,n_2,-n_3} & \text{when } n_3 \neq 0 \\ real & \text{when } n_3 = 0 \end{cases} \tag{5.67}$$

5.2.7 Hantzsche-Wendt space

Just like the previous Fundamental Domains, also the Hantzsche-Wendt space can be seen as the quotient of a Torus, although this is less clear at first sight. The three isometries of the

Hantzsche-Wendt space are:

$$\Lambda_1(\mathbf{x}) = \begin{pmatrix} 1 & 0 & 0 \\ 0 & -1 & 0 \\ 0 & 0 & -1 \end{pmatrix} + \begin{pmatrix} \frac{1}{2}L_x \\ \frac{1}{2}L_y \\ 0 \end{pmatrix} \tag{5.68}$$

$$\Lambda_2(\mathbf{x}) = \begin{pmatrix} -1 & 0 & 0 \\ 0 & 1 & 0 \\ 0 & 0 & -1 \end{pmatrix} + \begin{pmatrix} 0 \\ \frac{1}{2}L_y \\ \frac{1}{2}L_z \end{pmatrix} \tag{5.69}$$

$$\Lambda_3(\mathbf{x}) = \begin{pmatrix} -1 & 0 & 0 \\ 0 & -1 & 0 \\ 0 & 0 & 1 \end{pmatrix} + \begin{pmatrix} \frac{1}{2}L_x \\ 0 \\ \frac{1}{2}L_z \end{pmatrix} \tag{5.70}$$

Any of these isometries applied twice result in a translation, so indeed the Hantzsche-Wendt space is also a quotient of a torus (of size $L_xL_yL_z/8$). The fixed eigenmode of all 3 isometries is

$$\Upsilon_{k_x,k_y,k_z} + (-1)^{n_x-n_y}\Upsilon_{k_x,-k_y,-k_z} + (-1)^{n_y-n_z}\Upsilon_{-k_x,k_y,-k_z} + (-1)^{n_z-n_x}\Upsilon_{-k_x,-k_y,k_z} \tag{5.71}$$

when 2 of the indexes n_x, n_y, n_z is 0 this gets simplified; if $n_y = n_z = 0$ this reduces to $\Upsilon_{k_x,0,0} + \Upsilon_{-k_x,0,0}$ and respectively for the other combinations. By symmetry arguments we should again restrict the allowed values for n_x, n_y, n_z. This gives us values for χ_r as shown in table (5.5).

r	0	1	2	3	condition
χ_r	$\frac{1}{2}$	$\frac{(-1)^{n_x-n_y}}{2}$	$\frac{(-1)^{n_y-n_z}}{2}$	$\frac{(-1)^{n_z-n_x}}{2}$	for $(n_x, n_y \in \mathbb{Z}^+, n_z \in \mathbb{Z})$ or $(n_y, n_z \in \mathbb{Z}^+, n_x = 0)$ or $(n_x, n_z \in \mathbb{Z}^+, n_y = 0)$
	$\frac{1}{\sqrt{2}}$	0	$\frac{1}{\sqrt{2}}$	0	for $n_y = n_z = 0, n_x \in 2\mathbb{Z}^+$
	$\frac{1}{\sqrt{2}}$	0	0	$\frac{1}{\sqrt{2}}$	for $n_z = n_x = 0, n_y \in 2\mathbb{Z}^+$
	$\frac{1}{\sqrt{2}}$	$\frac{1}{\sqrt{2}}$	0	0	for $n_x = n_y = 0, n_z \in 2\mathbb{Z}^+$

Table 5.5: χ_r coefficients for the Hantzsche-Wendt space.

Chapter 6

Experimental Results

The results of our simulations are given in this chapter. We have simulated the cosmic microwave background (CMB) for each flat orientable multi connected universe. The simulated spaces are treated in the order below

- 3-Torus
- Chimney Space
- Slab Space
- Half Turn Space
- Quarter Turn Space
- Third Turn Space
- Sixth Turn Space
- Hantzsche-Wendt Space

For each space we took some dimensions with fixed size and varied the other. This way it is possible to determine how the signal(s) we might be able to measure depend on the size of the universe. Most of the simulations are done with us (the observers) in very special positions so possible effects of the topology on the CMB are the highest. E.g in the case of the half turn space we are located on the axis of rotation. For each space we generate a realization of a CMB sky along with the corresponding multipole vectors and pairs of matching circles.

6.1 Hypothesis

In a pure Gaussian simply connected space, the multipole vectors are randomly aligned with no preferred directions. All multi connected spaces (with the exception of the projective space) have intrinsic special directions. E.g. in the chimney space one direction is infinite while the others are not. The hypothesis which we pursue are:

1. The multipole vectors are dependent on special directions of the topology of the universe.
2. The multipole vectors become aligned (or anti-aligned) with each other.

The second hypothesis is directly related to the first, i.e. if all the quadrupole align with a specific axis they will also align with themselves. Note that unlike in the real world we have a priori knowledge of what the special directions of our Universe are. The second hypothesis is the only hypothesis we can therefore test in reality. If however, we do have prior knowledge about special directions in the sky — e.g. due to matching circles — we can use the results of this research to calculate probabilities of certain topological shapes.

6.2 Results

6.2.1 Euclidean Space

The simply connected Euclidean space was not simulated directly. The Euclidean case is the limit of the 3-torus, chimney and slap space if we take the closed dimensions very large (i.e. several times the distance of the surface of last scattering).

From figures (6.1(b)) and (6.1(d)) we can deduce that the dipole and quadrupoles indeed do not align themselves to a preferred direction. Note that the quadrupoles do anti-align slightly with each other in the Euclidean case.

6.2.2 Torus

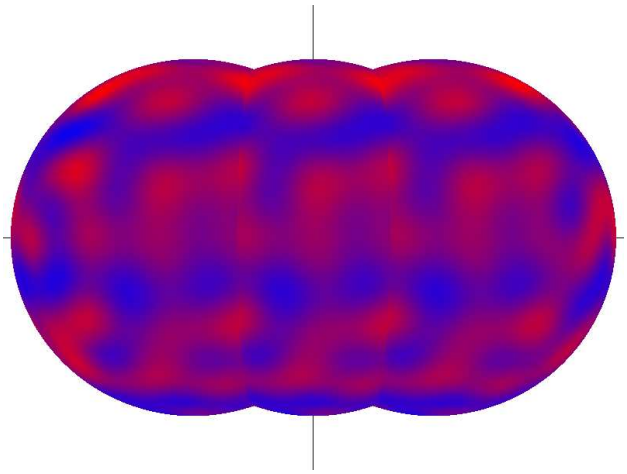

(a) The cosmic microwave background for a cuboid universe with a baselength of $0.8 r_{SLS}$.

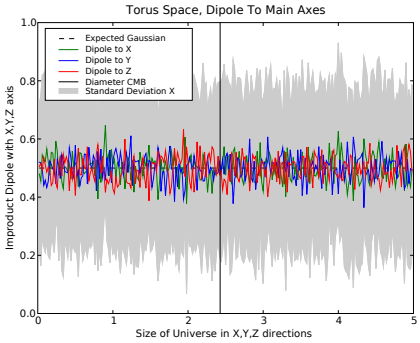

(b) The alignment of the dipole with the 3 axes of the cube is not existent.

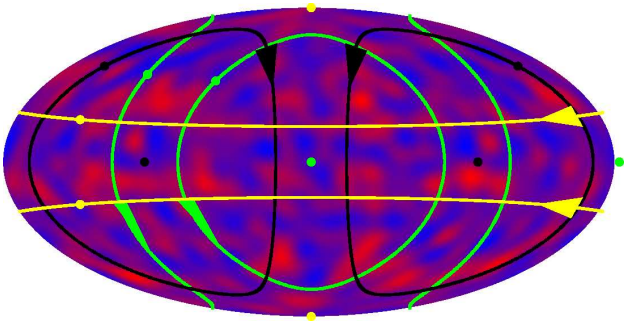

(c) The cosmic microwave background in Aitoff projection. The three largest pairs of matching circles are shown with identification.

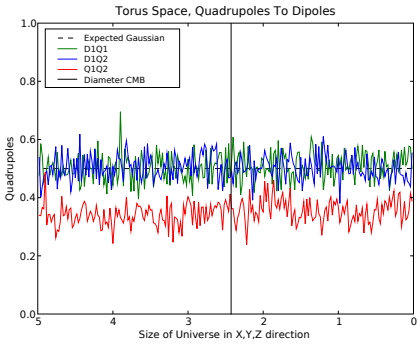

(d) The quadrupole alignment of the cube.

Figure 6.1: Torus

The torus is the simplest case to simulate. We simulated a perfect cuboid torus. The radius of the surface of last scattering is set at $r_{SLS} = 1.2134354$ which is dimensionless and sets the scale of our simulation. The size of the cube is varied between 5 and 0.

Figure (6.2(a)) shows the results of the simulation, 3 instances of the CMB. We (the observers) are in the center of all three spheres and the three CMB's are therefore identical. They fluently disperse into another at the circles where they intersect. Repetitive features can clearly be seen.

Figures (6.1(b)) and (6.1(d)) show the alignment of the dipole and the quadrupole respectively. The dipoles do not (cross)align themselves with any of the axis of the torus, neither with the quadrupoles. This is expected, since the dipole alignment is averaged, and on average there is no distinction between the 3 axes. No research is done on the actual distribution of the alignments, i.e. it might be possible that the dipoles always align with one of the axes but not with a specific one.

6.2.3 Chimney Spaces

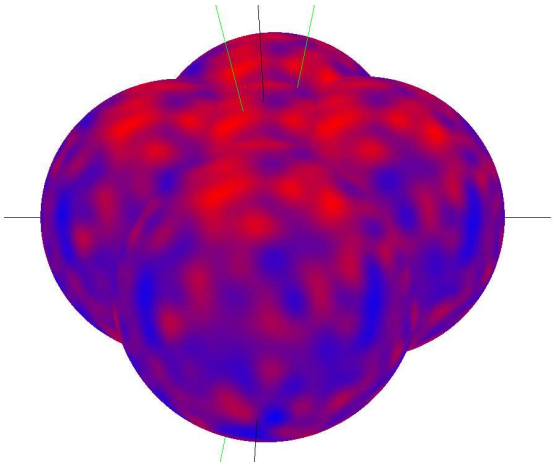

(a) The cosmic microwave background for a chimney space with a square base of $0.8 r_{SLS}$. The two quadrupole vectors are shown.

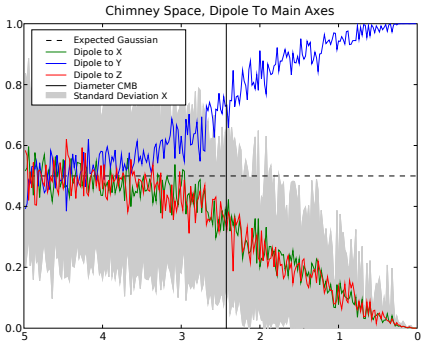

(b) The dipole alignment of the chimney space. The dipole aligns itself with the open direction (Y). It is interesting to see that the effect is already visible before the fundamental domain enters the horizon.

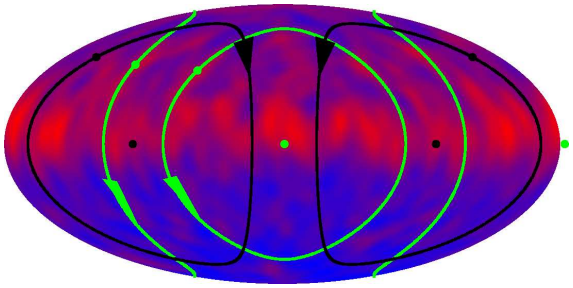

(c) The cosmic microwave background in Aitoff-projection.

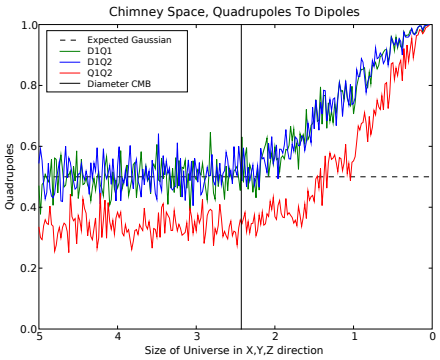

(d) The quadrupole alignments of the chimney space. It is clear that the quadrupoles will align with each other and with the dipole.

Figure 6.2: Chimney Space

For our purposes square chimney spaces are the most simple spaces to consider. For a square chimney space we use a cuboid as fundamental domain. Two sides are equal and will vary in radius, the third side is large, about 10 times the radius of the surface of last scattering to emulate an infinite direction. The finite third direction can be considered infinite for all considerations, the Euclidean case demonstrated this. The size of the square will be varied from 0.1 to 5. The radius of the surface of last scattering is set to $r_{SLS} = 1.2134354$.

Figure (6.2(a)) shows the results of the simulation. 5 instances of the CMB as seen from the outside and the quadrupole vectors are shown. The 5 surfaces of last scattering are chosen in such a manner that the 4 closest ghost copies of the center CMB are shown, corresponding to two generators of the holonomy group. Where two spheres intersect matching circles can be seen.

Note that since the lengths of the generating isometries are smaller then half the diameter of the CMB there are more matching circles from spheres not shown. It is clear that the quadrupole vectors do align themselves with the open direction of the space.

Figures (6.2(b)) and (6.2(d)) show the alignment of the dipole and quadrupole for the chimney space. From (6.2(b)) it is clear that the dipole aligns with the open direction. From (6.2(d)) we can conclude that the dipole and quadrupoles align with each other.

6.2.4 Slab Space

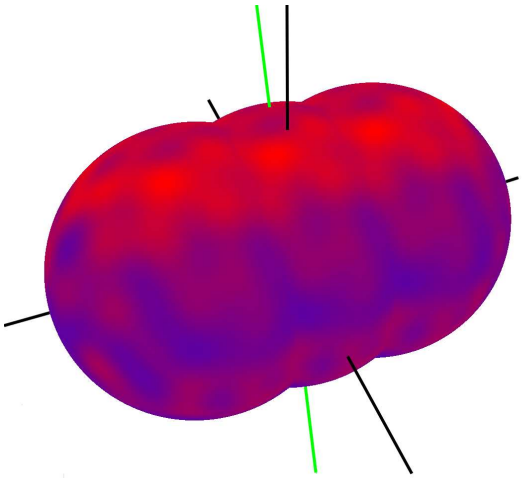

(a) The cosmic microwave background for a slab space with a 'thickness' of $0.8 r_{SLS}$. The dipole vector is shown.

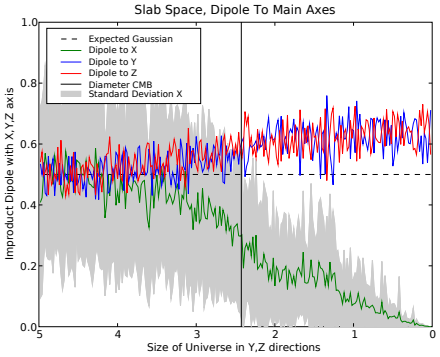

(b) The dipole alignment in the slab space. The dipole drops towards the infinite Y,Z plane. Also here the direction is visible before the short direction of the slab is smaller then the horizon.

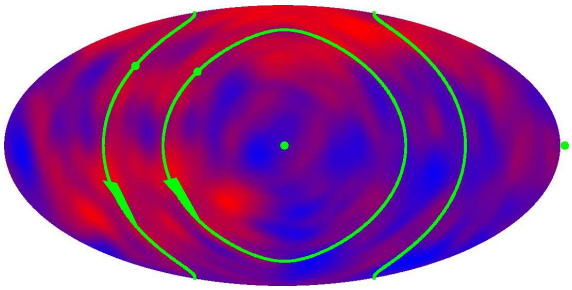

(c) The CMB in aitoff projection

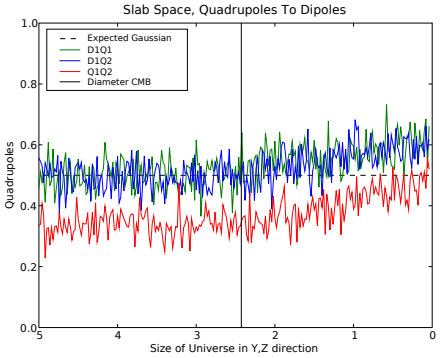

(d) The quadrupole alignment in the slab space. The quadrupoles slightly align with each other, and slightly with the dipole.

Figure 6.3: Slab Space

The slab space is simulated analogously with the chimney space. For a slab space two directions are set fixed at near infinity, the other varies in extent. The other parameters are the same as in the chimney space. Figure (6.3(a)) shows the results of the simulation, 3 instances of the CMB and the dipole vector. The dipole and quadrupole alignments in the slab space are shown in figures (6.3(b)) and (6.3(d)).

6.2.5 Half Turn Space

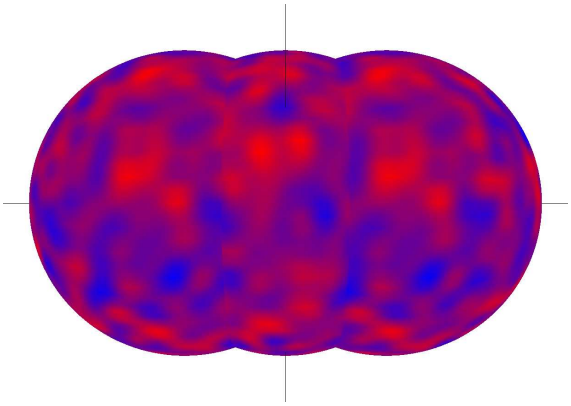

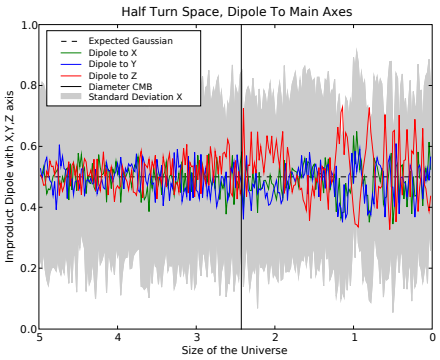

(b) The dipole alignment in the half turn space with a cube fundamental domain. The turn is in the Z-direction. The dipole aligns itself with the rotation axis when the size of the CMB is an integer multiple of the size of the FD.

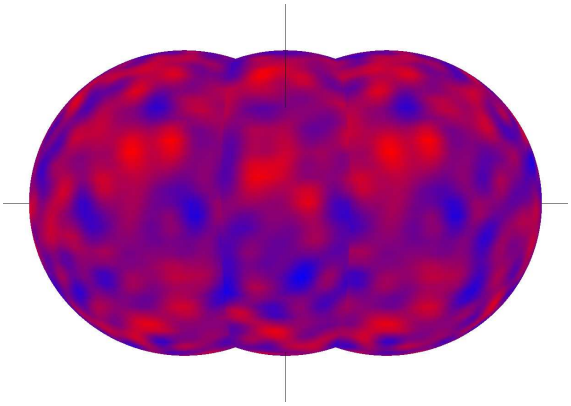

(c) Two images of three times the cosmic microwave background for a half turn space with a 'thickness' of $0.8r_{SLS}$. The lower image is rotated a half turn along the axis of the three spheres. The two outer spheres are the same as the inner spheres, but rotated half a turn so the CMB's have a fluent continuation on the borderlines. The bottom image is shown so it can be verified that all three spheres are actually the same: features on the outer two spheres in the top picture can be seen in the middle sphere in the bottom picture as well.

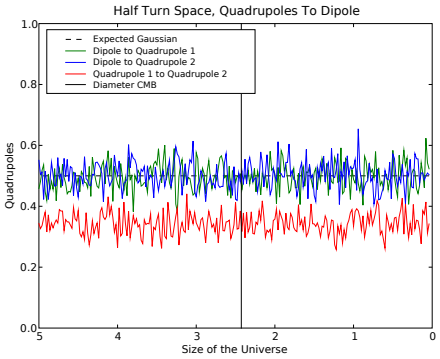

(d) The quadrupole alignment in the halfturn space. The quadrupole is unaligned with the dipole.

Figure 6.4: Half Turn Space

The half turn space is simulated with a cube fundamental domain. All sides are of equal length and varied between 5 and 0. Figure (6.4(c)) shows an realization of the simulation. The dipole and quadrupole alignments in the half turn space are shown in figures (6.4(b)) and (6.4(d)).

6.2.6 Quarter Turn Space

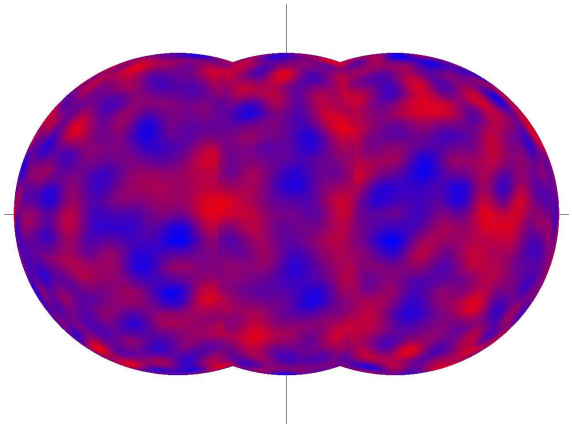

(a) The cosmic microwave background for a quarter turn space with a 'thickness' of $0.8 r_{SLS}$.

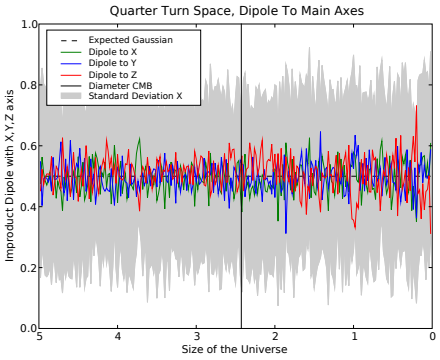

(b) The dipole alignment in the quarter turn space. Although some spikes appear to be visible it is hard to conclude alignment.

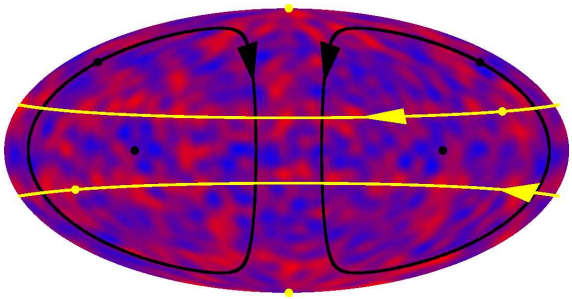

(c) The CMB in aitoff projection. Two pairs of matching circles are shown. The yellow circles have to be rotated a quarter circle as indicated by the yellow dot and arrow to match.

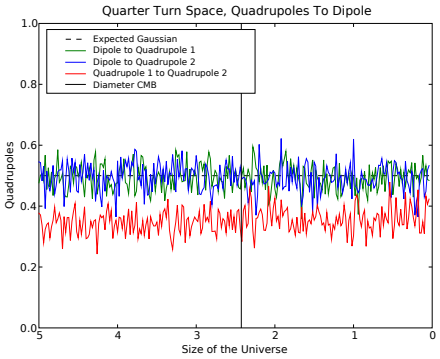

(d) The quadrupole alignment in the quarter-turn space. No alignment is visible.

Figure 6.5: Quarter Turn Space

The quarter turn space is simulated with a cube fundamental domain. All sides are of equal length and varied between 5 and 0. Figure (6.5(a)) shows an realization of the simulation. The dipole and quadrupole alignments in the quarter turn space are shown in figures (6.5(b)) and (6.5(d)).

6.2.7 Third Turn Space

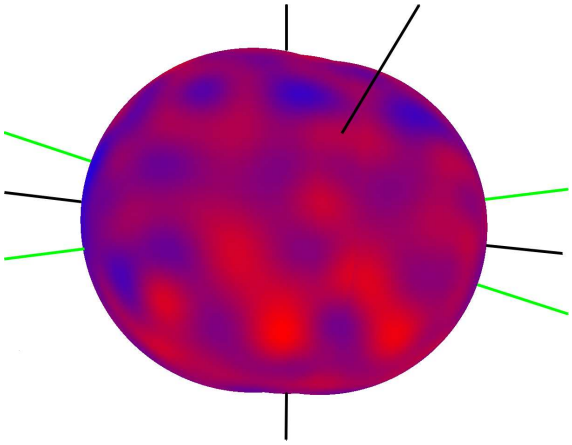

(a) The cosmic microwave background for a third turn space.

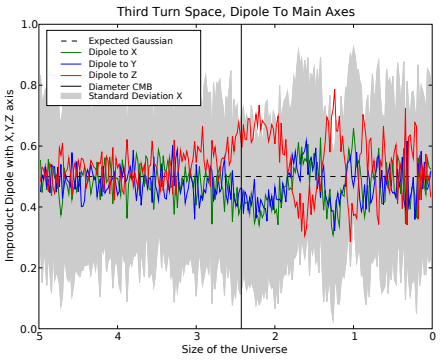

(b) The dipole alignment in the third turn space. The dipole aligns with the rotation axes often at certain sizes, but anti-aligns at other sizes.

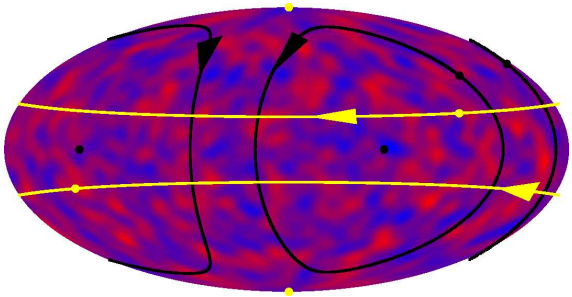

(c) The CMB in Aitoff projection.

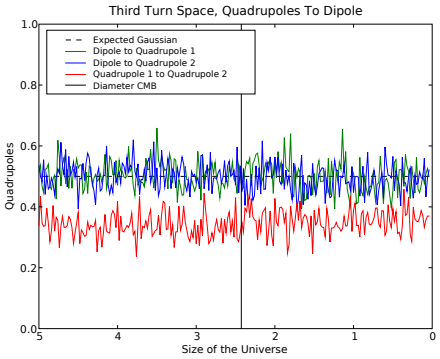

(d) The quadrupole alignment in the third turn space. There is no alignment between the quadrupoles and the dipole.

Figure 6.6: Third Turn Space

The third turn space is simulated with a hexagonal fundamental domain. All sides are of equal length and varied between 5 and 0. Figure (6.6(a)) shows an realization of the simulation. The dipole and quadrupole alignments in the third turn space are shown in figures (6.6(b)) and (6.6(d)).

6.2.8 Sixth Turn Space

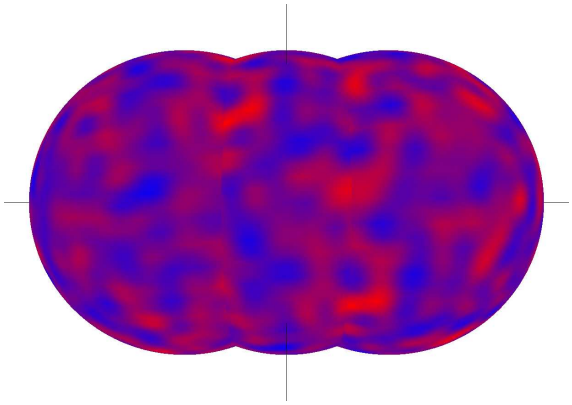

(a) The cosmic microwave background for a sixth turn space.

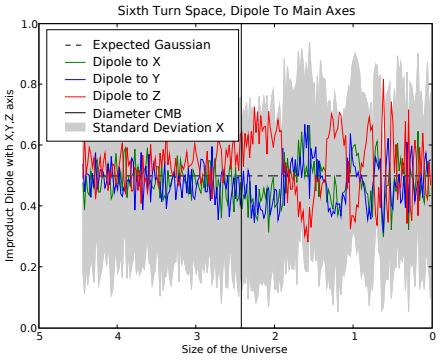

(b) The dipole alignment in the sixth turn space.

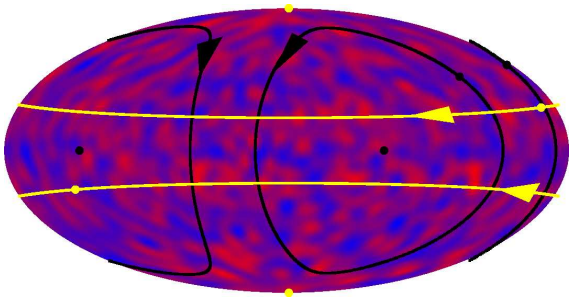

(c) The CMB in Aitoff projection.

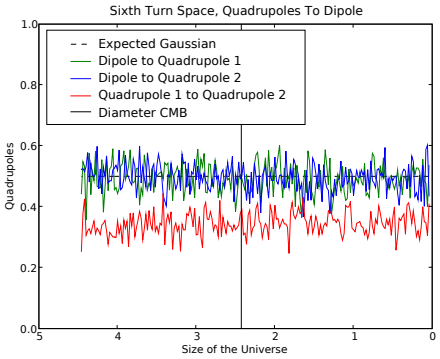

(d) The quadrupole alignment in the sixth turn space.

Figure 6.7: Sixth Turn Space

The sixth turn space is simulated with a hexagonal fundamental domain. All sides are of equal length and varied between 5 and 0. Figure (6.7(a)) shows an realization of the simulation. The dipole and quadrupole alignments in the sixth turn space are shown in figures (6.7(b)) and (6.7(d)).

6.2.9 Hantzsche-Wendt Space

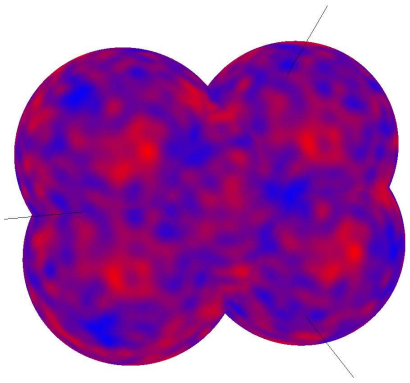

(a) The cosmic microwave background for a Hantzsche-Wendt space.

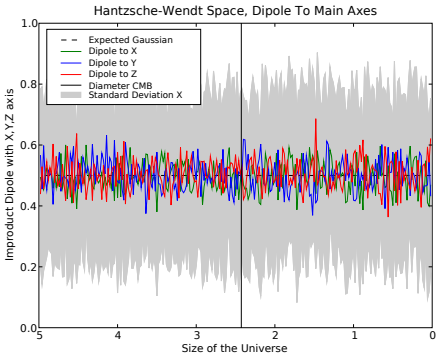

(b) The dipole alignment in the Hantzsche-Wendt space. There is no preference between the three primary direction, which this figure confirms.

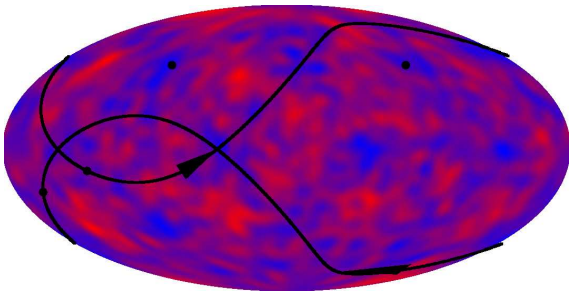

(c) The CMB in Aitoff projection. One pair of matching circles is shown. The circles intersect themselves.

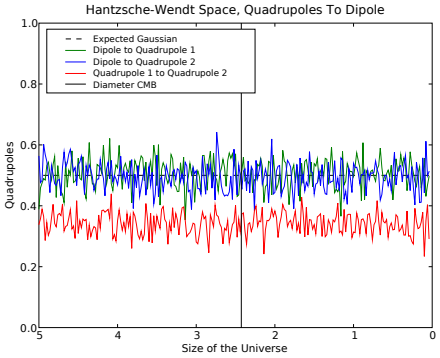

(d) The quadrupole alignment in the Hantzsche-Wendt space.

Figure 6.8: Hantzsche-Wendt Space

The Hantzsche-Wendt space is simulated with a size varied between 5 and 0. This is the size of the cube that has the same volume as the fundamental domain of the Hantzsche-Wendt space. Figure (6.8(a)) shows an realization of the simulation. The dipole and quadrupole alignments in the Hantzsche-Wendt space is shown in figures (6.8(b)) and (6.8(d)).

6.3 Conclusions

6.3.1 Conclusions

All simulated background radiations (CMB) resemble their topologies. By applying the isometries of the holonomy group corresponding to the topology in consideration, the CMB smoothly matches its ghost copy at their circle of intersection. From our simulation we can conclude that

- the effect of the topology on the multipole vectors is more dependent on the size of the fundamental domain than on its specific shape. In the semi-open spaces — the chimney and slab space — the effect on the direction of the multipole vectors is large: in the limit the vectors align themselves perfectly with the open directions.
- The effect of a specific shape is less pronounced. In most of the -turn cases, the dipole does align with the direction of the turn when the size of the fundamental domain in the direction of the rotation is a specific ratio of the size of the cosmic microwave background.
- Effects might be visible even if the scale at which the Universe is multi connected is larger then the diameter of the visible Universe. Figure 6.3(b) of the slab space show that the dipole aligns itself in an open direction even before the closed direction is visible.

6.3.2 Usability

The alignment of the poles with the special axes of the fundamental domain is not measurable a priori since we do not know these special direction before hand. Only if we have a model of a certain shape we can measure the probability that the poles align in the way they do. This is especially difficult with the dipole, i.e. it is hard to infer the intrinsic dipole as the resulting dipole of the Earth's motion is so large.

Therefore we have to conclude that at this moment it is not feasible to use the multipole vector analysis of the CMB to infer a specific topology of the Universe. Nonetheless it might be a valuable tool to check the probability of the existing CMB for a specific proposed model for the topology of the Universe.

6.3.3 Improvement

The simulations in this thesis are still limited in scope. Only spaces with very simple shapes are considered. It is possible to extend the shapes of the fundamental domains to take into account all degrees of freedom that the topologies have. E.g. a hexagonal space might be used for the torus as well and different sizes of the main axes of the FD can be used. Early exploration of these spaces show more statistical alignment anomalies so they might be more easily discovered using this technique.

Also, many of these simulated spaces have the Earth at a special position. In case of the -turn spaces the observer is placed on the axis of rotation, which would be a unlikely coincidence. Dependance on the specific position of the observer should be investigated further.

Appendix A

FLRW Conventions

In section (1.4.3) we used a non-standard notation of the Robertson-Walker metric (RW-metric). This notation is more generic and mathematically more sound. The general expression of the RW-metric used in this thesis is identical to the more commonly used ones. As the conventional metric's we use the one defined by Peacock in his book Cosmological Physics formula 3.12 and 3.10:

$$d\sigma^2 = R^2\left(dr^2 + S_k^2(r)d\Phi^2\right) \tag{A.1}$$

$$d\Phi^2 = d\theta^2 + \sin^2 d\phi^2 \tag{A.2}$$

with S_k depending on curvature

$$S_k(r) = \begin{cases} \sin(r) & (k=1) & \text{Spherical} \\ r & (k=0) & \text{Flat} \\ \sinh(r) & (k=-1) & \text{Hyperbolic} \end{cases} \tag{A.3}$$

where k is the constant of curvature.

Note that the r in the flat case is in units of present-day radius of curvature where r in the other spaces is the comoving angular distance. The r in the flat case has unit of distance, and can be arbitrarily large. The r in the other 2 cases is an dimensionless angle. In the spherical case it can only reach 2π. To convert from angular distance to comoving distance one has to multiply by the absolute value of R. Using different coordinates makes it intrinsically harder to understand the meaning of these metrics then is necessary. Peacock states: "There should of course be two different symbols for the different comoving radii, but each is often called r in the literature, so we have to learn to live with this ambiguity." While it is important to keep in mind that literature uses ambiguous definitions it is important to understand that these 3 metrics are just special cases of a generic one. In the rest of this section we will refer to the 'angular' r as ρ, to avoid confusion.

The generic expression we propose for the metric is

$$d\sigma^2 = dr^2 + \sin\left(\frac{r}{R}\right)^2 R^2 d\Phi^2 \tag{A.4}$$

We disregard the decomposition of the solid angle Φ, since it does not differ between the classical and generic definition. Using a generic solid angle also enables us to use this formula for a universe of arbitrary dimensions. From the general definition we can easily derive the classical spherical, flat and hyperbolic definitions.

Appendix B

Group Theory

A group is a set of elements accompanied by an operator. The operator applied to two elements of the group results in an element that also has to be in the group. In general, when we have a group G and an operator $\otimes$ we have

$$G = \{g_1, g_2, g_3, \ldots\} \tag{B.1}$$

$$g_a \otimes g_b = g_n \tag{B.2}$$

$$g_b \otimes g_a = g_m \tag{B.3}$$

Every group has to have an identity element I. When an element of G is combined with the identity element it returns the element itself. Every element g_a has an inverse element, g_a^{-1} that combined give the identity element.

$$g_a \otimes I = I \otimes g_a = g_a \tag{B.4}$$

$$g_a \otimes g_a^{-1} = g_a^{-1} \otimes g_a = I \tag{B.5}$$

If g_n and g_m from equations B.2 and B.3 are the same for all g_a and g_b we say the group is *Abelian*. The set *generators* of a group are the elements that can generate the entire group by repeatedly applying the operator to these elements. The generators should be independent, i.e. it should not be possible to construct one of the generators by combining the others.

An example of a group is the group of integers $\mathbb{Z} = \{\ldots, -2, -1, 0, 1, 2, \ldots\}$ with respect to the addition operator. The identity element of the integers is $I = 0$ and the inverse of every element is $g_a^{-1} = -g_a$. A possible set of generators of the integers is -1 and 1 since every integer can be generated by adding -1 and or 1 together a finite number of times. Besides an additive group, the set of real numbers form a multiplicative group as well with $I = 1$ and $g_a^{-1} = \frac{1}{g_a}$. The notation of a superscript -1 for the inverse element originates from the multiplicative groups, in general it should not literary be seen as a division. Both these groups are Abelian.

In general the elements of a group do not have to be numbers, they can be anything, from functions to abstract concepts, as long as there is an operator $\otimes$ and an identity element I that obey the rules above.

Appendix C

Simulation

C.1 Converting Linear Eigenmodes to Spherical

These two equations form the key to the conversion from linear to spherical eigenmodes:

$$\sum_{m=-\ell}^{\ell} Y_l^m(\Omega) Y_l^{m*}(\Omega') = \frac{2\ell+1}{4\pi} P_\ell(\cos(\Omega - \Omega') \tag{C.1}$$

$$e^{i\mathbf{kx}} = \sum_{\ell=0}^{\infty} (2\ell+1) i^\ell j_\ell(kx) P_\ell\left(\cos\theta_{\mathbf{k},\mathbf{x}}\right) \tag{C.2}$$

where $\theta_{\mathbf{k},\mathbf{x}}$ is the angle between $\mathbf{k}$ and $\mathbf{x}$. By combining these equations we can rewrite (5.1) as:

$$\begin{aligned}
\Upsilon_{\mathbf{k}}(\mathbf{x}) &= e^{i\mathbf{kx}} && \text{(C.3)}\\
&= \sum_{\ell=0}^{\infty} \sum_{m=-\ell}^{\ell} i^\ell j_\ell(kx) \frac{2\ell+1}{2\ell+1} 4\pi Y_l^m(\hat{x}) Y_\ell^{m*}(\hat{k}) && \text{(C.4)}\\
&= \sum_{\ell=0}^{\infty} \sum_{m=-\ell}^{\ell} \left(i^\ell Y_\ell^{m*}(\hat{k})\right) 4\pi j_\ell(kx) Y_l^m(\hat{x}) && \text{(C.5)}
\end{aligned}$$

With this result we can convert equation (5.8) to spherical eigenmodes:

$$\begin{aligned}
\phi(\mathbf{x}) &= \frac{(2\pi)^3}{V} \sum_{\mathbf{k}} \sum_{\ell=0}^{\infty} \sum_{m=-\ell}^{\ell} \left(i^\ell Y_\ell^{m*}(\hat{k})\right) 4\pi j_\ell(kx) Y_l^m(\hat{x}) \phi_k \hat{e}_{\mathbf{k}} && \text{(C.6)}\\
&= \frac{(2\pi)^3}{V} \sum_{\mathbf{k}} \sum_{\ell=0}^{\infty} \sum_{m=-\ell}^{\ell} \left(i^\ell Y_\ell^{m*}(\hat{k})\right) 4\pi j_\ell\left(kx\right) Y_\ell^m\left(\Omega\right) \phi_k \hat{e}_{\mathbf{k}} && \text{(C.7)}\\
&= \sum_{\ell=0}^{\infty} \sum_{m=-\ell}^{\ell} \frac{(2\pi)^3}{V} i^\ell \sum_{\mathbf{k}} \left(\left(Y_\ell^{m*}(\hat{k})\right) j_\ell\left(kx\right) \phi_k \hat{e}_{\mathbf{k}}\right) Y_\ell^m\left(\Omega\right) && \text{(C.8)}
\end{aligned}$$

C.2 Flat Eigenmodes

We derive the equations of section (5.2). For the isometries themselfs we refer to the main chapter.

C.2.1 Half Turn Space

When k_x, k_z are not both 0, the preserved element is:

$$\begin{aligned}\Upsilon^{\Gamma}_{\mathbf{k}} &= \Upsilon_{\mathbf{k}} + e^{i\mathbf{k}M^1T}\Upsilon_{\mathbf{k}M} \\ &= \Upsilon_{k_x,k_y,k_z} + e^{(-k_x,-k_y,k_z)(0,0,L_z/2)}\Upsilon_{-k_x,-k_y,k_z} \\ &= \Upsilon_{k_x,k_y,k_z} + e^{2\pi n_z/2)}\Upsilon_{-k_x,-k_y,k_z} \\ &= \Upsilon_{k_x,k_y,k_z} + (-1)^{n_z}\Upsilon_{-k_x,-k_y,k_z} \end{aligned} \tag{C.9}$$

otherwise it is:

$$\begin{aligned}\Upsilon^{\Gamma}_{0,0,k_z} &= \Upsilon_{\mathbf{k}} + e^{i\mathbf{k}M^1T}\Upsilon_{\mathbf{k}M} \\ &= \Upsilon_{0,0,k_z} + e^{(0,0,k_z)(0,0,L_z/2)}\Upsilon_{0,0,k_z} \\ &= \Upsilon_{0,0,k_z} + e^{2\pi n_z/2)}\Upsilon_{0,0,k_z} \\ &= \Upsilon_{0,0,k_z} + (-1)^{n_z}\Upsilon_{0,0,k_z} \\ &= 2\Upsilon_{0,0,k_z} \text{when } k_z \text{ is even} \end{aligned} \tag{C.10}$$

We see that $\Upsilon^{\Gamma}_{-k_x,-k_y,k_z}$ is essentially the same element as $\Upsilon^{\Gamma}_{k_x,k_y,k_z}$:

$$\begin{aligned}\Upsilon^{\Gamma}_{-k_x,-k_y,k_z} &= \Upsilon_{-k_x,-k_y,k_z} + (-1)^{n_z}\Upsilon_{k_x,k_y,k_z} \\ &= (-1)^{n_z}\left((-1)^{n_z}\Upsilon_{-k_x,-k_y,k_z} + \Upsilon_{k_x,k_y,k_z}\right) \\ &= (-1)^{n_z}\Upsilon^{\Gamma}_{k_x,k_y,k_z} \end{aligned} \tag{C.11}$$

To calculate the restrictions on $\hat{e}_{\mathbf{k}}$ we first calculate the complex conjugate of the eigenmode.

$$\begin{aligned}\Upsilon^{\Gamma*}_{k_x,k_z,k_z}e^*_{\mathbf{k}} &= \left(\Upsilon^*_{\mathbf{k}} + (-1)^{n_z}\Upsilon^*_{\mathbf{k}M}\right)e^*_{\mathbf{k}} \\ &= \left(\Upsilon^*_{\mathbf{k}} + (-1)^{n_z}\Upsilon^*_{\mathbf{k}M}\right)e^*_{\mathbf{k}} \\ &= \left(\Upsilon^*_{k_x,k_y,k_z} + (-1)^{n_z}\Upsilon^*_{-k_x,-k_y,k_z}\right)e^*_{\mathbf{k}} \\ &= \left(\Upsilon_{-k_x,-k_y,-k_z} + (-1)^{n_z}\Upsilon_{k_x,k_y,-k_z}\right)e^*_{\mathbf{k}} \\ &= (-1)^{n_z}\left((-1)^{n_z}\Upsilon_{-k_x,-k_y,-k_z} + \Upsilon_{k_x,k_y,-k_z}\right)e^*_{\mathbf{k}} \\ &= (-1)^{n_z}\Upsilon^{\Gamma}_{k_x,k_y,-k_z}e^*_{\mathbf{k}} \end{aligned} \tag{C.12}$$

Since the reality condition has to hold for all values of $\mathbf{k}$ and $\mathbf{x}$ — which is the (omitted) parameter of Υ — we have to collect all preserved eigenmodes with terms with the same $\mathbf{k}$ values. In this case this means combining with the preserved eigenmode generated by $\mathbf{k} = (k_x, k_y, -k_z)$. Doing this we get:

$$\hat{e}^*_{k_x,k_z,k_z} = (-1)^{n_z}\hat{e}_{k_x,k_y,-k_z} \tag{C.13}$$

this implies that when $k_z = 0$ the value $\hat{e}_k$ is a real (random) variable. Please note that during this derivation we made several implicit usage of $(-1)^{-n_z} = (-1)^{n_z}$ for $n_z \in \mathbb{Z}$.

C.2.2 Quarter Turn Space

The quarter turn space is very similar to the half turn space. The restrictions on $\hat{e}_{\mathbf{k}}$ are the same as at the half turn space:

$$\begin{aligned}\Upsilon^{\Gamma*}_{k_x,k_y,k_z} &= \Upsilon_{-k_x,-k_y,-k_z} + (-1)^{n_z}i^{n_z}\Upsilon_{k_y,-k_x,-k_z} \\ &\quad +(-1)^{2n_z}i^{2n_z}\Upsilon_{k_x,k_y,-k_z} + (-1)^{3n_z}i^{3n_z}\Upsilon_{-k_y,k_x,-k_z} \\ &= \Upsilon_{-k_x,-k_y,-k_z} + i^{3n_z}\Upsilon_{k_y,-k_x,-k_z} + i^{2n_z}\Upsilon_{k_x,k_y,-k_z} + i^{n_z}\Upsilon_{-k_y,k_x,-k_z} \\ &= (-1)^{n_z}\Upsilon^{\Gamma}_{k_x,k_y,-k_z} \end{aligned} \tag{C.14}$$

$$\sum \Upsilon^{\Gamma*}_{k_x,k_y,k_z}\hat{e}^*_{k_x,k_z,k_z} = \sum (-1)^{n_z}\Upsilon^{\Gamma}_{k_x,k_y,-k_z}\hat{e}_{k_x,k_y,-k_z} \tag{C.15}$$

This can only be fulfilled for all x when $k_z \neq 0$, k_z is a complex random variable fulfilling

$$\hat{e}^*_{k_x,k_z,k_z} = (-1)^{n_z} \hat{e}_{k_x,k_y,-k_z} \tag{C.16}$$

and when $k_z = 0$, $\hat{e}_k$ is a real variable.

Appendix D

Glossary

- **Acoustic Peaks (in the CMB)** Largest peaks in the *power spectrum*. After the *big bang* the (matter)densities Universe oscillated due to gravity and pressure. At *decoupling* the pressure dropped and the oscillations froze in phase. Densities in a maximum or minimum of their oscillations show as peaks in the *power spectrum* of the *CMB*.
- **Affine Point** The intersection point of two parallel *geodesics*. This point is not part of the plane in which the geodesics lie, on the *Poincaré* and *Klein disks* it lies on the boundary of the disk. (s.a *Ultra Affine Point*)
- **Big Bang** The singularity at the beginning of the Universe. At the time of the Big Bang the Universe was infinitely dense and hot. 'Before the Big Bang' is a meaningless concept, time began together with space with the Big Bang.
- **Black Body** An object that emits light with a specific radiation curve (Planck's law) depending on temperature.
- **Bolyai, János** A Transylvanian (Hungarian) mathematician (1802-1860). Published his works of hyperbolic geometry in 1832.
- **Circumcircle, Circumsphere** The smallest circle/sphere enclosing a polygon/polyhedron. (s.a. Circumscribed Circle, Inscribed Circle, Incircle)
- **Circumscribed Circle, Sphere** The unique circle/sphere passing through each vertex of a polygon/polyhedron. (s.a. Circumcircle, Inscribed Circle, Incircle)
- **Closed in Space** A universe with no infinite dimensions. Its volume is finite.
- **Closed in Time** A universe that stops expanding and starts contracting into a singularity.
- **CMB** see *Cosmic Microwave Background*
- **Cosmic Microwave Background, CMB** The radiation from the *surface of last scattering* that reaches us now. The radiation has cooled down due to expansion of the Universe to *black body* radiation of $3.7K$.
- **Copernicus, Nicolaus** a German or Polish astronomer (1473-1543) who popularized the heliocentric model of the Universe formulated the *Copernican Principle*.
- **Copernican Principle** The idea that we should not see us as special in the Universe.
- **Cosmology** Study of the Universe at its largest scales.
- **Clifford transformation** A transformation that translates all points the same distance.

- **Cosmological Principle** The idea that the Universe is homogeneous and isotropic.
- **Covering Transformations** The group of symmetries of the universal covering space. These are the group of transformations that translates the fundamental domain to its ghost copies. (s.a. Holonomy Group)
- **Dirichlet Domain** A special fundamental domain, corresponding to a certain point in the manifold, called the base point of that Dirichlet domain. The distance of every point in the Dirichlet domain to the base point is shorter then the distance to any ghost copies of the base point. In non globally homogeneous spaces the Dirichlet domain is different for different base points. Construction of the Dirichlet domain is given in figure (2.5).
- **Einstein, Albert** A German physicist (1879-1955). Einstein developed the theory of special and general relativity.
- **Einstein Tensor** A rank 2 tensor which describes the curvature of spacetime. Usually written as $G_{\mu\nu}$.
- **Stress-Energy Tensor** A rank 2 tensor used to describe the content of the Universe in *general relativity*. Usually written as $T_{\mu\nu}$.
- **Euclid** A Greek mathematician who lived in Alexandria around 325BC to 265BC. Euclid is famous for his book 'The Elements' in which the rules for *flat geometry* are described.
- **Euclidean Geometry** see *Flat Geometry*.
- **Equidistant Lines** Two lines with the attribute that every point on either line has a fixed distance to the other line. In Euclidean space a line equidistant to a geodesic is a geodesic itself, in spherical space it is a *small circle*. (s.a *Ultra Parallel Geodesics*, *Ultra Parallel Geodesics*)
- **Flat Geometry** Geometry of a simply connected locally isotropic space where through any given point only one geodesic does not intersect with another given geodesic. Also called Euclidean geometry. (s.a. *Spherical Geometry*, *Hyperbolic Geometry*)
- **Flat Torus** The truly flat torus, $\mathbb{T}^2 = \mathbb{S}^1 \times \mathbb{S}^1$ with 0 curvature everywhere. Possible to embed isometrically in $\mathbb{R}^4$.
- **Fundamental Domain, FD** A polyhedron in 3 dimensions or polygon in 2D, which contains every point of the manifold only once and can be used to construct the manifold by gluing together the appropriate sides with appropriate orientation. The universal covering space can be created by assembling several (infinite if the covering space is open) pieces of the fundamental domain together with proper identifications. Most fundamental domains discussed in this thesis are Dirichlet Domains.
- **General Relativity** A theory of physics in which spacetime is not a rigid manifold but where matter curves space and space influences the motion of matter. (s.a. Special Relativity)
- **Gauss, Carl Friedrich** A German mathematician (1777-1855) known for his many contributions to a large number of scientific fields. Discovered hyperbolic geometry around 1800 but did not publish it out of fear of his reputation being tarnished by other mathematicians.
- **Genus** The amount of holes (or better, handles) a manifold has.
- **Geodesics** The locally shortest path between two points on a manifold. In Euclidean space this path is usually called a straight line. On a spherical space it is a *great circle*.
- **Glide Reflection** A translations with a reflection along the line parallel to the translation.

- **Great Circle** A circle on a spherical space that intersects two antipodal points. (s.a *Small Circle*)
- **Great Debate** A discussion in the 1920s whether the Universe consisted of our Galaxy only, or whether it consists of several galaxies similar to our own.
- **Holonomy Group** The holonomy group Γ is a subset of the full isometry group G of the universal covering space which account for the identifications of the fundamental domain. The compact manifold can be represented by its group structure G/Γ.
- **Homotopy Group** The group of classes of loops that can be transformed smoothly into one another. On the sphere this group has only 1 element since all loops can be transformed into one another.
- **Hyperbolic Geometry** Geometry of a simply connected locally isotropic space where through any given point infinite geodesics do not intersect with another given geodesic. (s.a. *Spherical Geometry*, *Flat Geometry*)
- **Incircle, Insphere** The largest circle/sphere enclosed in a polygon/polyhedron. (s.a. Circumcircle, Circumscribed Circle, Inscribed Circle)
- **Inflation** The period shortly after the *Big Bang* when the Universe expanded exponentially. Inflation caused the quantum fluctuations in the primordial density field to expand to cosmic proportions.
- **Integrated Sachs-Wolfe effect** The effect that the entire gravitational field between the CMB and us has on the energy of a photon from the *CMB*. (s.a. *Sachs-Wolfe effect*)
- **Inscribed Circle, Sphere** The unique circle/sphere tangent to every side/face of a polygon/polyhedron. (s.a. Circumcircle, Circumscribed Circle, Incircle)
- **Isometry** A transformation (usually called Λ) that moves every point x of a manifold (which is usually the universal covering space) to another point on the manifold while preserving distances between points.

$$\Lambda : x \mapsto \Lambda(x) \tag{D.1}$$
$$dist(x,y) = dist(\Lambda(x),\Lambda(y)) \tag{D.2}$$

- **Isometry Group** The set of isometries of a manifold, usually of the universal covering space.
- **Klein, Felix** A German mathematician known for his work in group theory, function theory, non-Euclidean geometry.
- **Klein Bottle** The only closed non-orientable entirely flat 2 dimensional manifold.
- **Klein Disc** A model of the hyperbolic plane where the infinite plane is shrunk to the flat unit disk in such a manner that geodesics become straight lines.
- **Manifold** An n-dimensional surface, sometimes embedded in a larger dimensional space. e.g. The 2-dimensional surface of a torus, possibly embedded in 3 dimensions, or a 3-dimensional surface of a hypersphere, possibly embedded in 4 or more dimensions.
- **Metric** A rank 2 tensor (2 dimensional matrix) used for a notion of distance on a curved space.
- **Lobachevsky, Nikolai Ivanovich** A Russian mathematician (1792-1856). First publisher of studies of hyperbolic geometry in 1829. Hyperbolic geometry is also called after him *Lobachevsky space*.

- **Lobachevsky Space** see *Hyperbolic Geometry.*
- **Multi Connected** A manifold where some closed circles cannot be contracted to a point, e.g. the torus. (s.a. *Simply Connected*)
- **Multipole Vectors** A vector decomposition of the *CMB*. The multipole decomposition takes into account all degrees of freedom that the real density field of the CMB has. In an simply connected universe the multipole vectors should be unaligned, this is not the case in a multi connected universe.
- **Open in Space** A manifold with all dimensions of infinite size. A manifold with some directions finite and some infinite is called semi-open.
- **Open in Time** A Universe that will expand forever. (s.a. *Closed in Time*)
- **Orientability** A manifold that has 2 distinct orientations is orientable, a manifold with only 1 orientation is non-orientable.
- **Parallel Geodesics** Two geodesics that intersect in their extension to infinity. Parallel geodesics do not exist in spherical space. (s.a *Ultra Parallel Geodesics*, *Equidistant Lines*)
- **Poincaré Conjecture** A conjecture by Poincaré that states that if a 3 dimensional manifold has a trivial fundamental group (i.e. a simply connected manifold) is the 3-sphere. As of 2005 it is believed to be proved by Perelman in 2002 but his work is still under review by the mathematical community.
- **Poincaré Disk** A model for the hyperbolic plane where the entire plane is shrunk to the flat unit disk in such a manner that geodesics become arcs of circles perpendicular to the disc's boundary.
- **Poincaré, Henry** France mathematician who developed the Poincaré disk model for the hyperbolic plane. Famous for the *Poincaré conjecture.*
- **Ptolemy** Greek/Egyptian astronomer (90-168). Proposed the geocentric model of the Universe.
- **Recombination** The first combination of the ionized nuclei and electrons into atoms. This happened 379.000 years after the big bang when the Universe cooled to 3000K.
- **Riemann, Bernhard** A German mathematician (1826-1866) who made many contributions to differential geometry.
- **Sachs-Wolfe effect** The change of energy of a photon when it climbs out or falls into an potential well in the density field at recombination. Photons from high density regions have to climb out of a potential well which causes it to loose energy according to general relativity. Photons from a low density region fall into a potential well and gains energy. (s.a. *Integrated Sachs-Wolfe effect*)
- **Simply Connected** A manifold where every closed circle can be contracted to a point, e.g. the Euclidean plane or a sphere. (s.a. *Multi Connected*)
- **Small Circle** A circle on a spherical space that does not intersect two antipodal points. (s.a *Great Circle*)
- **Sound Speed** The speed at which oscillations in the primordial soup can propagate.
- **Special Relativity** A theory of physics which put space and time on equal footage and threats all unaccelerated motions equivalent. Its prime axioms are the fixed velocity of light and the principle of that all unaccelerated motions are indistinguishable. (s.a. General Relativity)

- **Spherical Geometry** Geometry of a simply connected locally isotropic space where through any given point every geodesic intersects with all other geodesics. (s.a. *Flat Geometry*, *Hyperbolic Geometry*)
- **Straight Line** In non-Euclidean geometries the term straight line is not well defined. Therefore it is better to speak of geodesics.
- **Surface of Last Scattering** The spherical surface which is the part of space where we see *recombination* occurring. Its distance is approximately $13.7 Glyr$.
- **Time of Last Scattering,** t_{SLS} The time of *last scattering*. (c.a. *Surface of Last Scattering*)
- **Torus** see *Flat torus* or *Torus of Revolution*.
- **Torus of Revolution** The (familiar) torus embedded in Euclidean 3space. Topologically the same as the flat torus T^2, but with different curvature (positive at some places, zero or negative at others).
- **Universal Time** The notion that at every point the time since the big bang is equal (disregarding small local fluctuations).
- **Ultra Affine Point** The intersection point of two *ultra parallel geodesics*. This point is not part of the plane in which the geodesics lie, on the *Poincaré disk* it lies outside the disk. (s.a *Affine Point*)
- **Ultra Parallel Geodesics** Two geodesics that do not intersect even in their extension to infinity. Ultra parallel geodesics do not exist in spherical or Euclidean space. (s.a *Parallel Geodesics*, *Equidistant Lines*)
- **Universal Covering (Space), UC or UCS** The simply connected space that can be created by gluing several pieces of the fundamental domain together. Occupants of a multi connected space at first glance appear to life in the universal covering space. In this thesis all universal covering spaces are homogeneous and isotropic.
- **Weyl, Hermann** A German mathematician (1885-1955), proposer of the *Weyl's postulate*.
- **Weyl's postulate** A postulate that states that it is possible to see space as a 3 dimensional manifold perpendicular to time.

Bibliography

Alpher, R. A., Bethe, H., and Gamow, G.: 1948, *Phys. Rev.* **73(7)**, 803

Baleisis, A., Lahav, O., Loan, A. J., and Wall, J. V.: 1998, *MNRAS* **297(2)**, 545

Cellarius, A.: 1708, *Harmonia Macrocosmica*, none

Cooray, A., Huterer, D., and Baumann, D.: 2004, *Phys. Rev. D* 69(2)

Copi, C., Huterer, D., Schwarz, D., and Starkman, G.: 2005, *MNRAS, astro-ph/0508047*

Copi, C., Huterer, D., and Starkman, G.: 2004, *Phys. Rev. D.* 70(043515)

Cornish, N., Spergel, D., Starkman, G., and Komatsu, E.: 2004, *Phys. Rev. Let* 92

Cyp, http://en.wikipedia.org/wiki/User:Cyp

Dineen, P., Rocha, G., and Coles, P.: 2005, *Mon.Not.R.Astron.Soc* **358(4)**, 1285

Eriksen, H., Hansen, F., Banday, A., Górski, K., and Lilje, P.: 2004, *Astrophys. Jour.* **605(1)**, 14

Gausmann, E., Lehoucq, R., Luminet, J.-P., Uzan, J.-P., and Weeks, J.: 2001, *Class. Quantum Grav* **18**, 5155

Gomero, G., Rebouças, M., and Teixeira, A.: 2000, *Phys. Let. A* **275(5-6)**, 355

Gomero, G., Teixeira, A., Rebouças, M., and Bernui, A.: 2002, *J. Mod. Phys. D* **11**, 869

Gundermann, J.: 2005, *Predicting the CMB power spectrum for binary polyhedral spaces*, arXiv:astro-ph/0503014v1

Hajian, A. and Souradeep, T.: 2003, *Astro. Jour.* **597**, L5

Hajian, A., Souradeep, T., and Cornish, N.: 2005, *Astro. Jour.* **618**, L63

Katz, G. and Weeks, J.: 2004, *Phys. Rev. D* 70(063527)

Lachièze-Rey, M. and Luminet, J.-P.: 1995, *Physics Reports* **254**, 135, arXiv:gr-qc/9605010v2

Land, K. and Magueijo, J.: 2005, *Phys. Rev. Lett.* **95**, 071301

Lehoucq, R., Lachièze-Rey, M., and Luminet, J.-P.: 1996, *Astron.Astrophys.* **313**, 339

Lehoucq, R., Luminet, J.-P., and Uzan, J.-P.: 1999, *Astron. Astrophys.* **344**, 735

Lehoucq, R., Uzan, J.-P., and Luminet, J.-P.: 2000, *A&A* **363**, 1

Lehoucq, R., Weeks, J., Uzan, J.-P., Gausmann, E., and Luminet, J.-P.: 2002, *Classical and Quantum Gravity* **19(18)**, 4683

Levin, J.: 2002, *Phys. Rept.* **365**, 251

Levin, J., Scannapieco, E., and Silk, J.: 1998, *Phys. Rev. D* 589(103516)

Luminet, J.-P. and Roukema, B.: 1999, *NATO science series. Series C.* **541**, 117, arXiv:astro-ph/9901364)

Luminet, J.-P., Weeks, J., Riazuelo, A., Lehoucq, R., and Uzan, J.-P.: 2003, *Nature* **425**, 593

Novacki, W.: 1934, *Commentarii Mathematici Helvetici* 7(81)

Park, C.-G.: 2004, *Mon.Not.R.Astron.Soc.* **349**, 313

Peterson, M.: 1979, *Am. J. Phys.* 47(12)

Poole, M.: 1995, *Beliefs and Values in Science Education.*, Open University Press

Przeworski, A.: 2003, *Topology and its Applications* **128(2-3)**, 103

Riazuelo, A., Uzan, J.-P., Lehoucq, R., and Weeks, J.: 2004, *Phys. Rev. D* 69(103514)

Rocha, G., Cayón, L., Bowen, R., Canavezes, A., Silk, J., Banday, A., and Górski, K.: 2004, *Mon. Not. R. Astron. Soc.* **351**, 769

Scannapieco, E., Levin, J., and Silk, J.: 1999, *Mon. Not. R. Astron.* **303**, 797

Schmoldt, I., Branchini, E., Teodoro, L., Efstathiou, G., Frenk, C. S., Keeble, O., McMahon, R., Maddox, S., Oliver, S., Rowan-Robinson, M., Saunders, W., Sutherland, W., Tadros, H., and White, S. D. M.: 1999, *MNRAS* **304(4)**, 893

Schwarz, D., Starkman, G., Huterer, D., and Copi, C.: 2004, *Phys. Rev. Lett.* **93(22)**, 221301

Smoot, G. F., Bennett, C. L., Kogut, A., Aymon, J., Backus, C., de Amici, G., Galuk, K., Jackson, P. D., Keegstra, P., Rokke, L., Tenorio, L., Torres, S., Gulkis, S., Hauser, M. G., Janssen, M. A., Mather, J. C., Weiss, R., Wilkinson, D. T., Wright, E. L., Boggess, N. W., Cheng, E. S., Kelsall, T., Lubin, P., Meyer, S., Moseley, S. H., Murdock, T. L., Shafer, R. A., and Silverberg, R. F.: 1991, *Astrophysical Journal, Part 2* **371**, L1

Spergel, D. N., Bean, R., Dore', O., Nolta, M. R., Bennett, C. L., Hinshaw, G., Jarosik, N., Komatsu, E., Page, L., Peiris, H. V., Verde, L., Barnes, C., Halpern, M., Hill, R. S., Kogut, A., Limon, M., Meyer, S. S., Odegard, N., Tucker, G. S., Weiland, J. L., Wollack, E., and Wright, E. L.: 2006, *astro-ph/0603449*

Thas, C.: 2002, *Bulletin of the Institute of Mathematics Academia Sinica* **30(2)**, 97

Tikhomirova, Y. Y. and Stern, B. E.: 2000, *Astronomy Letters* **26(10)**, 672

Vavrek, R., Balázs, L. G., Mészáros, A., Bagoly, Z., and Horváth, I.: 2004, *Baltic Astronomy* **13**, 231

Verde, L.: 2006, *WMAP returns*, Presentation Bernard's Cosmic Stories Conference

Weeks, J.: 1998, *Classical and Quantum Gravity* **15(9)**, 2599

Weeks, J.: 2002, *SnapPea*, http://www.geometrygames.org/SnapPea/

Weeks, J., Luminet, J.-P., Riazuelo, A., and Lehoucq, R.: 2004, *Mon.Not.R.Astron.Soc* **352(1)**, 258

WMAP Science Team: 2006, *LAMBDA - WMAP Images*, http://lambda.gsfc.nasa.gov/product/map/current/m_images.cfm

Wu, K., Lahav, O., and Rees, M.: 1999, *Nature* **397**, 225

Yadav, J., Bharadwaj, S., Pandey, B., and Seshadri, T. R.: 2005, *MNRAS* **364(8)**, 601